Theoretical and computational studies of the thermomechanics of magnetic materials

Thomas Nussle

UNIVERSITÉ DE TOURS

École Doctorale MIPTIS

Institut Denis Poisson UMR 7013 / CEA-DAM Le Ripault

THÈSE présentée par :

Thomas NUSSLE

soutenue le : 10 décembre 2019

pour obtenir le grade de : Docteur de l'université de Tours

Discipline/ Spécialité : Physique

Theoretical and computational studies of the thermomechanics of magnetic materials

THÈSE DIRIGÉE PAR :

NICOLIS Stam	Maître de conférences, Université de Tours

RAPPORTEURS :

KACHKACHI Hamid	Professeur, Université de Perpignan (UPVD)
LE HUR Karyn	Directeur de recherche, École polytechnique

JURY :

BARKER Joseph	Chercheur, University of Leeds
CHERNODUB Maxim	Directeur de recherche, Institut Denis Poisson, Président du jury
KACHKACHI Hamid	Professeur, Université de Perpignan (UPVD)
KLEIN Olivier	Directeur de recherche, CEA/Spintec
LE HUR Karyn	Directeur de recherche, École polytechnique
NICOLIS Stam	Maître de conférences, Université de Tours
RUELLO Pascal	Professeur, Université du Mans
THIBAUDEAU Pascal	Ingénieur-chercheur, CEA-DAM Le Ripault

Remerciements

Quand on achève quelque chose, on a tendance, bien trop souvent je trouve, à oublier les personnes sans lesquelles cela n'aurait pas été possible. J'espère, dans ce qui suit, remercier les personnes sans lesquelles je ne serais jamais parvenu jusqu'ici, sans trop en oublier.

Dans un premier temps, je voudrais remercier Karyn LE HUR et Hamid KACHKACHI, qui ont accepté la tâche contraignante d'être rapporteurs de ma thèse et qui ont ainsi consenti à donner de leur temps pour juger de la qualité de mes travaux de ces trois dernières années en relisant leur transcription manuscrite. Je remercie également les membres du Jury, sans lesquelles je ne pourrais pas présenter et soutenir ma thèse, ils acceptent de se déplacer afin d'entendre ma présentation et d'arbitrer de sa valeur et je leur en suis très reconnaissant.

Je souhaite aussi remercier tout particulièrement Stam NICOLIS, mon directeur de thèse, pour sa profusion d'idées et sa bonne humeur à toute épreuve. Il ne fait aucun doute qu'il fait partie des personnes qui m'ont donné envie de poursuivre dans cette voie. De même, je remercie Pascal THIBAUDEAU, co-directeur et encadrant CEA, pour la confiance qu'il m'a accordée tout au long de ces travaux et pour sa grande disponibilité à chaque étape de cette aventure et même avant, lors de mon stage de Master. Lui aussi m'a aidé à grandir pendant ces trois dernières années.

Je souhaite bien sûr aussi remercier le CEA le Ripault, pour m'avoir permis de mener mes travaux de recherches dans de bonnes conditions. Pour ne citer que quelques noms parmi ceux qui ont rendu mon séjour au Ripault plus agréable : Michael, Olivier, Yves, Sébastien, Joffrey, Marie, Jérémy, François, Nicolas, Hervé, Isabelle, Frédéric, Christophe, Charlotte, Luc, Jean-Louis, Karine, Corine, Louis, Julien, Augustin, Thibaut, Killian, Marjorie, Yohann ... et bien d'autres que j'oublie bien malgré moi. De plus, je remercie de tout cœur l'Université de Tours et plus encore, l'Institut Denis Poisson et tous ses membres, qui ont su faire de mes visites des moments parmi les plus agréables de cette aventure, que ce soit au futsal ou dans leurs locaux. Je ne saurais oublier également toute l'équipe enseignante de l'Université de Tours, qui a su m'apporter à la fois l'envie de continuer dans cette voie et les connaissances pour en avoir les moyens. Je tiens ici à remercier tout particulièrement Hector G, j'espère pouvoir un jour arriver à transmettre à mon tour les connaissances et l'expérience acquises avec autant de passion. Le groupe de doctorant de l'IDP également et pour n'en citer que quelques-uns : Abraham, Florestan, Jean-David, Amélie, Cam, Thomas (et il y en a plus d'un), Gabriel, Shinya ... et j'en oublie sûrement, mais ils ont tous contribué à ce sentiment de bien être que j'ai éprouvé

dans les locaux de l'université.

Il y a bien sûr aussi d'autres personnes qui ont contribué, de l'intérieur ou de l'extérieur de ces établissements. Je pense notamment à Xavier F, qui m'a apporté énormément et qui continue encore aujourd'hui à m'aider à évoluer humainement. Xavier L, également, qui m'a, dès mon stage de Master, aidé à me sentir chez moi à l'Université et avec qui j'ai partagé tellement de choses, je pense, notamment au séjour au Liban, en visite chez Salam K et Abdolhakim S (que je remercie également de tout cœur), qui fût une des plus belles expériences de ma vie. Mon camarade homonyme, Thomas R, qui fut également de la partie pour le Liban, et qui m'a lui aussi, tellement apporté. Il fait partie de ces personnes qui vous donnent foi en l'espèce humaine et je lui en suis reconnaissant. Il y a aussi Geoffroy K, d'abord camarade de bureau au CEA avant d'être un véritable ami, que je remercie pour m'avoir aidé à tenir lorsque le moral n'y était plus. Je pense que le hasard permet souvent de faire de très belles rencontres et il illustre parfaitement ce fait. Dans ce cadre je remercie également Jess B, rencontré au hasard d'un entraînement, mon acolyte d'escalade, avec qui je partage une vision commune de la vie et avec qui m'entretenir ou m'exercer est toujours, un véritable plaisir. Il y a bien sûr aussi parmi ceux qui m'ont aidé à faire baisser la pression, comme Jeremie D et nos petits séjours dans le Lot, le Tarn et la Jonte et Szabolcs B lors de mes petites escapades en Hongrie. Un petite pensée également pour mes amis de l'ESM, en particulier Ivan A et Nicolas M et pour les belles rencontres de conférences, Libor S et Joe B. Je pense aussi à Maxime D, Anthony M, Adrien H, Alexandre M, Sylvain M, Jérémie E, Gaëtan C, Guillaume L, Erwan R et bien d'autres encore que j'oublie, amis rencontrés grâce à mon frère Andréas.

D'ailleurs, venons-en à la famille. Ici avant tout je souhaite remercier du fond du cœur mes parents. Même si c'est cliché de dire ça, je ne serais pas ici sans eux aujourd'hui. Ils m'ont toujours permis de faire ce que je souhaitais dans les meilleures conditions qu'il leur était possible de m'offrir. Ils ont fait ce qu'ils ont pu malgré des conditions difficiles et je leur en suis extrêmement reconnaissant. Il y a également mes frères. Michaël qui a toujours été là à veiller sur moi lorsque j'en avais besoin étant plus jeune et Andréas qui m'a donné le goût de la science dès ma jeunesse et m'a dirigé sur les rails de la physique. Je peux dire aujourd'hui que je suis fier de faire partie de cette famille. Bien sûr, je remercie également toute ma famille en Allemagne que je suis si content de retrouver à chaque fois, même si ce n'est pas aussi fréquent que ce que je souhaiterais.

Pour ne pas m'éterniser, à la façon du soldat inconnu, je souhaite remercier ici tous ceux qui m'ont porté tout au long de ma vie et m'ont amené à être la personne que je suis aujourd'hui. Mes enseignants, que ce soit en maternelle, en primaire, au collège, au lycée ou à l'université. Mes amis d'enfance et de longue date pour lesquelles je vais m'autoriser une petite entorse à l'anonymat : Clément D, Olivier S, Léo B, Vincent G, Vincent P, Guillaume A, Ambroise D, Adrien B, Boris S ... et encore une fois, nombreux sont ceux qui ne me viennent pas à l'esprit, mais qui m'ont également façonné.

Pour finir, je souhaite également remercier du fond du cœur celle qui m'a accompagné et qui m'accompagne encore à travers les épreuves et les plaisirs de la vie et qui m'a soutenu lorsque j'en avais le plus besoin. Merci à toi Hermine et à toute ta famille de m'avoir accueilli et d'être si bienveillante à mon égard, même s'il est parfois difficile de l'exprimer ou de l'entendre, je te suis profondément reconnaissant de ce que tu fais et de

ce que tu es pour moi.

Résumé

Le magnétisme est l'un des plus anciens phénomènes rapportés de l'histoire des sciences naturelles et probablement l'un des plus fascinants. Véritable manifestation macroscopique de la physique quantique, il subit en s'y couplant, l'influence de nombreux réservoirs énergétiques et statistiques, dont ceux de la thermique et de la mécanique.

En remarquant qu'un moment magnétique élémentaire est un objet composite formé grâce à des variables anticommutantes inobservables, on peut engendrer une dynamique Hamiltonienne couplant ce degré de liberté à ceux provenant des autres réservoirs, eux-mêmes décrits par la dynamique de variables aléatoires.

La première étape est d'étudier la dynamique d'un moment magnétique, vu comme un spin classique dans de tels bains. À cette fin on considère un bain magnétique afin d'évaluer la possibilité de mimer les effets de couplage entre moments magnétiques ainsi que le couplage magnétoélastique par un tel modèle effectif.

Par la suite, nous montrons que la précession d'un spin classique peut être modélisée par une dynamique de Nambu qui facilite la description de la nature, additive ou multiplicative, des couplages stochastiques. La dynamique ainsi produite est d'abord étudiée numériquement de façon stochastique en moyennant les différentes réalisations obtenues; ensuite, un modèle déterministe sur la hiérarchie des moments statistiques est établi puis fermé afin de développer une méthode à la fois plus rapide, mais également déterministe de déduction des propriétés magnétiques.

Finalement, pour illustrer la pertinence tangible de toutes ces notions, nous construisons une dynamique étendue de particules "fictives" portant à la fois un moment magnétique et une déformation mécanique locaux exprimant la magnétoélasticité, d'une part dans une approche Lagrangienne puis Hamiltonienne. Pour chacune des deux approches nous étudierons la dynamique du retournement ultrarapide d'aimantation pour NiO, oxyde antiferromagnétique prototype, sous sollicitations mécanique et électrique.

Le formalisme, exposé ici, aussi bien conceptuel qu'informatique, ne sert pas, seulement, comme un exemple de l'état de l'art, mais permet une description des propriétés des milieux magnétiques, qui est fondamentale aussi bien pour la conception de nouveaux matériaux, que comme modèle pour aborder d'autres questions portant sur l'interaction entre bruit et variables dynamiques, plus généralement.

Mots clés : Dynamique stochastique de spin, fermeture de hiérarchie, magnétoélasticité, couplages magnétomécanique Lagrangien et Hamiltonien, dynamique de Nambu, antiferromagnétisme, intégration symplectique/géométrique, retournement du paramètre d'ordre de Néel, couple de transfert de spin.

Abstract

One of the utmost interesting properties of matter is magnetism. This property, which is a macroscopic consequence of quantum physics, is subjected and couples to several reservoirs. Among them, two are most relevant, namely the thermal and mechanical reservoirs. We build a Hamiltonian model for the coupling between – classical – magnetism and elasticity, which relies on the – underlying – anticommuting nature of spin, so as to describe the coupled dynamics of these degrees of freedom.

The first step is to study the behavior of the classical spin – or magnetic moment – when coupled to different – stochastic – baths. First a spin bath, so as to investigate if and how such an effective model can mimic the couplings, to different magnetic moments but also to the elastic structure of the compound. A different approach is then followed where, through a Nambu dynamics model for spin precession, the ways in which this spin can be coupled to a bath, additively or multiplicatively, are studied in order to make out which is better suited to describe coupling phenomena in magnetism. Those are then studied numerically, initially stochastically, with the appropriate averaging procedure over different realizations and then deterministically, by building an effective model for the moments of the statistical distributions. This model is obtained by truncating the thus derived hierarchy of moments, so as to construct a quicker and deterministic method to deduce magnetic properties of a system.

The second step is to construct models for magnetoelastic coupling, which we do via "virtual" particles carrying both localized magnetic moment and mechanical strain tensor. We begin by a Lagrangian formulation for the precession of spin, which is coupled to a dynamical elastic solid by a magnetoelastic coupling term. This enables us to study their coupled dynamics in a way that is fully consistent with all the symmetries, which ensures a consistent description.

We then shift to a Hamiltonian description where spin is interpreted as a composite – commuting – variable, which is a product of underlying and not observable – anticommuting – variables. Such a spin interacts with a couple of canonically conjugate variables representing the elastic medium, in an extended Poisson structure. Finally, for each of these two models, we numerically study the influence of an external stress on the switching behavior of the Néel order parameter and spin accumulation for a NiO toy model antiferromagnet, induced by an external spin-transfer-torque.

Keywords : Stochastic spin dynamics, hierarchy closing, magnetoelasticity, Lagrangian and Hamiltonian magnetomechanical coupling, Nambu dynamics, antiferromagnetism, symplectic/geometric integration, Néel order parameter switching, spin transfer torque.

Contents

List of Tables

List of Figures

Introduction

Qu'est-ce qu'une théorie effective ? Dans le contexte de la physique, il s'agit d'un formalisme qui décrit des effets à une échelle donnée, sans tenir compte explicitement de ce qui se passe à des échelles plus petites ou plus grandes. En d'autres termes, il s'agit de répondre plutôt à la question "qu'est-ce qui se passe et comment ?" qu'à la question "pourquoi est-ce que ça se passe ?". En ce sens, toute la physique moderne repose sur des approches effectives. Que ce soit pour les échelles les plus petites ou bien les échelles les plus grandes, il y a toujours des hypothèses sous-jacentes qui expriment un certain degré de subjectivité. Ce qu'il faut retenir de cela est qu'il est complexe de construire un modèle théorique qui explique réellement pourquoi quelque chose se produit afin de déterminer comment cela se réalise. Ainsi, la procédure habituelle est de fournir une interprétation a des résultats expérimentaux afin d'établir un formalisme théorique afin de tenter d'expliquer comment d'autres expériences, similaires, devraient se comporter. C'est également ce qui a été le cas pour la théorie du magnétisme.

Bien que nous comprenions aujourd'hui que ce phénomène est une manifestation macroscopique des propriétés quantiques de la matière [1], nombreuses sont les applications pour lesquelles les échelles considérées impliquent qu'un modèle classique ne tenant pas compte d'effets quantiques est suffisant.

Néanmoins, ces dernières décennies, avec les progrès expérimentaux en termes de réduction d'échelle, les ordres de grandeur des effets quantiques deviennent de plus en plus proches de ceux d'autres perturbations, comme par exemples thermiques ou liés au désordre.

De ce fait, il semble important de clairement définir les échelles des phénomènes auxquels nous nous intéressons et de construire un modèle pouvant décrire les propriétés magnétiques d'un tel objet. Malgré les premières observations des phénomènes magnétiques et les premières ébauches théoriques qui datent du XVI^e siècle, les théories plus modernes pour les moments magnétiques ont été construites de façon semi-empirique, sur des fondations de mécanique quantique. En effet le modèle de précession, déduit de l'algèbre de spin, ½ a été complété par un terme de couple. Ce terme, introduit pour reproduire les comportements expérimentaux, induit un "amortissement" pour la dynamique d'un moment magnétique vers un état d'équilibre, en général aligné avec le champ magnétique local dominant. Ultérieurement, et ce afin d'implémenter la prise en compte d'effets de température, une approche stochastique [2–4] a été construite.

Pour ce genre d'approche, l'idée est que la dynamique d'aimantation est gouvernée par des degrés de liberté qui ne sauraient être résolus au-delà de leur distribution statistique

Formellement, l'expression de la distribution de probabilité pour un moment magnétique en équilibre avec le bain dans lequel il est plongé est donnée par

$$P(\boldsymbol{s}) = Z^{-1} e^{-\int dt\, dt' \, \frac{1}{2}\left\{e(\boldsymbol{s})^{-1}\left(\frac{d\boldsymbol{s}}{dt}+\boldsymbol{A}(s)\right)(t) G(t-t') e^{-1}(\boldsymbol{s})\left(\frac{d\boldsymbol{s}}{dt}+\boldsymbol{A}(s)\right)(t')\right\}} \left|\det \frac{\delta \eta_I(t)}{\delta s_J(t')}\right| \qquad (1)$$

Bien évidemment, le défi est de réussir à donner un sens à cette expression. En pratique, la méthode est de travailler plutôt avec les moments de la distribution afin d'éviter d'avoir à manipuler cette formule. De fait, cette thèse s'intéresse aux conséquences de cette expression par l'intermédiaire de ses moments.

Ainsi on ne détermine pas la dynamique de l'aimantation elle-même, mais plutôt les propriétés de sa distribution à travers une hiérarchie ouverte d'équations différentielles pour ses moments. Dans ce cas, afin de pouvoir obtenir des observables à calculer, il faut procéder à la fermeture de cette hiérarchie par des hypothèses et des méthodes appropriées.

Des études récentes sur le retournement d'aimantation, des phénomènes liés au transport de l'aimantation ou plus généralement des propagations d'onde de spin (*i.e.*, magnons) ont fait émerger un nouveau type d'électronique : la spintronique. On entend même aujourd'hui, de plus en plus souvent, le terme magnonique, à savoir une électronique qui reposerait sur la propagation d'ondes de spin. Tous ces phénomènes sont sensibles à divers effets de couplage (entre moments magnétiques, structures mécaniques, distributions de charges ...), en plus bien sûr des effets thermiques, à savoir, par exemple, le couplage de l'aimantation à la structure mécanique des composés étudiés. Il a été montré en effet que certains matériaux changent de propriétés mécaniques lorsqu'ils sont exposés à un champ électrique et inversement (*i.e.*, la piézo-électricité [5]) et des observations similaires ont montré également ce genre de comportement pour des matériaux magnétiques exposés à des champs magnétiques externes. Ce phénomène est appelé la magnétostriction [6]. Dans ce cadre, des modèles théoriques relativement performants ont été développés, mais pour la plupart, ils reposent sur des approches énergétiques à l'équilibre qui ne s'intéressent pas à la dynamique des systèmes étudiés. Cela ne permet pas non plus de décrire correctement les aspects dynamiques liés à l'évolution temporelle de la structure mécanique. Ce que nous souhaitons donc construire, c'est un modèle dynamique de couplage entre les déformations mécaniques d'un réseau et les moments magnétiques d'un modèle de dynamique de spin atomique par une description locale de ces deux grandeurs. Ceci apparaît aujourd'hui comme nécessaire, car les échelles de temps des phénomènes deviennent très petites, comme par exemple pour les phénomènes de désaimantation ultrarapide, et la dépendance aux phénomènes thermiques requiert un modèle sensible aux fluctuations hors équilibre pour tous ces réservoirs énergétiques []. Sachant cela, nous avons développé un outil numérique pour lequel à chaque site d'une simulation (type dynamique de spin atomique), nous ajoutons une déformation mécanique locale. Les paramètres spécifiques à chaque composé doivent être déduits d'autres modèles *ab initio* ou à partir de données expérimentales. L'outil fournit ensuite l'évolution temporelle pour le moment magnétique et la déformation mécanique pour ce système couplé.

À cette fin, nous préparons cette étude avec un rappel des techniques existantes (chapitre 1). Dans ce cadre, la première étape est l'analyse détaillée des mouvements de précessions afin d'aboutir à une modélisation de la précession amortie expérimentalement constatée pour le moment magnétique. Nous retraçons ensuite les origines de la dy-

namique moléculaire magnétique qui permet de reproduire un couplage entre magnétisme et mécanique en permettant explicitement aux ”porteurs” de spin de se déplacer au sein du composé, ainsi que leurs implémentations numériques, à l'aide de schémas d'intégration symplectique, ceux-ci préservant le volume de l'espace des phases et l'énergie d'un système fermé. Puis nous étudions les techniques de dynamique de spin atomique utilisées notamment pour prédire les courbes d'aimantation de Curie. Nous nous intéressons également à la manière d'implémenter des effets de température finie dans ces modèles. La suite logique est donc d'étudier comment les systèmes magnétiques peuvent être couplés à des bains plus généraux et comment cela conduit soit à obtenir des systèmes d'équations stochastiques dépendant explicitement d'un bruit ou des systèmes d'équations déterministes sur les moments. Dans ce cadre nous nous intéressons également à la manière dont ces distributions statistiques ont été modifiées afin de mieux reproduire des effets quantiques, plus particulièrement à faible température. Ensuite, nous présentons quelques propriétés de la dynamique de Nambu et des crochets de Nambu-Poisson afin de décrire la précession du spin et nous donnons quelques interprétations intéressantes des symétries dans l'espace des phases du spin pour ce modèle. La partie suivante de cette revue concerne plus particulièrement l'élasticité mécanique et sa contribution à l'énergétique d'un système. Ici, nous étudierons brièvement des méthodes de couplages entre degrés de liberté mécanique et magnétique afin d'introduire la magnétoélasticité. Le dernier aspect traite de variables de Grassman (anticommutantes) et pourquoi celles-ci permettent de décrire les degrés de liberté de spin. Un bref résumé de l'émergence de couplage supersymétrique entre degrés de liberté spatiaux et de ces variables anticommutantes représentant le spin est également effectué.

Le (chapitre 2) commence par la présentation d'une méthode alternative pour décrire la dynamique d'aimantation d'un moment magnétique, couplé à une collection de moments magnétiques se comportant quant à eux comme un “bain macroscopique de spin”. Le nom qui nous a semblé le plus approprié pour cette approche est celui de modèle de spin “lourd” et de spin “léger”. La dynamique couplée pour ces deux objets se modélise par un ensemble d'équations différentielles stochastiques que nous résolvons numériquement à l'aide d'un schéma d'intégration symplectique. De même, nous construisons un modèle effectif déterministe pour les moments des distributions statistiques de ces deux moments magnétiques, en précisant des hypothèses de fermetures de hiérarchie et ce modèle est également intégré afin de pouvoir obtenir des résultats plus rapidement qu'avec l'approche stochastique. Ces deux méthodes sont ensuite comparées et nous évaluons si elles peuvent reproduire les effets attendus d'un couplage magnétoélastique. Ces travaux ont fait l'oeuvre de la publication [7]

Le (chapitre 3) est la construction d'une approche Lagrangienne pour le couplage magnétoélastique dans un modèle de dynamique de spin atomique. Dans cette approche, l'espace des phases étudié est constitué, pour chaque objet, d'un moment magnétique et d'un tenseur de déformation mécanique. Un Lagrangien est défini pour ce système et les équations du mouvement couplées sont obtenues. Une extension pour un modèle à plusieurs particules en interaction par échange magnétique est ensuite introduite. Nous en présentons la description à un modèle jouet pour simuler la dynamique de retournement ultrarapide de NiO. En particulier, nous étudions le retournement du paramètre de Néel sous contrainte mécanique externe pour ce système par l'application d'un couple de

transfert de spin. Ces travaux ont été publiés dans la référence [8].

Le (chapitre 4) présente une extension dissipante et fluctuante à la dynamique de Nambu pour la dynamique d'aimantation, qui implémente naturellement les contraintes de cette dernière. Dans ce contexte, nous étudions les différences entre bruit additif et bruit multiplicatif dans le cadre de systèmes magnétiques en étendant la dynamique de Nambu à des systèmes dissipants, dans le cas particulier de systèmes magnétiques dissipatifs . Pour cela, nous exposons comment déduire une dynamique de précession à partir d'un modèle de Nambu simple à deux Hamiltoniens. Ce modèle est ensuite complété par des termes dissipatifs. Ceux-ci sont identifiés avec les modèles habituels de dissipation afin de les interpréter comme issus d'une dynamique de Nambu dissipative. Nous introduisons ensuite des termes de fluctuations additives et multiplicatives afin de déterminer quelle forme est la plus adaptée à l'étude des fluctuations des systèmes magnétiques. Ces travaux ont été publiés sous la référence [9].

L'aboutissement de cette étude est l'établissement d'un modèle Hamiltonien pour décrire le couplage magnétoélastique (chapitre 5). Dans cette partie, nous commençons par construire un modèle de précession du spin en considérant que la variable de spin classique commutante (*i.e.*, dans le sens qu'elle satisfait des relations de commutation) est en fait une variable composée de deux variables anticommutantes (de Grassman, *i.e.*, dans le sens qu'elles satisfont des relations d'anticommutation) pour lesquelles nous montrons que l'algèbre associée décrit une précession. Grâce à ce formalisme, nous construisons un crochet de Poisson pour l'espace étendu des phases formé d'un vecteur de spin, d'un tenseur de déformation mécanique et de son tenseur conjugué. Une fois ce crochet établi, nous construisons un Hamiltonien pour le système couplé, afin de déduire les équations du mouvement pour celui-ci. Ensuite, comme dans le chapitre 2, ce modèle est étendu à des situations multi particulaires par un terme d'échange magnétique entre sites d'un réseau, chaque site portant son propre ensemble de variables dynamique et d'équations du mouvement correspondantes. Nous présentons ensuite un schéma d'intégration numérique symplectique pour ce système couplé. Cet outil est, de nouveau, utilisé pour étudier le retournement du paramètre de Néel pour NiO sous contrainte mécanique externe par un couple de transfert de spin. Ces résultats sont comparés à ceux du chapitre 1. Ces travaux ont été soumis et sont actuellement en cours d'évaluation pour "the Physical Review B".

Introduction

What is an effective approach ? Within the mind frame of physics, it consists of an approach which describes effects at a given scale without explicitly taking into account what happens at smaller or larger scale, yet delivers accurate results for calculations at this given scale. In other words, it answers the question *"what ?"* instead of *"why ?"* In this sense, all of modern physics is built through effective approaches. Even for the smallest or largest scales, there are always underlying assumptions which reflect at least some subjective views. The important idea to extract from this is that it is really difficult to build a theory which accurately answers the question *"why ?"* in order to be able to answer the question *"what ?"* So what is generally done is to interpret experimental results in some way which allows building a theoretical framework to try and explain how similar experiences should behave. This has been the case for the theory of magnetism.

Although, fundamentally, we understand that magnetism is an expression of the quantum nature of matter [1], many practical applications take place at scales, where the quantum effects, in fact, are not relevant and a classical description is appropriate, in terms of quantities, that do satisfy classical thermodynamics, as Curie and Weiss, already noticed.

However, since that time it has become possible to control matter at scales, where quantum effects, not only, cannot be neglected, but they become comparable to the host of perturbations, such as thermal or due to disorder.

Hence the smarter idea is to clearly define the scales for which we want to do computations, and then construct a model which enables us to study the magnetic properties and behavior reasonably. Even though the first observations of these phenomena are far from recent and scientists already speculated on magnetism, as early as the 16^{th} century (though the word is due to Thales, when coming across substances, found in ancient "Magnesia") the modern theories for the dynamics of magnetic moments have been constructed, mostly, by empirical approaches, though based on quantum mechanical foundations. The precessional model deduced from the spin ½ algebra was extended by adding a torque term. This term induces a "damping" for the dynamics of the magnetic moment towards an equilibrium state, aligned with the dominant magnetic field. In later studies, in order to implement thermal effects, a stochastic approach relying on Langevin dynamics [2–4] has been constructed.

It is remarkable that the expression for the probability distribution of a magnetic

moment, in equilibrium with its fluctuations, can be written, formally, in one line:

$$P(\boldsymbol{s}) = Z^{-1} e^{-\int dt\, dt' \, \frac{1}{2}\left\{e(\boldsymbol{s})^{-1}\left(\frac{d\boldsymbol{s}}{dt}+\boldsymbol{A}(s)\right)(t) G(t-t') e^{-1}(\boldsymbol{s})\left(\frac{d\boldsymbol{s}}{dt}+\boldsymbol{A}(s)\right)(t')\right\}} \left|\det \frac{\delta \eta_I(t)}{\delta s_J(t')}\right| \tag{2}$$

The challenge is to render this expression meaningful. In practice this is achieved by reconstructing it through its moments, in order to avoid dealing with it explicitly and this thesis focuses on ways of understanding its implications from the moments.

Thus what is finally computed for the magnetization itself refers to the properties of its statistical distribution, which can be encoded in an open hierarchy of ordinary differential equations–for a single spin, partial differential equations for a field–for the moments. For explicit calculations, beyond the Gaussian case, one therefore has to close said hierarchy using appropriate assumptions and methods that can, thus, shed light into understanding the implications of the distribution itself.

This is particularly cogent for magnetic materials, where exceptional breakthroughs in their experimental control have occurred in the last decades.

For instance, experimental studies on magnetic materials involving magnetization switching, magnetic transport and more general spin waves (*i.e.*, magnons) have given birth to a new kind of electronics *i.e.*, Spintronics. Even beyond this, one nowadays hears the term Magnonics more and more often, but these phenomena are most sensitive to coupling effects, different from thermal ones, namely coupling to the mechanical structures of the compounds. Indeed, in addition to thermal effects, experimental studies have revealed that some materials display a striking change in their mechanical properties, when exposed to an electrical field, i.e., piezoelectric effects [5] and similar observations have been made for magnetic materials exposed to a magnetic induction.

This phenomenon is called magnetostriction and other similar names such as magnetoelasticity have also emerged lately. Theoretical models have already been developed and have proven to be quite accurate. However, they mostly focus on the internal energy, which means that they only focus on equilibrium configurations and do not give much insight into fluctuations. This makes it complicated to describe dynamical aspects, related to the evolution of the mechanical structure of the compound system, taking into account how magnetic effects affect mechanical response and vice versa.

One of the objectives in this work is to construct a framework for describing models that can consistently take into account the mechanical deformation of a lattice at the scale of atomistic spin dynamics, by realizing a local description for both fields. This is necessary because, the timescales for the phenomena become very short, as for example in the case of ultrafast demagnetization. Furthermore, the dependence on thermal aspects as well, requires a model which is sensitive to the out of equilibrium fluctuations of these reservoirs. With this in mind, we set up a numerical toolkit for describing a crystal lattice with atomistic spins at each node, and we add a local mechanical deformation for each node as well. The properties of each structure are deduced from other ab initio calculations and experimental data and then the toolkit provides the time evolution for the coupled system.

We begin with an overview of existing techniques (chapter 1), recall the physical concepts necessary for our model. We review precessional models so as to recover damped

spin precession. We then recall the origins of magnetic molecular dynamics and how these have been implemented numerically, using symplectic integration schemes so as to preserve the phase space and the energy of the studied systems. Next, we study atomistic spin dynamics techniques for the study of magnetization dynamics and magnetization curves. We also investigate how to implement thermal effects in these models. The following step is to study how magnetic systems can be coupled to baths and how this leads to either deterministic equations on the moments of the distributions or stochastic equations on the noises. We also investigate how the distributions of these magnetic moments have been tampered with so as to recover quantum properties, especially at low temperatures. We then recall some features of Nambu dynamics and Nambu-Poisson brackets so as to describe spin precession and interesting physical interpretations of the spin phase space in this framework. The next part of this review deals with elasticity and more specifically on its contribution to the energy. Here we also review the coupling between magnetism and elasticity so as to introduce magnetoelasticity. The last part of the review focuses on Grassman – anticommuting – variables and how to describe spin degrees of freedom with it. A brief overview of the emerging coupled dynamics between spatial and spin degrees of freedom is also given.

Our study in proper begins in chapter 2, where we present an alternative method of describing magnetization dynamics, focusing on a single spin, coupled to a collection of spins behaving as a single macroscopic "spin-bath" variable. We call this the "light"-spin, "heavy"-spin model. We define the dynamics for both objects through a set of coupled stochastic equations of motion which we then solve numerically using a symplectic integration scheme. We also build an effective deterministic model for the moments of both statistical distributions from this stochastic system, using several motivated assumptions and then also integrate these so as to compare both dynamics and understand how accurately the stochastic approach can describe expected effects of magnetoelastic coupling. We also want to understand how close the resulting dynamics for both the stochastic and deterministic approaches are, as the deterministic model is quite likely much faster. This work has been published in [7].

We proceed in chapter 3 with the implementation of a Lagrangian approach to magneto-mechanically coupled atomistic spin-dynamics. In this model we introduce a phase space, for describing the state of a magnetic moment and a strain tensor degree of freedom. We show how an interaction Lagrangian for this coupled system can be defined and we obtain the equations of motion and thus, a description of the dynamics. We then generalize this model to multi-particle systems, which are taken to interact through magnetic exchange. We then show how this framework can be used for studying interesting properties of the antiferromagnetic compound NiO. In particular, we study the switching of the Néel order parameter for this system, that is triggered by an external spin transfer torque and the influence of external stress on the switching time and behavior. This work has been published in [9].

We then proceed to a systematic study of the influence of multiplicative vs. additive noise on magnetic systems, in particular, by generalizing Nambu dynamics to dissipative systems and illustrate this in the specific case of dissipative magnetic systems (chapter 4). To this end, we recall how to deduce spin precession from a simple – two-Hamiltonian – Nambu model, before extending this framework to include dissipative terms. We then

identify these terms with usual magnetic dissipation terms such as Landau-Lifshitz-Gilbert damping, so as to interpret dissipating magnetic systems as emerging from dissipative Nambu dynamics. We then introduce fluctuations in both additive and multiplicative fashion in order to evaluate which of these are best suited to describe magnetic fluctuations. This work has been published in [8].

The main study of this thesis is the Hamiltonian approach to magnetoelasticity (chapter 5). In this chapter we start by building the precessional model, by considering the – commuting (*i.e.*, satisfying commutation relations) – spin as a composite variable of two – anticommuting (Grassman) (*i.e.*, satisfying anticommutation relations) – variables, for which we show that we have a precessional algebra. Using this mixed anticommuting/-commuting formalism, we build a Poisson Bracket for the phase space of the spin vector, the strain and the strain-rate tensors. Once this bracket is constructed, we build a Hamiltonian for the coupling of these three objects, so as to deduce equations of motion for their coupled dynamics. Then, as we have done in chapter 1, we extend this single-particle model to multi-particle systems by introducing a magnetic exchange interaction between sites of a lattice, each site carrying its set of the single-particle equations of motion. We then build a numerical integration scheme using a symplectic integrator for the time evolution of the damped precessional motion of each spin for the mechanical – strain and strain-rate – system. We then implement this in our antiferromagnetic NiO compound toy model so as to compare our results. This work has been submitted and is currently under review for the Physical Review B.

Chapter 1

State of the art

Résumé

- Nous étudions l'émergence d'un modèle classique de précession, à partir de la description quantique du spin et comment ce modèle peut être étendu pour décrire des moments magnétiques en précession amortie.
- Nous rappelons les origines de la dynamique moléculaire magnétique et comment celle-ci a été implémentée numériquement en utilisant des schémas d'intégration symplectique.
- Nous faisons un rappel de la méthode de dynamique de spin atomique. Nous rappelons également comment inclure des effets thermiques à ce genre de simulations.
- Nous étudions ensuite comment les systèmes magnétiques peuvent être couplés à des bains (thermiques ou non) puis étudiés, de façon stochastique ou déterministe et comment modifier le couplage au bain(s) pour tenir compte d'effets quantiques à basse température.
- Nous rappelons le formalisme de la dynamique de Nambu et comment celui-ci peut permettre simplement de construire et de comprendre la précession non amortie d'un moment magnétique dans un champ externe.
- Nous nous intéressons ensuite aux effets de l'élasticité d'un composé et au couplage de ceux-ci aux effets magnétiques afin d'introduire la magnétoélasticité.
- Nous étudions finalement la description du spin comme variable – anticommutante – de Majorana et la construction d'une dynamique qui couple les degrés de liberté spatiaux à ceux du spin par ce formalisme.

1.1 Precessional models

Cohen-Tannoudji *et al.* wrote a well–known textbook on quantum mechanics [10]. One section is particularly relevant for understanding models of precession of spinning particles. In the fourth chapter of the first volume, one can find a thorough study of the spin$-\frac{1}{2}$ algebra. The first step is to start with a vector operator $\boldsymbol{S} = (S_x, S_y, S_z)$ in the basis of eigenvectors of S_z, namely $\{|\uparrow\rangle, |\downarrow\rangle\}$ which are the spin up and down – eigenstates. Then a complete set of commuting observables $\boldsymbol{S}^2$ and S_z is chosen with the following eigenvector/eigenvalue equations

$$\begin{cases} S_z|\uparrow\rangle = +\dfrac{\hbar}{2}|\uparrow\rangle \\ S_z|\downarrow\rangle = -\dfrac{\hbar}{2}|\downarrow\rangle \end{cases} \tag{1.1}$$

If an external magnetic field along the z-axis is added, then the Zeeman Hamiltonian reads as follows

$$H = \omega_0 S_z \tag{1.2}$$

where ω_0 is the frequency of the external field also expressed in terms of an external magnetic field B as

$$\omega_0 \equiv \frac{g\mu_B}{\hbar} B \tag{1.3}$$

Here μ_B is the Bohr magneton, $\hbar$ the reduced Planck constant and g the Landé factor.This yields the following eigenvector/eigenvalue for H

$$\begin{cases} H|\uparrow\rangle = \dfrac{\hbar\omega_0}{2}|\uparrow\rangle \\ H|\downarrow\rangle = \dfrac{-\hbar\omega_0}{2}|\downarrow\rangle \end{cases} \tag{1.4}$$

The state vector $|\psi\rangle$ can be expressed in the basis of eigenstates of the spin using polar angles θ and ϕ

$$|\psi\rangle = \cos\left(\frac{\theta}{2}\right)\exp\left(\frac{-i\phi}{2}\right)|\uparrow\rangle + \sin\left(\frac{\theta}{2}\right)\exp\left(\frac{i\phi}{2}\right)|\downarrow\rangle \tag{1.5}$$

The time evolution is formally given through the exponentiation of the Hamiltonian e^{-iHt} which is diagonal in the chosen basis and thus equivalent to the exponentiation of the eigenvalues, which in the Schrödinger picture can be expressed as

$$|\psi(t)\rangle = \cos\left(\frac{\theta}{2}\right)\exp\left(\frac{-i\left(\phi+\omega_0 t\right)}{2}\right)|\uparrow\rangle + \sin\left(\frac{\theta}{2}\right)\exp\left(\frac{i\left(\phi+\omega_0 t\right)}{2}\right)|\downarrow\rangle \tag{1.6}$$

Combining all this in taking the expectation values of the components of $\boldsymbol{S}$ such as $\langle\psi(t)|S_i|\psi(t)\rangle \equiv \langle S_i\rangle$ we get the following system

$$\begin{cases} \langle S_x\rangle = \dfrac{\hbar}{2}\sin(\theta)\cos(\phi+\omega_0 t) \\ \langle S_y\rangle = \dfrac{\hbar}{2}\sin(\theta)\sin(\phi+\omega_0 t) \\ \langle S_z\rangle = \dfrac{\hbar}{2}\cos(\theta) \end{cases} \tag{1.7}$$

which – indeed – is a precession motion in the spin space and, as is implied by Ehrenfest's theorem, the expectation value for the spin operator satisfies the same dynamics as the classical variable. By switching back to the Heisenberg picture, when only the operators are time-dependent, one can express this as

$$\imath\hbar\frac{\partial \boldsymbol{S}}{\partial t} = [H,\boldsymbol{S}] \Rightarrow \imath\hbar\frac{\partial\langle \boldsymbol{S}\rangle}{\partial t} = \langle[H,\boldsymbol{S}]\rangle \tag{1.8}$$

where the notation $\langle\boldsymbol{S}\rangle$ stands for $\langle\psi|\boldsymbol{S}|\psi\rangle$. It is straightforward to show that this, in turn, implies

$$\imath\hbar\frac{\partial \boldsymbol{S}}{\partial t} = \imath\hbar\omega_0\begin{pmatrix} S_y \\ -S_x \\ 0 \end{pmatrix} = \imath\hbar\boldsymbol{S}\times\boldsymbol{\omega} \tag{1.9}$$

where

$$\boldsymbol{\omega} = \omega_0\boldsymbol{z} \tag{1.10}$$

as $\boldsymbol{\omega}$ is independent of $\boldsymbol{S}$ one can indeed deduce from eq. (1.9) the evolution equation for the classical spin $\langle\boldsymbol{S}\rangle$

$$\frac{\partial\langle \boldsymbol{S}\rangle}{\partial t} = \langle\boldsymbol{S}\rangle\times\boldsymbol{\omega} \tag{1.11}$$

This exhibits the quantum "origin" of the precession of magnetization, which yields the Larmor precession eq. (1.11).

However, in the presence of a magnetic field, the magnetization of a magnetic medium does not simply precess, but also relaxes towards the dominant field [11], which implies the presence of additional terms, that should be added to eq. (1.11).

One way of describing the appearance of such terms is by the interaction of the magnetization with external fields, produced by the medium. In addition, it should be stressed that the non-relativistic approximation used above can break down in real materials; however the medium defines a preferred frame and, in this way, it is possible to develop more sophisticated models that take into account such effects, in order to understand the dynamics of real particles carrying –classical– spins (or magnetic moments) in the presence of an external field.

The prototypical example is in the paper by Bargmann *et al.* [12], for investigating the precession of the spin of a point particle in a homogeneous magnetic field in a fully relativistic framework.

They start with the 4-vector $\boldsymbol{S}$, such as

$$\boldsymbol{S} = (s_0, \boldsymbol{s}) \tag{1.12}$$

where $\boldsymbol{s}$ is the classical magnetic moment. In the rest frame of the particle, the time component of such a 4-vector is zero *i.e.*,

$$\boldsymbol{S} = (0, \boldsymbol{s}) \tag{1.13}$$

In addition, a precession equation for the space components of the spin is postulated using the quantum-mechanical equivalent form

$$\frac{d\boldsymbol{s}}{d\tau} = \frac{ge}{2m}\boldsymbol{s} \times \boldsymbol{H} \tag{1.14}$$

where $\boldsymbol{H}$ is the external (magnetic) field, τ is the proper time of the rest frame of the particle, m its mass, e its electric charge and g its Landé factor. They then compute the equations of motion (EOM) in the relativistic case for an arbitrary – moving – frame. They obtain the following expression

$$\frac{d\boldsymbol{S}}{d\tau} = \frac{ge}{2m}\left[\bar{\bar{\boldsymbol{F}}}\boldsymbol{S} + \left(\boldsymbol{S}\bar{\bar{\boldsymbol{F}}}\boldsymbol{u}\right)\boldsymbol{u}\right] - \left[\frac{d\boldsymbol{u}}{d\tau}\boldsymbol{S}\right]\cdot\boldsymbol{u} \tag{1.15}$$

where $\bar{\bar{\boldsymbol{F}}}$ is the electromagnetic tensor, $\boldsymbol{u}$ is the 4-velocity of the moving frame. They then recast their expressions in terms of two unit polarization 4-vectors $\boldsymbol{e}_l$ (longitudinal) and $\boldsymbol{e}_t$ (transverse)–with respect to the external field–in the laboratory frame, as

$$\frac{\boldsymbol{S}}{\sqrt{-\boldsymbol{S}\cdot\boldsymbol{S}}} = \boldsymbol{e}_l\cos(\phi) + \boldsymbol{e}_t\sin(\phi) \tag{1.16}$$

where

$$\begin{cases} \boldsymbol{e}_l &= \gamma\left(v, \dfrac{\boldsymbol{v}}{v}\right) \\ \boldsymbol{e}_t &= (0, \boldsymbol{n}) \end{cases} \tag{1.17}$$

such that $\boldsymbol{n}.\boldsymbol{n} = 1$ and $\boldsymbol{n}.\boldsymbol{v} = 0$. Here, γ is the Lorentz factor, and v the relative velocity. In this description, they define the rate $\Omega = \frac{d\phi}{dt} = \frac{d\phi}{\gamma d\tau}$ at which longitudinal polarization is transformed into transverse polarization. They obtain the following expression

$$\Omega = \frac{e}{m}\left\{\boldsymbol{E}\cdot\frac{\boldsymbol{n}}{v}\left[\left(\frac{g}{2}-1\right) - \frac{g}{2\gamma^2}\right] + \left(\frac{\boldsymbol{v}}{v}\cdot(\boldsymbol{H}\times\boldsymbol{n})\right)\left(\frac{g}{2}-1\right)\right\} \tag{1.18}$$

where $\boldsymbol{E}$ is the electric field. In usual terms, the fact that transverse polarization is transformed into longitudinal polarization can be understood as the relaxation of the polarization towards the "longitudinal axis" *i.e.* damping. More detailed calculations, describing the significance of this effect for the dynamics of the classical magnetic moment in the laboratory frame for a relativistic magnetic moment can be found in [13] as well as in the textbook [14]. Even though the interpretation of this term is not straightforward, it already provides a first hint towards identifying damping in magnetic systems. The origin of this term is, however, due to relativistic effects, and although this can be relevant for some magnetic moments, for example close to the Fermi surface [15], this is not the only

plausible "fundamental" way to understand damping in magnetic materials. We shall thus investigate a different formulation of dissipation in magnetic systems through a Lagrangian approach, in which it is possible to investigate relativistic and non-relativistic effects in a unified way. This approach has the advantage of computational ease, as well as conceptual clarity.

In 2011, Bose *et al.* [16] considered a Lagrangian formulation for dissipative magnetic systems. Their approach follows the idea of a classical magnetic system, described by $\boldsymbol{m}$, whose phase space is enlarged by bath variables – of undefined origin – $\boldsymbol{\sigma}$. They start by presenting symmetry arguments enabling them to construct the following Lagrangian density

$$\mathcal{L}[\boldsymbol{m}, \dot{\boldsymbol{m}}, \nabla\boldsymbol{m}; \boldsymbol{\sigma}, \nabla\boldsymbol{\sigma}] = \mathcal{L}^{(m)}[\boldsymbol{m}, \dot{\boldsymbol{m}}, \nabla\boldsymbol{m}] + \mathcal{L}^{(\sigma)}[\nabla\boldsymbol{\sigma}] + \mathcal{L}^{(m\sigma)}[\dot{\boldsymbol{m}}, \nabla\boldsymbol{m}; \boldsymbol{\sigma}, \nabla\boldsymbol{\sigma}] \tag{1.19}$$

that comprises three terms, respectively the magnetic term, the (vector)bath term, and the coupling term.

$$\begin{cases} \mathcal{L}^{(m)} = \dfrac{1}{2} J^{(m)}_{\alpha\beta} \dfrac{\partial m_\nu}{\partial x_\alpha} \dfrac{\partial m_\nu}{\partial x_\beta} + A_\nu(\boldsymbol{m})\dot{m}_\nu \\ \mathcal{L}^{(\sigma)} = \dfrac{1}{2} J^{(\sigma)}_{\alpha\beta} \dfrac{\partial \sigma_\nu}{\partial x_\alpha} \dfrac{\partial \sigma_\nu}{\partial x_\beta} \\ \mathcal{L}^{(m\sigma)} = J^{(m\sigma)}_{\alpha\beta} \dfrac{\partial m_\nu}{\partial x_\alpha} \dfrac{\partial \sigma_\nu}{\partial x_\beta} + B_\nu(\boldsymbol{\sigma})\dot{m}_\nu \end{cases} \tag{1.20}$$

where $J^{(m)}_{\alpha\beta}$ is the magnetic exchange coupling, $J^{(\sigma)}_{\alpha\beta}$ is the coupling within the bath and $J^{(m\sigma)}_{\alpha\beta}$ is the coupling between the magnetic and bath degrees of freedom. In the isotropic case, all these are diagonal matrices. $\boldsymbol{A}$ and $\boldsymbol{B}$ are vector potentials for the couplings which imply that $\mathcal{L}^{(m)}$ and $\mathcal{L}^{(m\sigma)}$ are not gauge fixed. Furthermore, they assume that small, local, variations of the bath are related to small variations of the magnetization *i.e.*, $\delta\sigma_\beta = -\kappa\delta m_\beta$, $\kappa > 0$. By taking

$$\begin{cases} B_\nu &= -c\sigma_\nu \\ J_{\alpha\beta} &= J\delta_{\alpha\beta} \end{cases} \tag{1.21}$$

time-reversal symmetry is broken, thus leading to a net flow (in phase space). They then deduce the equations of motion as constrained Euler-Lagrange equations. They end up with the following expression for the magnetization dynamics

$$\frac{\partial \boldsymbol{m}}{\partial t} = \frac{1}{g}(\boldsymbol{m} \times \boldsymbol{H}_{\text{eff}}) - \frac{\kappa c}{g}\left(\boldsymbol{m} \times \frac{\partial \boldsymbol{m}}{\partial t}\right) \tag{1.22}$$

where one has

$$\begin{cases} g = \dfrac{-1}{\gamma} \\ \dfrac{\kappa c}{g} = -\alpha \end{cases} \tag{1.23}$$

and

$$\boldsymbol{H}_{\text{eff}} = (J^{(m)} - \kappa J^{(m\sigma)})\boldsymbol{\Delta m} - c\dot{\boldsymbol{\sigma}} + (J^{(m\sigma)} - \kappa J^{(\sigma)})\boldsymbol{\Delta\sigma} \tag{1.24}$$

Here γ is the gyromagnetic ration and α the Gilbert damping parameter. As one can notice, this is very similar to the LLG [17] equation which reads

$$\dot{\boldsymbol{m}} = \gamma \boldsymbol{B} \times \boldsymbol{m} + \alpha \boldsymbol{m} \times \dot{\boldsymbol{m}} \tag{1.25}$$

where $\boldsymbol{B}$ is the magnetic field.

The formalisms described in this chapter are, however, intended to describe either single particles, as for example a single electron of spin ½, or domains which can be considered as single isolated magnetic moments in a magnetic field. What is also interesting to notice is that in the last part of this section, the "microscopic" degrees of freedom, that make up the bath itself remain undefined. There have been attempts to exploit similar models with thermal baths described by a collection of harmonic oscillators [18]. However, in many cases, such descriptions are insufficient, since they neglect the back reaction of, either a collection of magnetic moments, or of magnetic moments, interacting with the medium in which they are embedded. In the next section, we will thus investigate how one can describe the coupled evolution of a collection of moving magnetic moments using the framework of magnetic molecular dynamics.

1.2 Magnetic molecular dynamics

In 1980 Yang *et al.* [19] and Ruijgrok *et al.* [20], independently, published papers, in which they investigated generalizations of Poisson brackets that include spin variables. [1]

They begin by recalling the equations of motion, which can be deduced from the Breit-Pauli Hamiltonian $\mathcal{H}$,

$$\frac{d\boldsymbol{s}_j}{dt} = -\boldsymbol{s}_j \times \frac{\partial \mathcal{H}}{\partial \boldsymbol{s}_j} \tag{1.26}$$

where $\mathcal{H}$ is a function of positions $\{\boldsymbol{r}_j\}$, conjugate momenta $\{\boldsymbol{p}_j\}$ and spins $\{\boldsymbol{s}_j\}$. These equations are canonical, since the Hamiltonian structure is preserved *i.e.*,

$$\begin{cases} \dfrac{\partial \mathcal{H}}{\partial \boldsymbol{p}_j} = \dfrac{d\boldsymbol{r}_j}{dt} \\ \dfrac{\partial \mathcal{H}}{\partial \boldsymbol{r}_j} = -\dfrac{d\boldsymbol{p}_j}{dt} \end{cases} \tag{1.27}$$

Applying the chain rule for the time derivative of $\mathcal{H}$ to positions $\boldsymbol{q}_j$, momenta $\boldsymbol{p}_j$ and spin variables $\boldsymbol{s}_j$, they find that

$$\frac{d\mathcal{H}}{dt} = \frac{\partial \mathcal{H}}{\partial t} + \sum_j \left(\frac{d\boldsymbol{p}_j}{dt} \cdot \frac{\partial \mathcal{H}}{\partial \boldsymbol{p}_j} + \frac{d\boldsymbol{r}_j}{dt} \cdot \frac{\partial \mathcal{H}}{\partial \boldsymbol{r}_j} + \frac{d\boldsymbol{s}_j}{dt} \cdot \frac{\partial \mathcal{H}}{\partial \boldsymbol{s}_j} \right) \tag{1.28}$$

Because $\mathcal{H}$ does not explicitly depend on time, their expression for the "extended" Poisson bracket, which includes spin, reads as follows

$$\{f, g\} = \sum_j \left(\frac{\partial f}{\partial \boldsymbol{r}_j} \cdot \frac{\partial g}{\partial \boldsymbol{p}_j} - \frac{\partial f}{\partial \boldsymbol{p}_j} \cdot \frac{\partial g}{\partial \boldsymbol{r}_j} + \boldsymbol{s}_j \cdot \left(\frac{\partial f}{\partial \boldsymbol{s}_j} \times \frac{\partial g}{\partial \boldsymbol{s}_j} \right) \right) \tag{1.29}$$

[1] Their approach is quite different from that of Casalbuoni [21] Berezin and Marinov [22] or Brink et al. [23]. Their approach shall be reviewed in section 1.7

for solutions of the equations of motion (1.26).

Moreover, they show that this bracket satisfies all the properties of a Lie bracket:

$$\begin{array}{lll} \{f,g\} = -\{g,f\} & & \text{(Antisymmetry)} \\ \{af+bg,h\} = a\{f,h\} + b\{g,h\} & \forall a,b \in \mathbb{R} & \text{(Bilinearity)} \\ \{hf,g\} = h\{f,g\} + \{h,g\}f & & \text{(Leinbiz rule)} \\ \{f,\{g,h\}\} + \{h,\{f,g\}\} + \{g,\{h,f\}\} = 0 & & \text{(Jacobi identity)} \end{array} \tag{1.30}$$

Therefore the equations of motion can be expressed as

$$\begin{cases} \dfrac{d\boldsymbol{r}_j}{dt} = \{\boldsymbol{r}_j, \mathcal{H}\} \\ \dfrac{d\boldsymbol{p}_j}{dt} = \{\boldsymbol{p}_j, \mathcal{H}\} \\ \dfrac{d\boldsymbol{s}_j}{dt} = \{\boldsymbol{s}_j, \mathcal{H}\} \end{cases} \tag{1.31}$$

and they preserve the volume in the extended phase space *i.e.*,

$$\sum_{I,j} \frac{\partial \dot{s}_j^I}{\partial s_j^I} + \frac{\partial \dot{r}_j^I}{\partial r_j^I} + \frac{\partial \dot{p}_j^I}{\partial p_j^I} = 0 \tag{1.32}$$

where the upper indices stand for the components of each variable and the lower indices are labels for the different sites. This bracket is the foundation for what later turned into magnetic molecular dynamics (MMD), where the phase space of molecular dynamics is extended by the spin variables and hence leads to a way to describe the interaction between mechanical and magnetic degrees of freedom. The Hamiltonian, that describes the dynamics need not be of Breit-Pauli type, of course.

The next step was thus to study specific magnetic systems – numerically – through this approach. For this, efficient and consistent integration schemes are required.

These were developed by Beaujouan *et al.* [24] for the study of thermally induced dynamics of a Cobalt nanowire on a (111)Pt substrate. They describe their approach as an effective model in which magnetic moments, moving through an "active" medium, interact with each other through magnetic exchange. In order to take into account the back reaction of the medium, they supplement their description by effective anisotropy terms, which also allow them to account for magnetostrictive effects. In order to describe the dynamics of their system, they use the following Hamiltonian

$$\begin{aligned} \mathcal{H} = &\sum_{i=1}^{N} \frac{||\boldsymbol{p}_i||^2}{2m_i} + \sum_{i<j}^{N} \left(V(r_{ij}) - J(r_{ij})\boldsymbol{s}_i \cdot \boldsymbol{s}_j - K(r_{ij})\left[(\hat{r}_{ij} \cdot \boldsymbol{s}_i)(\hat{r}_{ij} \cdot \boldsymbol{s}_j)\right]\right) \\ &+ \sum_{i<j}^{N} \left(-\frac{1}{3}(\boldsymbol{s}_i \cdot \boldsymbol{s}_j) + \boldsymbol{D}(r_{ij}) \cdot (\boldsymbol{s}_i \times \boldsymbol{s}_j)\right) - g\mu_B\mu_0 \boldsymbol{H}_{\text{ext}} \cdot \sum_{i=1}^{N} \boldsymbol{s}_i \end{aligned} \tag{1.33}$$

where, $V(r_{ij})$ is a potential term, r_{ij} is the distance–in the medium–between particles i and j, $\hat{r}_{ij}$ is the corresponding unit vector, $K(r_{ij})$ is the diagonal exchange interaction

and $\boldsymbol{D}(r_{ij})$ is the Dzyaloshinskii-Moriya vector. They take a Bethe-Slater form for the isotropic exchange function $J(r_{ij})$ such that

$$J(r_{ij}) = -4\varepsilon\left(-\frac{r^2}{\sigma^2} + \delta\frac{r^4}{\sigma^4}\right)\exp\left(-\frac{r^2}{\sigma^2}\right)\Theta(R_c - r_{ij}) \tag{1.34}$$

where R_c is a cutoff scale, taken up to second and third nearest neighbors, which has to be parametrized properly, using *ab initio* calculations. They use the expression for the Poisson bracket eq. (1.29) to derive the equations of motion (EOM) for $\{\boldsymbol{r}_i(t), \boldsymbol{p}_i(t), \boldsymbol{s}_i(t)\}$ from their Hamiltonian eq. (1.33). They then focus on how to solve these EOM numerically by implementing a symplectic/geometric integration scheme: For any function $\rho \equiv \rho(t)$

$$\frac{d\rho(t)}{dt} = \{\rho(t), \mathcal{H}\} \equiv (L_r + L_p + L_s)\rho(t) \tag{1.35}$$

where the corresponding time evolution operators L_r, L_p and L_s are

$$L_r = \sum_{i=1}^{N} \frac{d\boldsymbol{r}_i}{dt}\cdot\frac{\partial}{\partial \boldsymbol{r}_i}, \quad L_p = \sum_{i=1}^{N} \frac{d\boldsymbol{p}_i}{dt}\cdot\frac{\partial}{\partial \boldsymbol{p}_i} \quad \text{and} \quad L_s = \sum_{i=1}^{N} \frac{d\boldsymbol{s}_i}{dt}\cdot\frac{\partial}{\partial \boldsymbol{s}_i} \tag{1.36}$$

One can formally find a solution for the time evolution of $\rho(t)$ starting from an initial condition $\rho(0)$ such that

$$\rho(\tau) = \exp\left[\tau(L_s + L_r + L_p)\right]\rho(0) \tag{1.37}$$

which is approximated by the Suzuki-Trotter (ST) decomposition

$$\exp\left[\tau(L_s + L_r + L_p)\right] = \exp\left(\frac{\tau}{2}L_p\right)\exp\left(\frac{\tau}{2}L_r\right)\exp(\tau L_s)\exp\left(\frac{\tau}{2}L_r\right)\exp\left(\frac{\tau}{2}L_p\right) + \mathcal{O}(\tau^3) \tag{1.38}$$

Moreover, the time evolution operators satisfy $\exp(\tau L_r) = \prod_{i=1}^{N}\exp(\tau L_{r_i})$ and $\exp(\tau L_p) = \prod_{i=1}^{N}\exp(\tau L_{p_i})$. This is not true for the spins, however, thus a ST decomposition up to the same order is also considered for $\exp(\tau L_s)$ *i.e.*,

$$\exp(\tau L_s) = \exp\left(\frac{\tau}{2}L_{s_1}\right)\ldots\exp\left(\frac{\tau}{2}L_{s_{N-1}}\right)\exp\left(\tau L_{s_N}\right)\exp\left(\frac{\tau}{2}L_{s_{N-1}}\right)\ldots\exp\left(\frac{\tau}{2}L_{s_1}\right) + \mathcal{O}(\tau^3) \tag{1.39}$$

This enables the construction of a robust integration algorithm which preserves the phase space volume and structure of the equation hence minimizing the propagated error. This formalism enabled them to simulate Cobalt nanowires, and obtain magnetization curves for different structures, hence demonstrating the usefulness of this approach.

Recent implementations of similar approaches [25] have been shown to properly describe the spin-orbit coupling, due to the coupling between the atomic and electronic subsystems and symmetry breaking due to phonons and defects. Indeed, as both subsystems can exchange angular momentum, this formalism is required, in order to correctly capture the fluctuations and nonequilibrium processes, that are of interest in magnetic materials. In addition, structural phase transitions in Fe have been shown to be captured by such an approach [26]. One issue, however, is that the strength of the interactions is encoded in the distances between the particles which makes approximation schemes, such as

the "Verlet-radius choice" for nearest neighbors difficult to apply and computationally less efficient. More generally, this approach is difficult to scale up to large – supra-nanoscopic – systems, even though there are attempts to adapt these methods in such a fashion that they can be scaled up to much larger systems, for example by developing parallelization algorithms which highly enhance its efficiency [27].

1.3 Atomistic spin dynamics

In 2008, Skubic *et al.* [28] presented a method for performing atomistic spin dynamics and showed how it could be implemented computationally. This method is inspired by previous implementations of *ab initio* approaches [29] for constructing the equations of motion for the dynamics of spin systems from general principles.

The first step is to use the Born-Oppenheimer approximation, which disentangles the atomistic spins (slow) from the electronic motion (fast); this amounts to solving the equations of motion (EOM) for both systems separately. The starting point is the dynamical evolution of the quantum spin operator $\hat{\boldsymbol{S}}$, given by

$$\frac{\partial \hat{\boldsymbol{S}}}{\partial t} = \frac{1}{\imath\hbar}[\hat{\boldsymbol{S}}, \mathcal{H}_{KS}] \tag{1.40}$$

where $\mathcal{H}_{KS}$ is the Kohn-Sham Hamiltonian of density functional theory. They show that this yields the following EOM of the spin moment $\boldsymbol{S}_i$ (expectation value) where i labels each atom of the atomistic simulation.

$$\frac{\partial \boldsymbol{S}_i}{\partial t} = -\gamma \boldsymbol{S}_i(t) \times \boldsymbol{B}_i \tag{1.41}$$

$\boldsymbol{B}_i$ being some effective field at site i and γ the gyromagnetic ratio. They define the relation between field and frequency by the *Ansatz*

$$\boldsymbol{B}_i = \frac{\partial \mathcal{H}}{\partial \boldsymbol{S}_i} \tag{1.42}$$

where $\mathcal{H}$ is a Hamiltonian, that consists of standard terms

$$\mathcal{H} = \mathcal{H}_{\text{iex}} + \mathcal{H}_{\text{ma}} + \mathcal{H}_{\text{dd}} + \mathcal{H}_{\text{ext}} \tag{1.43}$$

describing, namely, interatomic exchange (Heisenberg), magnetic anisotropy (uniaxial), dipolar interactions and the Zeeman term for interaction with the external magnetic field. Finally, they add a phenomenologically motivated damping term, consistent with the Landau-Lifshitz form, in order to take into account energy and angular momentum dissipation, without providing, however, too much detail on why this particular term is introduced

$$\frac{\partial \boldsymbol{S_i}}{\partial t} = -\gamma \boldsymbol{S}_i \times \boldsymbol{B}_i - \gamma \frac{\alpha}{S} [\boldsymbol{S}_i \times [\boldsymbol{S}_i \times \boldsymbol{B}_i]] \tag{1.44}$$

where S is the norm of the spin and α the damping parameter.

The fluctuation dissipation theorem implies relations between the dissipative processes of a physical system and the fluctuations of the corresponding degrees of freedom. Such relations can be illustrated when discussing thermal fluctuations.

In the case at hand, three thermal reservoirs are introduced, corresponding, to the electronic, the lattice and the spin degrees of freedom; the corresponding characteristic timescales are given in Figure 1.1.

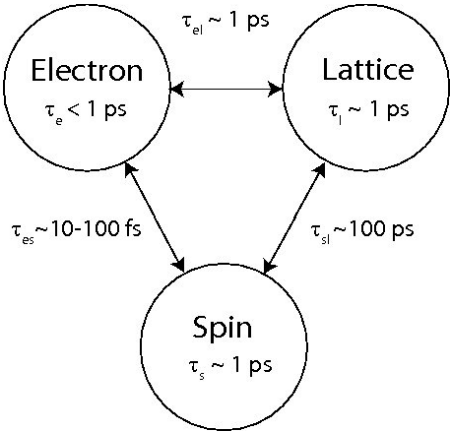

Figure 1.1: Characteristic interaction and relaxation timescales for thermodynamic electron, lattice and spin reservoirs

Following [30], thermal effects can be taken into account by using a stochastic formulation through a vector bath variable $\boldsymbol{b}_i$ drawn from a Gaussian stochastic process such that

$$\langle b_{i,\mu}(t)\rangle = 0, \quad \langle b_{i,\mu}(t) b_{j,\nu}(s)\rangle = 2D\delta_{ij}\delta_{\mu\nu}\delta(t-s) \tag{1.45}$$

where the expression for D is given through the fluctuation dissipation theorem (as discussed in the appendix of the paper, which describes calculations using the Langevin formalism and Fokker-Planck equation, which spell out the relation between D and the temperature T). Now taking into account the scales of the different relaxation times, namely that one only needs to distinguish the dynamics for the lattice and the electronic system when timescales are significantly below picoseconds, it is possible to deduce the EOM at finite temperature

$$\begin{aligned}\frac{\partial \boldsymbol{S}_i}{\partial t} &= -\gamma \boldsymbol{S}_i \times [\boldsymbol{B}_i + \boldsymbol{b}_i(t)] \\ &- \gamma \frac{\alpha_e}{S} \boldsymbol{S}_i \times [\boldsymbol{S}_i \times [\boldsymbol{B}_i + \boldsymbol{b}_i(t)]] \\ &- \gamma \frac{\alpha_l}{S} \boldsymbol{S}_i \times [\boldsymbol{S}_i \times [\boldsymbol{B}_i + \boldsymbol{b}_i(t)]]\end{aligned} \tag{1.46}$$

where α_e is the electronic damping parameter and α_l is the lattice damping parameter. It is, thus, possible to extract information for specific systems from atomistic spin dynamics simulations, namely, from phase space trajectories, magnetization curves, correlations between magnetic moments and energy distributions. This method is also applied for the description of the magnetic switching of bcc Fe under strong magnetic fields, where previous macrospin approaches are not sufficient for obtaining accurate results, because

the emergence of spin wave instabilities alters the macrospin size, especially for large anisotropy. This approach is, however, inconsistent when trying to reproduce low – much below Curie – temperature effects, as it has been shown [31] not to reproduce the experimental "plateau" for magnetization curves at very low temperatures, that can be taken to be $T = 0\,K$ in the simulations.

In 2015, Evans *et al.* [32] also used atomistic spin dynamics to investigate temperature dependent properties. They begin by imposing the usual constraints of atomistic spin dynamics namely

$$\boldsymbol{S}_i = \mu_s \boldsymbol{s}_i \quad \text{and} \quad |\boldsymbol{s}_i| = 1 \tag{1.47}$$

where μ_s is the magnetic moment, and quickly focus on how to reproduce low temperature – quantum – effects as in this kind of scheme, basically any spin orientation is possible, whereas quantum mechanics is drastically less permissive. One consequence is that the statistical laws behave very differently. For low temperature, the classical magnetization satisfies

$$m_c(T) \approx 1 - \frac{1}{3}\frac{T}{T_c}, \tag{1.48}$$

where

$$m_c = \frac{M(T)}{M(0)} \tag{1.49}$$

with M the magnetization and T_C the Curie temperature. The quantum law, which is more accurate for low temperatures, yields

$$m_q(T) = 1 - \frac{1}{3} s \left(\frac{T}{T_c}\right)^{3/2} \tag{1.50}$$

where s is a slope factor given by

$$s = S^{1/2}(2\pi W)^{-3/2}\zeta\left(\frac{3}{2}\right) \tag{1.51}$$

with S being the spin quantum number, $\zeta(x)$ is the Riemann ζ function and W is a Watson integral. For the whole range of T, up to T_C, they propose the following rescaling for the magnetization depending on $\tau = \frac{T}{T_c}$

$$m(\tau) = (1 - \tau^{\alpha})^{\beta} \tag{1.52}$$

where $\beta \approx 1/3$ is the critical exponent and α is a single empirical constant used for better fitting. Typical values for α are 2.37 for Co and 2.32 for Ni. In order to check the magnetization curves, they compare them to those obtained from another rescaling model by Kuz'min [33] given by

$$m(\tau) = \left[1 - s\tau^{3/2} - (1 - s)\tau^{p}\right]^{\beta} \tag{1.53}$$

Next they carry out simulations for Co, Fe, Ni and Gd using a nearest neighbor exchange model. They show that indeed, their model is able to predict the correct magnetization curves, as the model which was developed by Kuz'min, but with fewer parameters, hence a more effective fit. They also show how to use this model in practice to fit the α parameter.

They end by performing a more elaborate simulation, that involves coupling the electron and the lattice thermodynamic reservoirs to the spin reservoir in order to predict the correct demagnetization curves for Ni, shown in Figure 1.2, where the EOM for each spin site is the stochastic Landau-Lifshitz-Gilbert equation

$$\frac{\partial \boldsymbol{S}_i}{\partial t} = -\frac{\gamma_e}{1+\lambda^2}\left[\boldsymbol{S}_i \times \boldsymbol{H}^i_{\text{eff}} + \lambda \boldsymbol{S}_i \times \left(\boldsymbol{S}_i \times \boldsymbol{H}^i_{\text{eff}}\right)\right] \tag{1.54}$$

Here λ is the Gilbert damping factor, $\boldsymbol{H}$ the magnetic field and γ_e the gyromagnetic ratio. In their framework, the time evolution for the electronic T_e^{exp} and the lattice T_l^{exp} temperatures are given by a 2-temperature model

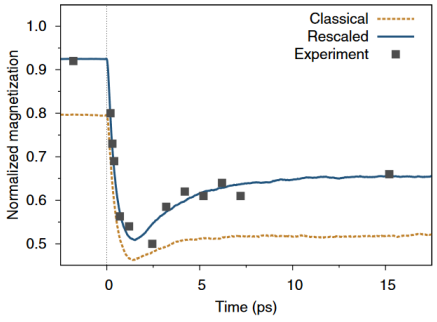

Figure 1.2: Demagnetization of Ni : classical vs. rescaled thermostat

$$\begin{cases} C_e \dfrac{\partial T_e^{\text{exp}}}{\partial t} = -G(T_e^{\text{exp}} - T_l^{\text{exp}}) + \phi(t) \\ C_l \dfrac{\partial T_l^{\text{exp}}}{\partial t} = -G(T_l^{\text{exp}} - T_e^{\text{exp}}) \end{cases} \tag{1.55}$$

where $\phi(t)$ is a time-dependent Gaussian light pulse, C_e the specific heat for the electronic system, G is the electron-lattice coupling constant and C_l the specific heat of the lattice. They show that indeed their rescaled model is in better agreement with experimental data than the classical atomistic spin dynamics simulation.

In this context, one can explore finite temperature effects for spin dynamics simulations in a deterministic fashion. There are however different approaches to the implementation of these in which the coupling to thermal degrees of freedom is realized by stochastic noises, defined by bath variables [34]. Whereas the deterministic models imply either that one builds effective 2 or even 3-temperature models [35] for each subsystem's reservoir to properly describe the dynamics or that one focuses rather on the equilibrium magnetization than the actual approach to it; the stochastic models allow for a more natural definition of the temperature through fluctuation-dissipation relations, and also, they make it possible to follow the actual time evolution of the spin dynamics, modified by the coupling to thermal reservoirs, as we shall see in the next section.

1.4 Noisy dynamics

In 2012, Thibaudeau *et al.* [36] published an article in which they investigated forced thermalization of a spin system in an extended phase space, whose symmetry is deliberately broken, in order to simulate overdamped spin dynamics. Their starting point is a Hamiltonian, which includes only a Heisenberg exchange term. Their formulation leads to the following equations of motion for each spin on sites i of a regular lattice

$$\dot{s}_i = \{s_i, \mathcal{H}\} = G_{ij}\left(s_k\right)\omega_j\left(s_k\right) \tag{1.56}$$

where $G_{ij} = C_{ijk}s_k$ is an antisymmetric Poisson tensor.

They, then, couple their model to a heat bath through a function $g(\zeta)$, where ζ is a pseudo friction term or "demon", such that

$$\dot{s}_i = G_{ij}\left(s_k\right)\left(\omega_j\left(s_k\right) - g(\zeta)A_j\right) \tag{1.57}$$

since this equation cannot be recast in Hamiltonian form by a redefinition of variables. Here $\boldsymbol{A}$ is a vector field through which the coupling is achieved.

It is straightforward to generalize this expression to any number of such friction terms and if $g(\zeta)$ is constant in time, one recovers the Landau-Lifshitz form [37]. They then introduce a canonical probability distribution that describes the new ensemble

$$f(\{s_i\}, \zeta) = f_0 \exp\left(-\beta\mathcal{H} - \mathcal{G}(\zeta)\right) \tag{1.58}$$

and they derive equations of motion for the bath variable ζ, which enables them to recover, at equilibrium ($i.e$ when $\dot{\zeta} = 0$), the expected spin temperature

$$T_s = \frac{\hbar\left(\omega_i\omega_i - \left(\omega_l s_l\right)^2\right)}{3k_b\omega_j s_j} \tag{1.59}$$

Once this is established, they focus on building a symplectic numerical scheme to integrate their equations of motion. In particular they derive an exact expression for the precession of a single spin around a fixed axis $\boldsymbol{\omega}$, such that $||\boldsymbol{\omega}|| = \omega$, depending on the bath realization.

$$\boldsymbol{s}(t) = A(t)\boldsymbol{s}(0) + B(t)\frac{\boldsymbol{\omega}}{\omega} + C(t)\boldsymbol{s}(0) \times \frac{\boldsymbol{\omega}}{\omega} \tag{1.60}$$

where

$$\begin{cases} A(t) = \dfrac{2\cos(\omega t)\exp(-\zeta\omega t)}{1 + \exp(-2\zeta\omega t) + \chi(1 - \exp(-2\zeta\omega t))} \\ B(t) = \dfrac{1 - \exp(-2\zeta\omega t) + \chi(1 + \exp(-2\zeta\omega t)) - 2\chi\cos(\omega t)\exp(-\zeta\omega t)}{1 + \exp(-2\zeta\omega t) + \chi(1 - \exp(-2\zeta\omega t))} \\ C(t) = \dfrac{2\sin(\omega t)\exp(-\zeta\omega t)}{1 + \exp(-2\zeta\omega t) + \chi(1 - \exp(-2\zeta\omega t))} \end{cases} \tag{1.61}$$

and $\chi = \boldsymbol{s}(0) \cdot \frac{\boldsymbol{\omega}}{\omega}$. By introducing a second bath variable and hence building a chain of thermostats, they show that this procedure is a fast alternative to previous methods in determining thermal equilibrium solutions. An issue of this method is that it "fakes" quicker

dynamics in order to fall into an energy well, hence only focusing on the "destination" and not on the "journey". An alternative which preserves the averaged path of the dynamics for the spin variables is to study the moments of the distribution so as to build an effective – deterministic – model for the dynamics of the stochastic variables.

Later, Tranchida *et al.* [38] considered stochastic magnetization dynamics through an effective – deterministic – approach. They begin with the standard damped precession equation in the form of the Landau-Lifshitz-Gilbert equation (cast in the Landau-Lifshitz form)

$$\frac{\partial s_i}{\partial t} = \frac{1}{1+\lambda^2}\epsilon_{ijk}\left[\omega_j + \tilde{\omega}_j - \lambda\epsilon_{jlm}\omega_l s_m\right] s_k \tag{1.62}$$

where $\tilde{\omega}_j$ are the components of a stochastic Ornstein-Uhlenbeck noise distribution satisfying

$$\langle\tilde{\omega}_i(t)\tilde{\omega}_j(t')\rangle = \frac{D}{\tau}\delta_{ij}\exp\left(-\frac{|t-t'|}{\tau}\right) \tag{1.63}$$

to get from the stochastic system eq. (1.62) to a deterministic hierarchy of moments

$$\begin{cases} \dfrac{\partial\langle s_i\rangle}{\partial t} = \dfrac{1}{1+\lambda^2}\epsilon_{ijk}\left[\omega_j\langle s_k\rangle + \langle\tilde{\omega}_j s_k\rangle - \lambda\epsilon_{jlm}\omega_l\langle s_m s_k\rangle\right] \\ \dfrac{\partial\langle s_i s_j\rangle}{\partial t} = \dfrac{1}{1+\lambda^2}\epsilon_{jkl}\left(\omega_k\langle s_i s_l\rangle + \langle\tilde{\omega}_k s_i s_l\rangle - \lambda\epsilon_{lmn}\omega_m\langle s_i s_l s_n\rangle\right) + (i \leftrightarrow j) \\ \qquad \dots \end{cases} \tag{1.64}$$

and they take advantage of the noise distribution to use the Shapiro-Loginov formula [39] to express mixed moments between the noise and the spin components such that

$$\frac{\partial\tilde{\omega}_i s_j}{\partial t} = \langle\tilde{\omega}_i\frac{\partial s_j}{\partial t}\rangle - \frac{1}{\tau}\langle\tilde{\omega}_i s_j\rangle \tag{1.65}$$

Assuming that the third order cumulants vanish (Gaussian closing [40]) it is possible to close the hierarchy eq. (1.64) and a deterministic system on the first and second-order moments of the spin distribution is obtained. This system is integrated numerically and compared to the stochastic integration of eq. (1.62). All this enables them to construct a deterministic model which amounts to the Landau-Lifshitz-Bloch [41] equation, without the need for imposing a longitudinal dissipation term *ad-hoc*. On top of this, this framework enables the study of effects of colored noise distributions on magnetic systems in a manner which is independent of the number of realizations of the noise and thus is significantly faster for resolving the properties of the statistical distribution of the magnetic system. The limitations, which are highlighted by the authors, amount to the Gaussian closure, in particular whether the distribution does become Gaussian at long times.

A further issue is that this closure assumption leads to the conclusion that the average value satisfy the classical equations of motion, which at low temperature is expected to break down anyway, since it amounts to neglecting quantum correlations, arising from the intrinsic quantum nature of magnetic properties. Such properties are usefully described in terms of magnons, when these can be resolved.

Coherent superpositions of magnons (*i.e.*, spin waves) are typical excitations of magnetic materials [42]. At low occupation number, the individual magnons can be resolved and their statistical distribution becomes relevant.

According to the Holstein-Primakoff representation, their statistical distribution is of Bose-Einstein form (see [43] for a thorough review on this subject).

However it is possible to describe them in terms of an effective angular momentum algebra. In terms of this algebra, the statistic distribution is, in fact "intermediate", an example of anyons, cf. [44].

The Bose–Einstein distribution was used by Woo *et al.* [31] in order to study the effects of the noise field at low temperatures, with the aim of improving the simulations for the behavior of magnetic materials, below the Curie point. After a brief review on noisy spin-lattice dynamics and temperature dependence of phonons and magnons, a modified quantum fluctuation-dissipation relation (QFDR) for the lattice is computed. The kinetic energy is found to be given by the expression $\langle E_k \rangle = \frac{3N\eta_l}{2}$ where $\eta_L(T)$ is given by the expression

$$\eta_L(T) = \int_0^\infty \hbar\omega \left[\frac{1}{e^{\hbar\omega/k_B T} - 1} + \frac{1}{2} \right] g_P(\omega, T) d\omega \tag{1.66}$$

and the phonon density of states (DOS) is of the form

$$g_P(\omega(\boldsymbol{k}), T) = \frac{4\pi k^2 \Omega}{(2\pi)^3} \left[\nabla_{\boldsymbol{k}} \omega(T) \right]^{-1} \tag{1.67}$$

$\hbar$ is the reduced Planck constant, N the number of particles, ω the frequency, k_B the Boltzmann constant, k stands for the k^{th} mode, Ω is the atomic volume. A similar expression holds for the spin part, where $\langle E \rangle = N\eta_S - \frac{1}{2} N H_0 S$,

$$\eta_S(T) = \int_0^\infty \frac{\hbar\omega}{e^{\hbar\omega/k_B T} - 1} g_m(\omega, T) d\omega \tag{1.68}$$

and the magnon DOS is given by

$$g_m(\omega, T) = \frac{\Omega}{(2\pi)^3} \frac{4\pi k^2}{\nabla_k \omega(T)} \tag{1.69}$$

This enables them to study specific cases such as Debye crystals or other low-temperature models for which they have an analytic expression respectively for the phonon and magnon DOS so as to obtain QFDR modified heat capacities for the lattice and spin parts of the system. They show that, indeed, their modified QFDR is better suited for the description of the low temperature magnon energy and the magnetization, especially for obtaining vanishing slope close to 0 K and also for describing the low-temperature magnon heat capacity. They end their discussion by a dynamical spin-lattice simulation of bcc Fe in which they show that their model can reproduce low-temperature behavior, measured in experiments, in particular the vanishing slope at $T = 0K$ for the magnetization curve. This effective approach is thus capable of describing, certain, quantum effects at low temperatures, without any extra computational cost.

In the above sections, the methods which were used to describe spin dynamics were all, somehow, relying on a Hamiltonian, or equivalently Lagrangian description. In this

context, the classical spin dynamics realizes constraints that, for example, imply the conservation of the norm of the spin. These constraints can be encoded much more naturally in a more general framework which is Nambu mechanics, a generalization of Hamiltonian dynamics [45] to phase spaces of arbitrary – including odd – dimensions. What is interesting is that the same is true for Nambu dynamics and higher order (*i.e.*, $N+1$ dimensional phase space, where N is the dimension of the corresponding Nambu phase space) Hamiltonian dynamics which in turn can encode the constraints of the initial Nambu dynamics [46]. In the following section, we will thus proceed to review some properties of Nambu dynamics and how this framework more naturally allows for the construction of undamped precessional spin dynamics.

1.5 Nambu mechanics

In 2009, Axenides *et al.* [47] published an article in which the main focus is the quantization of Nambu dynamics. What is more interesting here is that they begin by recalling the main features of Nambu dynamics. In $\mathbb{R}^3$, the time evolution for a variable $\boldsymbol{x}$ implicitly depending on time and living in a Nambu phase space is given by

$$\dot{x}_i \equiv \{x_i, H_1, H_2\} \tag{1.70}$$

where H_1 and H_2 are the two conserved quantities, the Nambu Hamiltonians. The bracket, on the RHS, is a generalization of the Poisson Bracket, to more than two entries:

$$\{f, g, h\} = \varepsilon_{ijk} \frac{\partial f}{\partial x_i} \frac{\partial g}{\partial x_j} \frac{\partial h}{\partial x_k} \tag{1.71}$$

As in the case of Hamiltonian dynamics, such a Nambu bracket must satisfy a certain set of properties :

- It is antisymmetric for any functions f, g and h of the phase space variables

$$\{f, g, h\} = -\{f, -g, h\} = \{f, -g, -h\} = -\{-f, -g, -h\} \tag{1.72}$$

- It satisfies the Leinbiz property

$$\{f, g, hj\} = \{f, g, h\}j + h\{f, g, j\} \tag{1.73}$$

- It satisfies a generalization of the Jacobi identity, called the Fundamental Identity

$$\{\{f_1, f_2, f_3\}, f_4, f_5\} + \{f_1, \{f_4, f_2, f_3\}, f_5\} + \{f_1, f_4, \{f_5, f_2, f_3\}\} = \{\{f_1, f_4, f_5\}, f_2, f_3\} \tag{1.74}$$

It is possible to describe the precession dynamics of a magnetic moment as an example of a linear Nambu flow. For this, they take $H_1 = \boldsymbol{a} \cdot \boldsymbol{x}$ and $H_2 = \frac{1}{2}\boldsymbol{x} \cdot B\boldsymbol{x}$. Here $\boldsymbol{a}$ is a real–valued vector and B is a real, symmetric matrix. This yields the following dynamics

$$\dot{x}_i = \varepsilon_{ijk} a_j B_{kl} x_l \tag{1.75}$$

If one now takes $\boldsymbol{a} \equiv \boldsymbol{\omega}$ the precession frequency, $B \equiv \mathbb{1}$ the identity matrix and $\boldsymbol{x} \equiv \boldsymbol{s}$ the classical spin – or magnetic moment, we recover

$$\dot{\boldsymbol{s}} = \boldsymbol{\omega} \times \boldsymbol{s} \tag{1.76}$$

which is, up to a possible numerical factor, the usual precession equation for a classical – undamped – spin.

Even though this formalism has been developed more than forty years ago, it has been forgotten for quite a while, apart from applications to fluid mechanics [48, 49]. It was revived in the context of the description of membranes in the so–called Bagger–Lambert–Gustafsson approach to multiple M2-branes [50], but was, once more, forgotten, when the expected relation between classical bracket and quantum commutator turned out to be much more difficult to establish than expected–and, indeed, it remains an open problem to this day.

What is interesting about linear Nambu flows that are relevant for spin precession is that it is possible to evade the problem of constructing the quantum Nambu bracket, since it is possible to construct the unitary evolution operator itself.

On the other hand, already at the classical level, how to describe dissipative effects in Nambu mechanics, that could be used to understand quantum fluctuations for deterministically chaotic systems, has provided insights for magnetic systems. We may cite here [51, 52]. It should be stressed that Nambu's original motivation was to describe the phase space of extended objects and it is noteworthy that the classical formalism has been applied to elastic strings [53] which can be identified as Goto–Nambu strings. Interestingly, a common way to study the coupling between mechanical and magnetic degrees of freedom has been derived from fluid dynamics [54]. However, these approaches often rely on studying the extrema of an appropriate energy functional, without paying attention to the dynamics. So, while they can provide useful insights for the couplings between magnetism and elasticity, also known as magnetostriction, they do not allow us to explore the phase space as fully as desired. Our aim being the study of the dynamical interplay between magnetism and elasticity, the next section's focus will be how to describe these couplings in a different fashion, namely from the symmetries that constrain the interaction between magnetic moments and mechanical strain tensors [6].

1.6 From elasticity to magnetoelasticity

In a review article about ferromagnetic domains, Kittel [55] focuses an entire section on how "magnetoelasticity", the interaction between magnetic and elastic DOF contributes to the total energy of a magnetic material. In this section, the magnetoelastic energy is defined as the energy arising from the interaction of the magnetization and the mechanical strain. For a crystal with cubic symmetry, a useful starting point consists in defining the elastic energy density as

$$f_{\text{el}} = \frac{c_{11}}{2}(e_{xx}^2 + e_{yy}^2 + e_{zz}^2) + \frac{c_{44}}{2}(e_{xy}^2 + e_{yz}^2 + e_{zx}^2) + c_{12}(e_{yy}e_{zz} + e_{xx}e_{zz} + e_{xx}e_{yy}) \tag{1.77}$$

where the c_{ij} are the elastic moduli and the e_{ij} are the mechanical strain tensor components. Here one may recall that, usually [56–58], the coupling between magnetism and

strain is due to the shape of the crystal, hence it is interpreted as a modification of the magnetic anisotropy which depends on the strain. By expanding the effective magnetic anisotropy energy f_k in a Taylor series of the mechanical strain, it is possible to define

$$f_k = (f_k)_0 + \sum_{i \geq j} \left(\frac{\partial f_k}{\partial e_{ij}} \right)_0 e_{ij} + \dots \tag{1.78}$$

where $(f_k)_0$ is the strain–independent part of this effective magnetic anisotropy. The different terms which are to be taken into account are

$$\begin{cases} \dfrac{\partial f_k}{\partial e_{xx}} = B_1 \alpha_1^2; & \dfrac{\partial f_k}{\partial e_{yy}} = B_1 \alpha_2^2; \\ \dfrac{\partial f_k}{\partial e_{zz}} = B_1 \alpha_3^2; & \dfrac{\partial f_k}{\partial e_{xy}} = B_2 \alpha_1 \alpha_2; \\ \dfrac{\partial f_k}{\partial e_{yz}} = B_2 \alpha_2 \alpha_3; & \dfrac{\partial f_k}{\partial e_{xz}} = B_2 \alpha_1 \alpha_3 \end{cases} \tag{1.79}$$

The B's are called magnetoelastic constants, and the α's are the direction cosines of the magnetization

$$\begin{cases} \alpha_1 &= \sin(\theta)\cos(\phi) \\ \alpha_2 &= \sin(\theta)\sin(\phi) \\ \alpha_3 &= \cos(\theta) \end{cases} \tag{1.80}$$

where, θ and ϕ are the spherical angles for the magnetization direction. Hence the total energy including strain, anisotropy and magnetoelastic terms, for a crystal displaying cubic symmetry reads

$$\begin{aligned} f &= K(\alpha_1^2\alpha_2^2 + \alpha_2^2\alpha_3^2 + \alpha_3^2\alpha_1^2) + B_1(\alpha_1^2 e_{xx} + \alpha_2^2 e_{yy} + \alpha_3^2 e_{zz}) \\ &+ B_2(\alpha_1\alpha_2 e_{xy} + \alpha_2\alpha_3 e_{yz} + \alpha_3\alpha_1 e_{zx}) + \frac{c_{11}}{2}(e_{xx}^2 + e_{yy}^2 + e_{zz}^2) \\ &+ \frac{c_{44}}{2}(e_{xy}^2 + e_{yz}^2 + e_{zx}^2) + c_{12}(e_{yy}e_{zz} + e_{xx}e_{zz} + e_{xx}e_{yy}) \end{aligned} \tag{1.81}$$

Now for more general systems [59] – beyond cubic symmetry –, the mechanical strain energy f_{el} is given by

$$f_{\text{el}} = \frac{1}{2} C_{ijkl} e_{ij} e_{kl} \tag{1.82}$$

where the C_{ijkl} is the tensor of elastic constants and, in a similar fashion, for crystals with lower symmetry, one can define a more general expression for the linear magnetoelastic energy [6]

$$f_{\text{mel}} = B_{ijkl} e_{ij} s_k s_l \tag{1.83}$$

where $\boldsymbol{s}$ are the components of the magnetization vector.

A key aspect of this approach is that it does not simply couple vector to vector but instead allows for a more subtle directional dependence through tensor quantities which can encode the direction with respect to the surroundings as well. But even though these structures are mathematically quite different, of course, they remain very similar as, they commute *pointwise*, *viz.*, $e_{ij}e_{kl} = e_{kl}e_{ij}$. (This, of course, does not mean that the matrices commute.)

What is interesting is that the spin degrees of freedom are qualitatively different, since their equations of motion–that describe precession–are first order. To handle the constraints that this implies, it is fascinating that other algebraic structures, namely Grassmann variables, turn out to be of practical relevance [21, 22]. Through these, it turns out to be possible to represent spin systems either using non-local, but commuting, variables; or by using local, but, anticommuting, variables. Thus, in the next section, we will review, how spin systems can be described in terms of Grassmann variables. In this way, it is possible to understand how a new kind of symmetry, called supersymmetry, appears, that mixes together commuting and anticommuting variables in a way that has quite profound implications for physics–especially for magnetic materials.

1.7 Grassmann variables and supersymmetry

Berezin *et al.* [22] proposed to use Grassmann variables for describing the dynamics of classical spinning point particles. They begin by introducing the notion of anticommuting c-numbers (complex numbers) using the Grassmann algebra formalism, which is presented in textbooks for fermionic field theories [60]. The particularity is that Grassmann algebras do not involve commutators, but anticommutators. The corresponding generalizations of Lie algebras are known as graded Lie algebras or superalgebras [61].

It is possible to summarize the work of Berezin and Marinov by stating the salient results, namely the action principle for the spinning particle in an external field.

The appropriate description for a spinning particle, indeed, turns out to involve functions of time, $\xi_i(t)$, that realize a Clifford algebra

$$\xi_i \xi_j + \xi_j \xi_i = 2\delta_{ij} \tag{1.84}$$

The reason, that took some time to be understood properly (in particular through the subsequent work of Brink et al.) is that it is indeed this algebra, rather than the usual Grassmann algebra

$$\xi_i \xi_j + \xi_j \xi_i = 0 \tag{1.85}$$

that ensures that the target space can describe the propagation of spinning particles, thanks to the consistent realization of the appropriate constraints.

The classical action on any time interval $[t_i, t_f]$ is given by the expression

$$\mathscr{A}_\xi(t_i, t_f) = \int_{t_i}^{t_f} dt \left[\frac{1}{2}\tilde{\omega}_{kl}\xi_k\dot{\xi}_l - H(\xi)\right] \tag{1.86}$$

where $\tilde{\omega}$ is a symmetric imaginary matrix (*i.e.*, antihermitian) for which the simplest possible form is taken, as $\tilde{\omega}_{kl} = \imath\delta_{kl}$ and $H(\xi)$ is an even polynomial (of degree lower or equal to 3), because an even product of odd numbers is an even number, as is required by the first term in the integral of the LHS of eq. (1.86). Hence

$$H(\xi) = \frac{-\imath}{2}\epsilon_{klm}B_k\xi_l\xi_m \tag{1.87}$$

and the B_k's are real. Thus the equations of motion deduced from the requirement that the action eq. (1.86) be extremal are

$$\dot{\xi}_k = iH\overleftarrow{\partial}_k = \epsilon_{klm}B_l\xi_m \tag{1.88}$$

where the $A\overleftarrow{\partial}_k$ notation simply denotes a derivative which acts on the right of the term A instead of on the left of it (as would the $\overrightarrow{\partial}_k A$), which one needs to specify, as the ξ's anticommute. Thus

$$(\xi_j\xi_l)\overleftarrow{\partial}_k = \xi_j\delta_{kl} - \xi_l\delta_{kj} = -\overrightarrow{\partial}_k(\xi_j\xi_l) \tag{1.89}$$

Equations (1.88) can be identified as describing spin precession in an external field $\boldsymbol{B}$ in analogy with eq. (1.76). The appropriate generalization of the Poisson bracket turns out to be

$$\{f,g\}_{P.B.} \equiv \imath(f\overleftarrow{\partial}_k)(\overrightarrow{\partial}_k g) \tag{1.90}$$

One can then define the rotation group in the extended phase space by the action of the spin angular momentum as

$$S_k = \frac{-\imath}{2}\epsilon_{klm}\xi_l\xi_m \tag{1.91}$$

Indeed it is the fact that the ξ_l generate a Clifford algebra that implies that the S_k generate the algebra of rotations.

Hence, the most general expression for the action, that describes the motion of a spinning particle in an external field, in this extended phase space (which, in fact, is a "superspace") $\{\boldsymbol{q},\boldsymbol{p},\boldsymbol{\xi}\}$ is described by

$$\mathscr{A}(t_i,t_f) = \int_{t_i}^{t_f} dt\left[\boldsymbol{p}\cdot\dot{\boldsymbol{q}} + \frac{\imath}{2}\boldsymbol{\xi}\cdot\dot{\boldsymbol{\xi}} - \frac{p^2}{2m} - V_0(\boldsymbol{q}) - (\boldsymbol{L}\cdot\boldsymbol{S})V_1(\boldsymbol{q}) - \boldsymbol{S}\cdot\boldsymbol{B}(\boldsymbol{q})\right] \tag{1.92}$$

where $\boldsymbol{L} = \boldsymbol{q}\times\boldsymbol{p}$ is the angular momentum, V_0 and V_1 are potential functions and $\boldsymbol{B}$ is the external field. We have used the notation $\boldsymbol{f}\cdot\boldsymbol{g} \equiv \sum_{i=1}^{3} f_i g_i$. This action yields the following equations of motion

$$\begin{cases} \dot{\boldsymbol{q}} = \dfrac{\boldsymbol{p}}{m} + (\boldsymbol{S}\times\boldsymbol{q})V_1, \\ \dot{\boldsymbol{p}} = -\boldsymbol{\nabla}V_0 - (\boldsymbol{L}\cdot\boldsymbol{S})\boldsymbol{\nabla}V_1 + (\boldsymbol{S}\times\boldsymbol{p})V_1 - \boldsymbol{\nabla}(\boldsymbol{S}\cdot\boldsymbol{B}), \\ \dot{\boldsymbol{\xi}} = (\boldsymbol{L}\times\boldsymbol{\xi})V_1 + (\boldsymbol{B}\times\boldsymbol{\xi}) \end{cases} \tag{1.93}$$

where $-\boldsymbol{\nabla}V_0$ is the field generated by the potential V_0,

$$(\boldsymbol{S}\times\boldsymbol{q})V_1, \quad (\boldsymbol{L}\cdot\boldsymbol{S})\boldsymbol{\nabla}V_1, \quad (\boldsymbol{S}\times\boldsymbol{p})V_1, \quad (\boldsymbol{L}\times\boldsymbol{\xi})V_1 \tag{1.94}$$

describe the spin-orbit interaction and

$$\boldsymbol{\nabla}(\boldsymbol{S}\cdot\boldsymbol{B}), \quad (\boldsymbol{B}\times\boldsymbol{\xi}) \tag{1.95}$$

correspond to the interaction with the external field $\boldsymbol{B}$. One interesting aspect to notice is that the dynamics for the spin itself is described by Grassmann variables $\boldsymbol{\xi}$, that satisfy

anticommutation relations, even though the coupling to the "spatial" degrees of freedom is done through the composite variables $\boldsymbol{S}$, that satisfy commutation relations. Through this formalism it has been possible to construct, from first principles, a representation of the algebra of the dynamical DOFs, that include position, momentum and spin in one multiplet, and define a Hamiltonian function and an appropriate graded Poisson bracket, thus defining the dynamical evolution for the system. Furthermore, such a description allows a smoother transition to describing fluctuations in general, more particularly quantum properties and how classical symmetries get realized [62]. This in turn implies a more straightforward implementation of the relations between the couplings, that are an expression of such symmetries. For instance, one can now see that the coupling of $\{\boldsymbol{q}, \boldsymbol{p}\}$ to the composite variable $\boldsymbol{S}$ is not simply to be imposed *ad hoc* but can be understood in terms of "deeper" symmetries. In this thesis we shall show in a specific example, pertaining to magnetostriction, how this formalism can be put to practical use in understanding the symmetries of the magnetoelastic interaction.

In this brief overview, we have seen different approaches describing spin dynamics, either for single – isolated – particles or for collections of them, in both cases interacting with an external field. For these methods we have seen that there are several issues, such as requiring a lot of computational power or failing to describe effects due to temperature or more general couplings. We have, thus, also investigated how these spin DOF's can then be coupled either to a thermal (or generic) noise reservoir or to the strains of the medium in which they are embedded. Current models for coupling to strains neither focus on the dynamical interplay between strains and spins nor consider any back reaction of the spins on the strains. In addition, we have investigated alternative, more natural, ways to take into account the constraints of spin degrees of freedom, depending on their bosonic or fermionic nature, through using Nambu mechanics or Grassmann – anticommuting – variables. These tools are not especially recent but what has not been considered thoroughly is how to use them together in a common approach describing finite temperature magneto-elasticity. Current advances in material science now open the possibility of studying matter under conditions, where fluctuations can be probed to unprecedented precision, which requires a good description of their dynamics. As our aim is to study the coupling between thermal, mechanic and magnetic degrees of freedom, these tools shall prove, indeed, particularly useful in building numerical methods to investigate their dynamics and dynamical interplay.

Summary

- Precession as an emergent property of the quantum nature of spin and the generalization of this simple model to describe damped precession of magnetic moments by equations such as LL or LLG.
- Construction of a consistent magnetic molecular dynamics and a review of how the framework can be used to numerically study magnetic materials. How symplectic integration schemes can be constructed in this context.
- A review of the atomistic spin dynamics model for numerical simulations of magnetic structures and the implementation of thermal effects in this method.
- Coupling of magnetic systems to baths and the quantitative description, either in terms of a stochastic dynamics, which needs to be averaged, or in terms of a deterministic – effective – approach for the moments of the distribution. We also investigated how to recover quantum effects, especially at low temperature, through an effective model of the fluctuations.
- A review of some interesting features of Nambu dynamics and Nambu brackets. We have shown how this framework can describe spin precession and how this can bring forth interesting physical interpretations.
- We reviewed some properties of elasticity and the description in terms of an energy functional and how the couplings between magnetism and elasticity give rise to magnetoelasticity, the dynamic alter ego to magnetostriction.
- Finally, we have presented Grassmann – anticommuting – variables and how to use them to describe spins and their coupling to mechanical degrees of freedom.

Chapter 2

Simulating magneto-thermo-mechanical dynamics through a spin/spin-bath coupling model

Résumé

- Nous construisons un modèle théorique stochastique pour le couplage d'un spin à un bain de spins afin d'explorer comment modéliser les effets de la magnétoélasticité. Ce modèle est décrit par des équations différentielles stochastiques.
- Nous établissons un modèle déterministe pour les moments de la distribution du spin, à partir du modèle stochastique. Ce modèle est décrit par des équations différentielles ordinaires, où les effets stochastiques sont implicites.
- Nous développons un intégrateur numérique stochastique pour simuler le comportement du premier système. Pour cela, nous utilisons un schéma symplectique/géométrique qui conserve le volume de l'espace des phases et permet de garder l'énergie du système bornée.
- Nous développons un intégrateur pour le système effectif – déterministe – à l'aide des bibliothèques GSL afin d'explorer dans quelle mesure ce système peut reproduire les propriétés du modèle stochastique, de façon plus rapide et explicite.

In the field of magnetic materials, "effective" theories are quite common. In order to take into account thermal effects, for example, one can construct a model for the interaction of a macroscopic magnetic moment with a stochastic bath, whose statistical properties define the "physical" temperature of the system [63], but whose degrees of freedom are not and need not be specified. Thus, one can understand the macroscopic behavior of a system in terms of this effective model, whose purpose is to "mimic" the influence of temperature on the initial system. In this chapter, we will, therefore, propose a model, which is based on this idea. In fact, we shall describe the way of coupling a magnetic moment (or spin) not only to a thermal bath, but, also, to another spin, which behaves as a collection of them (i.e., a spin bath [64]). Our aim is to have a way to take into account not only thermal effects but, also, the interaction between magnetic degrees of freedom, where we can single out some of them, with respect to others (that define the bath). In addition, we shall explore the effects of the elastic medium in which the magnetic moment is embedded [65] and construct the corresponding magneto-elastic interaction [18]. Thus in what follows, we will build a theoretical model for coupling a spin to a thermal bath, a spin bath and a reactive medium, so as to explore new ways for understanding dissipation in magnetic materials [66].

2.1 How to define a theoretical model for the spin/spin-bath coupling

For a classical spin (or magnetic moment) $\boldsymbol{s}(t)$ the simplest evolution model describes a precession [12] motion around a field $\boldsymbol{\omega}$ such that

$$\dot{\boldsymbol{s}}(t) = \boldsymbol{\omega} \times \boldsymbol{s}(t) \tag{2.1}$$

When one wants to couple this system to a bath, one can either introduce an additive $\boldsymbol{\omega} \times \boldsymbol{s} \to \boldsymbol{\omega} \times \boldsymbol{s} + \boldsymbol{\eta}$ or a multiplicative noise $\boldsymbol{\omega} \times \boldsymbol{s} \to (\boldsymbol{\omega} + \boldsymbol{\eta}) \times \boldsymbol{s}$, depending on the physical interpretation and the intrinsic properties of the system [67], where $\boldsymbol{\eta}$ is a vector of random variables, drawn from a fixed distribution that defines the bath. This induces a map between the probability distributions of the variables $\boldsymbol{s}$ and of the variables $\boldsymbol{\eta}$. These can be reconstructed from the moments $\langle s_i \dots s_n \rangle$ defined as

$$\langle s_i \dots s_n \rangle = \frac{\int D\boldsymbol{\eta} \mathcal{P}[\boldsymbol{\eta}] s_i[\boldsymbol{\eta}] \dots s_n[\boldsymbol{\eta}]}{\int D\boldsymbol{\eta} \mathcal{P}[\boldsymbol{\eta}]} \tag{2.2}$$

where $\mathcal{P}[\boldsymbol{\eta}]$ is the noise probability density and if it is normalized, then one simply has $\int D\boldsymbol{\eta} \mathcal{P}[\boldsymbol{\eta}] = 1$.

By assuming that the studied system is ergodic, which is by no means trivial [68], we will rather use the more convenient definition

$$\langle s_i[\boldsymbol{\eta}] \rangle = \lim_{N \to \infty} \frac{1}{N} \sum_{j=1}^{N} \tilde{s}_i^{(j)}[\boldsymbol{\eta}] \tag{2.3}$$

where the $\tilde{\boldsymbol{s}}^{(j)}$ label each stochastic realization. In order not to overload the notation, we will drop this specific distinction and simply keep in mind that the variables in brackets are averages, and the variables by themselves describe individual stochastic realizations.

Such a stochastic approach has been shown to be able to describe spin relaxation [69], for instance, by imposing a fluctuating field described by a Langevin equation. The probability distribution for the spin can then be determined as the solution to the corresponding Fokker-Planck equation, and a fluctuation-dissipation theorem can be shown to hold. In a "high-temperature" limit, this model was shown to produce LL or Bloch equations.

One shortcoming of this approach is that dissipation is introduced *ad hoc*. This particularly annoying for the Bloch equation, where the longitudinal damping is introduced by hand. It would be useful to have a framework for describing the stochastic properties of the spin, whatever the particular way dissipation may be realized. In particular, we would like to find a framework, where the longitudinal damping is the output, rather than the input.

One way to set up such a stochastic framework is to separate the spin variables into two classes $\boldsymbol{s}$ and $\boldsymbol{S}$, where $\boldsymbol{S}$ is drawn from a stochastic "spin" distribution. We will thus introduce the following system

$$\left\{ \begin{array}{rcl} \dot{\boldsymbol{s}} & = & \boldsymbol{\omega}[\boldsymbol{s}, \boldsymbol{S}] \times \boldsymbol{s} \\ \dot{\boldsymbol{S}} & = & \boldsymbol{\Omega}[\boldsymbol{s}, \boldsymbol{S}, \boldsymbol{\eta}] \times \boldsymbol{S} \end{array} \right. \tag{2.4}$$

The immediate consequence is that

$$\left\{ \begin{array}{rcl} \boldsymbol{s} \cdot \dot{\boldsymbol{s}} & = & 0 \\ \boldsymbol{S} \cdot \dot{\boldsymbol{S}} & = & 0 \end{array} \right. \tag{2.5}$$

i.e., the norms of $\boldsymbol{s}$ and $\boldsymbol{S}$ are constant over time. The approach constructed throughout this chapter introduces a "light" spin $\boldsymbol{s}$, representing a single magnetic moment, interacting with a "heavy" spin $\boldsymbol{S}$ [70], behaving as a collection of spins which can be resolved only through their statistical distribution.
This is represented if Figure 2.1. The red spin represents the single light magnetic moment, taken independently among all the spins. The bigger blue spin represents the heavy spin which mimics the interaction with the collection of the other (gray) spins. The idea is that the coupling between the noise and the heavy spin should encode the structural changes of the gray lattice so as to describe both, purely magnetic, as well as magnetoelastic, effects. Indeed, instead of directly having access to all the positions and orientations of the small magnetic moments, the heavy spin encodes this information as if it were only possible to detect the statistical properties of the noise induced by them. Thus different mechanical and magnetic structures are to be "translated" into statistical moments of the noise distribution.

So, the first property we want this system to reflect is that for each realization of the noise, the norm of the magnetic moment has to be conserved over time, since; otherwise, we would have introduced dissipation by hand. This rules out additive noise for the precession equation and calls for implementing multiplicative noise[28]

$$\left\{ \begin{array}{rcl} \dot{\boldsymbol{s}} & = & \boldsymbol{\omega}[\boldsymbol{s}, \boldsymbol{S}] \times \boldsymbol{s} \\ \dot{\boldsymbol{S}} & = & (\boldsymbol{\Omega}[\boldsymbol{s}, \boldsymbol{S}] + \boldsymbol{\eta}) \times \boldsymbol{S} \end{array} \right. \tag{2.6}$$

Next we must discuss how to define the interaction between the light $\boldsymbol{s}$ and heavy $\boldsymbol{S}$ spins.

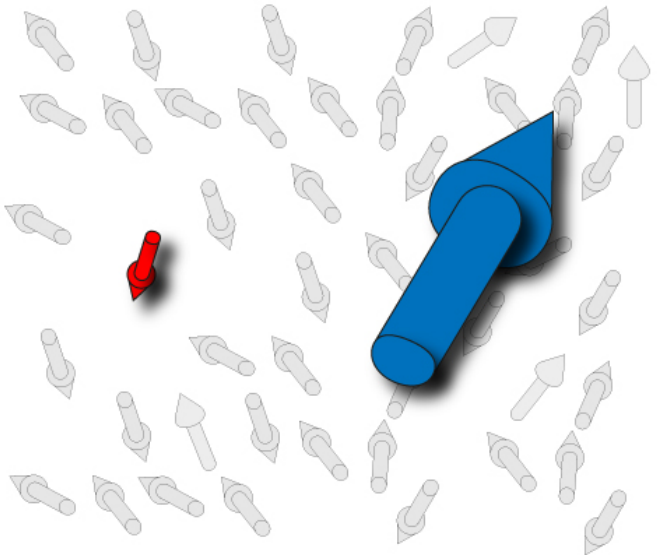

Figure 2.1: Light spin depicted in red and heavy spin depicted in blue, representing the collective effects of all the gray collection of spins.

We shall do this by introducing an exchange coupling constant J such that

$$\left\{\begin{array}{rcl} \dot{\boldsymbol{s}} & = & (\boldsymbol{\omega}[\boldsymbol{s}] + J\boldsymbol{S}) \times \boldsymbol{s} \\ \dot{\boldsymbol{S}} & = & (\boldsymbol{\Omega}[\boldsymbol{S}] + J\boldsymbol{s} + \boldsymbol{\eta}) \times \boldsymbol{S} \end{array}\right. \tag{2.7}$$

For simplicity, we take the same constant for both equations. We will, also, implement the usual Gilbert term (as a torque: $-\alpha\dot{\boldsymbol{S}} \times \boldsymbol{S}$) [71]–for the heavy spin, only, as it does describe collective, rather than individual, behavior:

$$\dot{\boldsymbol{S}} = \left(\boldsymbol{\Omega}[\boldsymbol{S}] - \alpha\dot{\boldsymbol{S}} + J\boldsymbol{s} + \boldsymbol{\eta}\right) \times \boldsymbol{S} \tag{2.8}$$

Since these equations conserve the norm of the spins, we can set the initial value for them so that $\boldsymbol{s}^2 = 1$ and $\boldsymbol{S}^2 = 1$; and, then, we can recast eq. (2.8)in the more familiar Landau-Lifshitz form

$$\dot{\boldsymbol{S}} = \frac{1}{1+\alpha^2}\left(\boldsymbol{\Omega}_{\text{eff}} - \alpha\boldsymbol{\Omega}_{\text{eff}} \times \boldsymbol{S}\right) \times \boldsymbol{S} \tag{2.9}$$

where the effective frequency is given by

$$\boldsymbol{\Omega}_{\text{eff}} = \boldsymbol{\Omega} + J\boldsymbol{s} + \boldsymbol{\eta} \tag{2.10}$$

Bertotti *et al.* [72] have shown that the noise term can be omitted in the effective frequency $\boldsymbol{\Omega}_{\text{eff}}$ for the double cross product, without any incidence on the dynamics. Hence the coupled system we will consider is given by

$$\left\{\begin{array}{l} \dot{\boldsymbol{s}} = (\boldsymbol{\omega} + J\boldsymbol{S}) \times \boldsymbol{s} \\ \dot{\boldsymbol{S}} = \dfrac{1}{1+\alpha^2}\left[(\boldsymbol{\Omega} + J\boldsymbol{s} + \boldsymbol{\eta}) - \alpha\left(\boldsymbol{\Omega} + J\boldsymbol{s}\right) \times \boldsymbol{S}\right] \times \boldsymbol{S} \end{array}\right. \tag{2.11}$$

from which it is straightforward to compute the variation in the phase space volume

$$\frac{\partial \dot{S}_i}{\partial S_i} + \frac{\partial \dot{s}_i}{\partial s_i} = -\frac{2\alpha}{1+\alpha^2}(J\boldsymbol{s} + \boldsymbol{\Omega}) \cdot \boldsymbol{S} \tag{2.12}$$

and find that it does not vanish. This means that the combined system is not closed. In addition, this implies that, depending on the orientation between $(J\boldsymbol{s} + \boldsymbol{\Omega})$ and $\boldsymbol{S}$ the volume of the phase space can either contract, or expand, which indicates the possibility for instabilities of the dynamical system. While this is a fascinating topic, it is beyond the subject of this thesis.

Explicit solutions of this system of equations are not available, for the noise distributions of interest, so a numerical treatment will be presented in section 2.3; but it is interesting to note that an alternative way to understand the behavior of this system is available: we can also determine the properties of the statistical distributions for the light and heavy spins, or equivalently the hierarchy of moments [73], which we shall study in the next section.

2.2 The hierarchy, its closure and the equivalent deterministic system

As mentioned before, once a random variable is introduced, the dynamical variables, depending on it , also become random and the system becomes stochastic. This means that computing the time evolution for one realization of the noise no longer has physical meaning. The quantities which express Ehrenfest's theorem are the averages over the noise $\langle \boldsymbol{s} \rangle$ and $\langle \boldsymbol{S} \rangle$ or, to be even more precise

$$\begin{cases} \dfrac{d}{dt}\langle \boldsymbol{s} \rangle = \langle (\boldsymbol{\omega} + J\boldsymbol{S}) \times \boldsymbol{s} \rangle \\ \dfrac{d}{dt}\langle \boldsymbol{S} \rangle = \dfrac{1}{1+\alpha^2}\langle [(\boldsymbol{\Omega} + J\boldsymbol{s} + \boldsymbol{\eta}) - \alpha\,(\boldsymbol{\Omega} + J\boldsymbol{s}) \times \boldsymbol{S}] \times \boldsymbol{S} \rangle \end{cases} \tag{2.13}$$

It is possible to gain considerable insight into the properties of these equations, under the assumption that $\boldsymbol{\Omega}$ and $\boldsymbol{\omega}$ be "external," fields which do not depend on $\boldsymbol{s}$ and $\boldsymbol{S}$. A further simplification, without any loss of generality, is that they are, indeed, constant vectors.

As such we can rewrite eq. (2.13)

$$\begin{cases} \dfrac{d}{dt}\langle \boldsymbol{s} \rangle = \boldsymbol{\omega} \times \langle \boldsymbol{s} \rangle + J\langle \boldsymbol{S} \times \boldsymbol{s} \rangle \\ \dfrac{d}{dt}\langle \boldsymbol{S} \rangle = \dfrac{1}{1+\alpha^2}\left[\boldsymbol{\Omega} \times \langle \boldsymbol{S} \rangle + J\langle \boldsymbol{s} \times \boldsymbol{S} \rangle + \langle \boldsymbol{\eta} \times \boldsymbol{S} \rangle - \alpha\left(J\langle (\boldsymbol{s} \times \boldsymbol{S}) \times \boldsymbol{S} \rangle - \boldsymbol{\Omega} \times \langle \boldsymbol{S} \times \boldsymbol{S} \rangle\right)\right] \end{cases} \tag{2.14}$$

and we immediately notice a problem: these equations do not define a closed hierarchy. They depend on higher order (as well as mixed) moments of these spins, namely $\langle s_i s_j \rangle$, $\langle s_i S_j \rangle$, $\langle S_i S_j \rangle$, $\langle s_i S_j S_k \rangle$, ... which in turn implies that we need equations of motion for all *these* moments as well.

To attempt to "close" this hierarchy, we proceed as follows:

We shall use the *Ansatz* that the averaging procedure and time derivative commute, which implies, for example

$$\frac{d}{dt}\langle s_i S_j\rangle = \langle \dot{s}_i S_j\rangle + \langle s_i \dot{S}_j\rangle \tag{2.15}$$

By replacing $\dot{\boldsymbol{s}}$ and $\dot{\boldsymbol{S}}$ in the resulting expressions, we end up with the following system for the second-order moments

$$\begin{cases} \dfrac{d}{dt}\langle s_i s_j\rangle = \langle \varepsilon_{ilm}\left(\omega_l + JS_l\right) s_m s_j\rangle + \langle s_i \varepsilon_{jlm}\left(\omega_l + JS_l\right) s_m\rangle \\ \dfrac{d}{dt}\langle s_i S_j\rangle = \langle \varepsilon_{ilm}\left(\omega_l + JS_l\right) s_m S_j\rangle \\ \qquad\qquad + \left\langle s_i \left(\dfrac{1}{1+\alpha^2}\varepsilon_{jlp}\left[\left(\Omega_m + Js_m + \eta_m\right) - \alpha\varepsilon_{lmn}\left(\Omega_m + Js_m\right) S_n\right] S_p\right)\right\rangle \\ \dfrac{d}{dt}\langle S_i S_j\rangle = \left\langle \left(\dfrac{1}{1+\alpha^2}\varepsilon_{ilp}\left[\left(\Omega_l + Js_l + \eta_l\right) - \alpha\varepsilon_{lmn}\left(\Omega_m + Js_m\right) S_n\right] S_p\right) S_j\right\rangle \\ \qquad\qquad + \left\langle S_i \left(\dfrac{1}{1+\alpha^2}\varepsilon_{jlp}\left[\left(\Omega_l + Js_l + \eta_l\right) - \alpha\varepsilon_{lmn}\left(\Omega_m + Js_m\right) S_n\right] S_p\right)\right\rangle \end{cases} \tag{2.16}$$

which involve even higher-order moments, namely $\langle s_i S_j S_k S_l\rangle$. If we tried to continue to write down equations of motion for these moments, we would only find even higher-order moments, thus giving rise to an infinite hierarchy of equations [73]. What is now required is a way to consistently truncate this hierarchy in order to keep only a finite number of terms. Here we chose a "Gaussian closure," which implies that the third-order cumulants vanish:

$$\langle\!\langle \mathcal{F}_i[\boldsymbol{\eta}]\mathcal{G}_j[\boldsymbol{\eta}]\mathcal{H}_k[\boldsymbol{\eta}]\rangle\!\rangle = 0. \tag{2.17}$$

where $\mathcal{F}[\boldsymbol{\eta}]$, $\mathcal{G}[\boldsymbol{\eta}]$ and $\mathcal{H}[\boldsymbol{\eta}]$ are general functionals of the noise. This is a highly non-trivial choice, which we make in order to keep things simple enough to be computed within a reasonable amount of time. However the consistency of this choice can be checked much more easily. This has been thoroughly investigated [38]. The closure assumption, in particular, means that one can rewrite the third- and fourth-order moments as functions of the first and second order ones

$$\begin{aligned} \mathcal{C}^{\boldsymbol{ABC}}_{ijk} &= \langle A_i B_j\rangle\langle C_k\rangle + \langle A_i C_k\rangle\langle B_j\rangle \\ &+ \langle B_j C_k\rangle\langle A_i\rangle - 2\langle A_i\rangle\langle B_j\rangle\langle C_k\rangle, \end{aligned} \tag{2.18}$$

$$\begin{aligned} \mathcal{E}^{\boldsymbol{ABCD}}_{ijkl} &= \langle A_i B_j\rangle\langle C_k D_l\rangle \\ &+ \langle A_i C_k\rangle\langle B_j D_l\rangle + \langle A_i D_l\rangle\langle B_j C_k\rangle \\ &- 2\langle A_i\rangle\langle B_j\rangle\langle C_k\rangle\langle D_l\rangle. \end{aligned} \tag{2.19}$$

where we introduce the following notation to keep the expressions as compact as possible: $\{A, B, C, D\}$ are to be chosen in $\{\boldsymbol{s}, \boldsymbol{S}\}$. As an example $C^{sSs}_{ijk} \equiv \langle s_i S_j s_k\rangle$. In this way, we

can express the components of the first-order moments as

$$\left\{\begin{array}{rcl} \dfrac{d}{dt}\langle s_i\rangle & = & \varepsilon_{ijk}\left(\omega_j\langle s_k\rangle + J\langle S_j s_k\rangle\right) \\ \dfrac{d}{dt}\langle S_i\rangle & = & \dfrac{1}{1+\alpha^2}\left\{\varepsilon_{ijk}\Big(\Omega_j\langle S_k\rangle + J\langle s_j S_k\rangle + \langle \eta_j S_k\rangle\Big)\right\} \\ & - & \dfrac{\alpha}{1+\alpha^2}\Big[\Omega_m\langle S_m S_i\rangle - \Omega_i + J\Big(\mathcal{C}^{\boldsymbol{sSS}}_{mmi} - \langle s_i\rangle\Big)\Big] \end{array}\right. \tag{2.20}$$

and the full expression for the components of the second-order moments are given by

$$\left\{\begin{array}{rcl} \dfrac{d}{dt}\langle s_i s_m\rangle & = & \varepsilon_{ijk}\left\{\omega_j\langle s_k s_m\rangle + J\mathcal{C}^{\boldsymbol{Sss}}_{jkm}\right\} + \varepsilon_{mjk}\left\{\omega_j\langle s_k s_i\rangle + J\mathcal{C}^{\boldsymbol{Sss}}_{jki}\right\} \\ \dfrac{d}{dt}\langle s_i S_m\rangle & = & \varepsilon_{ijk}\left\{\omega_j\langle s_k S_m\rangle + J\mathcal{C}^{\boldsymbol{SsS}}_{jkm}\right\} + \dfrac{\varepsilon_{mlp}}{1+\alpha^2}\left\{\Omega_l\langle s_i S_p\rangle\right. \\ & + & \left. J\mathcal{C}^{\boldsymbol{ssS}}_{ilp} + \langle s_i\eta_l\rangle\langle S_p\rangle + \langle S_p\eta_l\rangle\langle s_i\rangle\right\} \\ & - & \dfrac{\alpha}{1+\alpha^2}\Big[\Omega_p\mathcal{C}^{\boldsymbol{sSS}}_{imp} + J\mathcal{E}^{\boldsymbol{ssSS}}_{ipmp} - \Omega_m\langle s_i\rangle - J\langle s_i s_m\rangle\Big] \\ \dfrac{d}{dt}\langle S_i S_m\rangle & = & \dfrac{\varepsilon_{mlp}}{1+\alpha^2}\left\{\Omega_l\langle S_i S_p\rangle + J\mathcal{C}^{\boldsymbol{SsS}}_{ilp} + \langle S_i\eta_l\rangle\langle S_p\rangle\right. \\ & + & \left.\langle S_p\eta_l\rangle\langle S_i\rangle\right\} + \dfrac{\varepsilon_{ilp}}{1+\alpha^2}\left\{\Omega_l\langle S_m S_p\rangle + J\mathcal{C}^{\boldsymbol{SsS}}_{mlp}\right. \\ & + & \left.\langle S_m\eta_l\rangle\langle S_p\rangle + \langle S_p\eta_l\rangle\langle S_m\rangle\right\} - \dfrac{\alpha}{1+\alpha^2}\left\{2\Omega_p\mathcal{C}^{\boldsymbol{SSS}}_{imp}\right. \\ & + & \left. 2J\mathcal{E}^{\boldsymbol{SsSS}}_{ipmp} - \Omega_m\langle S_i\rangle - \Omega_i\langle S_m\rangle\right. \\ & - & \left. J\Big[\langle s_i S_m\rangle + \langle s_m S_i\rangle\Big]\right\} \end{array}\right. \tag{2.21}$$

The next step which remains to be elucidated is how to perform averages involving mixed components of the spins and the noise, such as $\langle \eta_i s_j\rangle$ and $\langle \eta_i S_j\rangle$ and, also to this end, which kind of noise to consider. Obviously, these are very tricky questions and can significantly enhance, or mitigate, the difficulty of the analysis of these kinds of systems. We will investigate ways to study a relatively simple noise distribution and review the mathematical tricks which will help us to have a better grasp on how this system relates to usually more ad hoc, although experimentally more widely used, approaches. An example of the noise distribution that's simple enough for analytical treatment, but, also, of physical relevance, is the Ornstein-Uhlenbeck distribution, whose salient features we review now.

The next few subsections are quite technical in character and involve describing *how* the mixed spin–noise moments are computed. They can be skipped on first reading, and one may jump directly to subsection 2.2.4.

2.2.1 The Ornstein-Uhlenbeck noise distribution

There are two very different kinds of noise distributions. The first kind describes so-called white noise, which is uncorrelated. This simply means that their components are independent at different times and for different components. A notable example is the Gaussian white noise distribution (which we can assume of mean zero), where each component is defined by the probability distribution of standard deviation $\sqrt{2D}$

$$P(x) = \frac{1}{\sqrt{4\pi D}} e^{-\frac{x^2}{4D}} \tag{2.22}$$

with $D > 0$ and such that

$$\int_{-\infty}^{\infty} P(x)dx = 1 \tag{2.23}$$

This distribution can, equivalently, be defined in terms of its first- and second-order moments

$$\begin{cases} \langle \eta_i(t) \rangle &= 0 \\ \langle \eta_i(t)\eta_j(t') \rangle &= 2D\delta_{ij}\delta(t-t') \end{cases} \tag{2.24}$$

There are, however, noise distributions, for which the different components, or the same components at different times, are no longer independent, *i.e.,* they are correlated [38]. An example of these "colored" noises is the Ornstein-Uhlenbeck process

$$\begin{cases} \langle \eta(t) \rangle &= 0 \\ \langle \eta_i(t)\eta_j(t') \rangle &= \frac{D}{\tau} \exp\left(\frac{-|t-t'|}{\tau}\right) \delta_{ij} \end{cases} \tag{2.25}$$

where τ is the autocorrelation time of the process. One reason why we are particularly interested in this process is that, in the limit $\tau \to 0$, we recover the Gaussian white noise given by eq. (2.24). A very interesting feature of this process is that it no longer involves distributions but only analytical, and more importantly, differentiable functions. This means that one can more easily differentiate and manipulate these moments and recover a Gaussian white noise by taking the aforementioned limit.

Now that we have defined the Ornstein-Uhlenbeck process and its limit when $\tau \to 0$, namely the Gaussian (normal) distribution, we shall continue with the next step, for computing the mixed moments of spin and noise, $\langle \eta_i S_j \rangle$. To this end, we use the Shapiro-Loginov theorem [39], which we describe in the following section.

2.2.2 Applying the Shapiro-Loginov theorem to compute derivatives of the noise for the spin bath

In order to close the established hierarchy, we need to have evolution equations for every quantity which remains after truncation and approximation. For the case at hand, we need them for $\langle s_i \rangle$, $\langle S_i \rangle$, $\langle s_i S_j \rangle$, $\langle s_i s_j \rangle$, $\langle S_i S_j \rangle$, $\langle \eta_i s_j \rangle$ and $\langle \eta_i S_j \rangle$. For those last two expressions, the mixed moments involving the noise, we need to compute $\frac{d}{dt}\langle \eta_i S_j \rangle$ and $\frac{d}{dt}\langle \eta_i s_j \rangle$.

In this section we will focus on $\langle \eta_i S_j \rangle$. The Shapiro-Loginov theorem [74], which yields a formula of differentiation for averages enables us to write, for the case of the Ornstein-Uhlenbeck process,

$$\frac{d}{dt}\langle \eta_i S_j \rangle = \langle \eta_i \frac{dS_j}{dt} \rangle - \frac{1}{\tau}\langle \eta_i S_j \rangle \tag{2.26}$$

If we replace $\dot{S}_j$ by its expression in eq. (2.26), we get

$$\frac{d}{dt}\langle \eta_i S_j \rangle = \left\langle \frac{\eta_i}{1+\alpha^2}\varepsilon_{jrp}\left[(\Omega_r + Js_r + \eta_r) - \alpha\varepsilon_{rlm}\left(\Omega_l + Js_l\right) S_m\right] S_p \right\rangle - \frac{1}{\tau}\langle \eta_i S_j \rangle \tag{2.27}$$

What is interesting to notice is that there is only one term in the RHS of eq. (2.27), which is linear in $\frac{1}{\tau}$, namely,

$$\frac{\varepsilon_{jrp}}{1+\alpha^2}\langle \eta_i \eta_r S_p \rangle \propto \frac{1}{\tau} \tag{2.28}$$

Here, once more, we apply the Gaussian closure, where the third-order moment of any function of the noise can be expressed in terms of products of the first- and second-order moments or equivalently, the third-order cumulant vanishes as given by eq. (2.17). This in turn means that $\langle \eta_i \eta_r S_p \rangle = \langle \eta_i \eta_r \rangle \langle S_p \rangle$, since the other terms vanish. We end up with

$$\langle \eta_i(t)\eta_r(t')S_p(t)\rangle = \frac{D}{\tau}\exp\left(\frac{-|t-t'|}{\tau}\right)\delta_{ij}\langle S_p(t)\rangle \tag{2.29}$$

The idea is to multiply eq. (2.27) by τ and then take the limit $\tau \to 0$ to recover the Gaussian white noise, which leads to the following expression

$$\langle \eta_i(t) S_j(t)\rangle = \frac{-D}{1+\alpha^2}\varepsilon_{ijk}\langle S_k(t)\rangle \tag{2.30}$$

Now we can simply replace this expression in eqs. (2.20) and (2.21), instead of computing $\frac{d}{dt}\langle \eta_i S_j \rangle$. As elementary functional analysis tells us, it is not generally true that one can simply commute averaging (*i.e.*, integration) and differentiation especially as the behavior of some terms in the $\tau \to 0$ can be subtle [75] but here, as a simplifying hypothesis, for this first step, it is postulated that these assumptions hold. It should be stressed that this simplification does not prejudge the properties of the long-time limit, which, however, can be checked *a posteriori*.

Now that we have managed to express $\langle \eta_i S_j \rangle$ in terms of available quantities, we shall turn our attention towards $\langle \eta_i s_j \rangle$ for which, as we shall see in the next section, we will need to make use of the Furutsu-Novikov-Donsker theorem in the case of a Gaussian white noise.

2.2.3 Using the Furutsu-Novikov-Donsker theorem to compute derivatives of the noise for the spin

The simplification of $\langle \eta_i s_j \rangle$ requires a bit more work. One could ask why we do not use the same procedure as previously with the Shapiro-Loginov approach for $\langle \eta_i S_j \rangle$. The

reason is that there is no explicit dependence on the noise in the expression for $\dot{s}_i$; thus we cannot apply the same procedure.

We are thus going to use another tool which is the Furutsu-Novikov-Donsker theorem [76], which yields a formula for Gaussian noise path integrals of functional derivatives.

In our case it reads

$$\langle \eta_i(t) s_j(t) \rangle = \int dt' \langle \eta_i(t) \eta_l(t') \rangle \left\langle \frac{\delta s_j(t)}{\delta \eta_l(t')} \right\rangle \tag{2.31}$$

What remains to be computed is the functional derivative $\dfrac{\delta s_j(t)}{\delta \eta_l(t')}$. One way to do this is to use the chain rule [77] for functional differentiation

$$\left\langle \frac{\delta s_i(t)}{\delta \eta_j(t')} \right\rangle = \int dt'' \left\langle \frac{\delta s_i(t)}{\delta S_k(t'')} \frac{\delta S_k(t'')}{\delta \eta_j(t')} \right\rangle . \tag{2.32}$$

The evaluation of the derivatives on the RHS is quite delicate:

Formally one can always write

$$\begin{cases} s_i(t) &= s_i(0) + \int_0^t dt' \dot{s}_i(t') \\ S_i(t) &= S_i(0) + \int_0^t dt' \dot{S}_i(t') \end{cases} \tag{2.33}$$

As implied by the different integral, the times t, t' and t'' are ordered as shown in Figure 2.2

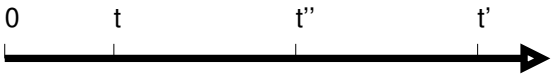

Figure 2.2: Timeline for the times t, t' and t''

One can now obtain expressions for the functional derivatives of s_i and S_i as

$$\begin{cases} \dfrac{\delta s_i(t)}{\delta S_k(t'')} = J \displaystyle\int_0^t dt' \frac{\delta \dot{s}_i(t')}{\delta S_k(t'')} = \frac{J}{2} \varepsilon_{ikm} \int_0^t dt' s_m(t') \delta(t' - t'') \\ \dfrac{\delta S_k(t'')}{\delta \eta_j(t')} = \displaystyle\int_0^{t''} dt \frac{\delta \dot{S}_k(t)}{\delta \eta_j(t')} = \frac{\varepsilon_{kjp}}{2\,(1+\alpha^2)} \int_0^{t''} dt \delta(t - t') S_p(t) \end{cases} \tag{2.34}$$

keeping in mind that $\langle \eta_i(t) \eta_l(t') \rangle = 2D\delta(t - t')\delta_{il}$, for a white noise, we get the full expression for the mixed moment of the noise with the light spin

$$\langle \eta_i(t) s_j(t) \rangle = \frac{JD}{2\,(1+\alpha^2)} \left(\langle S_j(t) s_i(t) \rangle - \delta_{ij} \langle S_m(t) s_m(t) \rangle \right) \tag{2.35}$$

Using these tools we can, finally, write down a completely closed system of equations, which involve only the first and second moments of the corresponding distributions. For the benefit of the reader, who only wishes to use the equations, we write them out in the following subsection.

2.2.4 The equations for the closed system

We, now, can write the completely closed system of equations for the first and second moments of the distributions. For the first moments, we have

$$\left\{\begin{array}{rcl} \frac{d}{dt}\langle s_i\rangle & = & \varepsilon_{ijk}\left(\omega_j\langle s_k\rangle + J\langle S_j s_k\rangle\right) \\ \frac{d}{dt}\langle S_i\rangle & = & \frac{1}{1+\alpha^2}\left\{\varepsilon_{ijk}\left[\Omega_j\langle S_k\rangle + J\langle s_j S_k\rangle\right]\right\} - \frac{2D}{(1+\alpha^2)^2}\langle S_i\rangle \\ & - & \frac{\alpha}{1+\alpha^2}\left[\Omega_m\langle S_m S_i\rangle - \Omega_i + J\left(\mathcal{C}^{\boldsymbol{sSS}}_{mmi} - \langle s_i\rangle\right)\right] \end{array}\right. \tag{2.36}$$

and for the second, including mixed, moments, we have

$$\begin{array}{rcl} \frac{d}{dt}\langle s_i s_m\rangle & = & \varepsilon_{ijk}\left\{\omega_j\langle s_k s_m\rangle + J\mathcal{C}^{\boldsymbol{Sss}}_{jkm}\right\} + \varepsilon_{mjk}\left\{\omega_j\langle s_k s_i\rangle + J\mathcal{C}^{\boldsymbol{Sss}}_{jki}\right\} \\ \frac{d}{dt}\langle s_i S_m\rangle & = & \varepsilon_{ijk}\left\{\omega_j\langle s_k S_m\rangle + J\mathcal{C}^{\boldsymbol{SsS}}_{jkm}\right\} + \frac{\varepsilon_{mlp}}{1+\alpha^2}\left\{\Omega_l\langle s_i S_p\rangle\right. \\ +J\mathcal{C}^{\boldsymbol{ssS}}_{ilp} & + & \left.\frac{JD}{2(1+\alpha^2)}\left(\langle S_i s_l\rangle - \delta_{il}\langle S_n s_n\rangle\right)\langle S_p\rangle - \frac{D}{1+\alpha^2}\varepsilon_{lpn}\langle S_n\rangle\langle s_i\rangle\right\} \\ & - & \frac{\alpha}{1+\alpha^2}\left[\Omega_p\mathcal{C}^{\boldsymbol{sSS}}_{imp} + J\mathcal{E}^{\boldsymbol{ssSS}}_{ipmp} - \Omega_m\langle s_i\rangle - J\langle s_i s_m\rangle\right] \\ \frac{d}{dt}\langle S_i S_m\rangle & = & \frac{\varepsilon_{mlp}}{1+\alpha^2}\left\{\Omega_l\langle S_i S_p\rangle + J\mathcal{C}^{\boldsymbol{SsS}}_{ilp} - \frac{D}{1+\alpha^2}\varepsilon_{lin}\langle S_n\rangle\langle S_p\rangle\right. \\ & - & \left.\frac{D}{1+\alpha^2}\varepsilon_{lpn}\langle S_n\rangle\langle S_i\rangle\right\} + \frac{\varepsilon_{ilp}}{1+\alpha^2}\left\{\Omega_l\langle S_m S_p\rangle\right. \\ & + & \left. J\mathcal{C}^{\boldsymbol{SsS}}_{mlp} - \frac{D}{1+\alpha^2}\varepsilon_{lmn}\langle S_n\rangle\langle S_p\rangle - \frac{D}{1+\alpha^2}\varepsilon_{lpn}\langle S_n\rangle\langle S_m\rangle\right\} \\ & - & \frac{\alpha}{1+\alpha^2}\left\{2\Omega_p\mathcal{C}^{\boldsymbol{SSS}}_{imp} + 2J\mathcal{E}^{\boldsymbol{SsSS}}_{ipmp} - \Omega_m\langle S_i\rangle - \Omega_i\langle S_m\rangle\right. \\ & - & \left. J\left[\langle s_i S_m\rangle + \langle s_m S_i\rangle\right]\right\} \end{array} \tag{2.37}$$

where the expressions for $\mathcal{C}$ and $\mathcal{E}$ are given in eq. (2.18).

Now that we have consistently closed this hierarchy we can check the validity of our closure assumptions and ancillary hypotheses, we need to solve these equations. Obtaining analytical solutions for this effective system, for arbitrary couplings and conditions is not an easy task. There are, however, ways to solve them, numerically, and this is what we will focus on in the next sections. Solving equations numerically, of course, is an experimental task, as one has to check that the solutions to the numerical approximations actually are approximations to the solutions of the original equations. In order to have a reference point to compare the solutions for the effective, deterministic, system, we will start by integrating the stochastic system. To this end it is necessary to construct an appropriate numerical integrator for this spin/spin-bath coupling model. This is the topic to which we now turn.

2.3 A stochastic numerical integrator for the spin/spin-bath dynamics

In this section, we will turn our focus back to the initial, stochastic, system eq. (2.11). In order to solve these equations, we shall study only white noise, so as to keep things simple. We define two effective precession frequencies, $\boldsymbol{\Omega}^{\text{eff}}$ and $\boldsymbol{\omega}^{\text{eff}}$, such that

$$\begin{cases} \dot{s}_i &= \varepsilon_{ijk}\omega_j^{\text{eff}} s_k \\ \dot{S}_i &= \varepsilon_{ijk}\Omega_j^{\text{eff}} S_k \end{cases} \tag{2.38}$$

These equations can be identified as Liouville equations [78], by defining operators $\mathcal{L}_{\boldsymbol{s}}$ and $\mathcal{L}_{\boldsymbol{S}}$

$$\begin{cases} \mathcal{L}_{\boldsymbol{s}} \equiv \dot{\boldsymbol{s}}_i(t)\dfrac{\partial}{\partial \boldsymbol{s}_i(t)} \\ \mathcal{L}_{\boldsymbol{S}} \equiv \dot{\boldsymbol{S}}_i(t)\dfrac{\partial}{\partial \boldsymbol{S}_i(t)} \end{cases} \tag{2.39}$$

where $i \in \{1,2,3\}$ and summation over repeated indices is implied. It is possible to show that the operators $\mathcal{L}_{\boldsymbol{s}}$ and $\mathcal{L}_{\boldsymbol{S}}$ do, indeed, satisfy the properties expected of Liouville operators.

Applying these operators on the heavy and light spin directly yields

$$\begin{cases} \dot{\boldsymbol{s}}(t) &= [\mathcal{L}_{\boldsymbol{s}}]\,\boldsymbol{s}(t) \\ \dot{\boldsymbol{S}}(t) &= [\mathcal{L}_{\boldsymbol{S}}]\,\boldsymbol{S}(t) \end{cases} \tag{2.40}$$

Formally, one can integrate these equations using operator exponentials, since the time evolution depends only on the initial conditions $\{\boldsymbol{s}(0), \boldsymbol{S}(0)\}$

$$\begin{cases} \boldsymbol{s}(t) &= \left[e^{t\mathcal{L}_{\boldsymbol{s}}}\right]\boldsymbol{s}(0) \\ \boldsymbol{S}(t) &= \left[e^{t\mathcal{L}_{\boldsymbol{S}}}\right]\boldsymbol{S}(0) \end{cases} \tag{2.41}$$

A consequence of the fact that these are Liouville operators is that their exponentials are symplectic operators.

Therefore, the complete solution is given by

$$\{\boldsymbol{s}(t), \boldsymbol{S}(t)\} = e^{\mathcal{L}t}\{\boldsymbol{S}(0), \boldsymbol{s}(0)\} \tag{2.42}$$

where $\mathcal{L} = \mathcal{L}_{\boldsymbol{s}} + \mathcal{L}_{\boldsymbol{S}}$. There is, however, a remaining issue. These operators do not commute, as the time evolution for each spin depends on the other. This can be shown by a direct computation of the commutator, $[\mathcal{L}_{\boldsymbol{S}}, \mathcal{L}_{\boldsymbol{s}}]f[\boldsymbol{s}, \boldsymbol{S}]$

$$\mathcal{L}_{\boldsymbol{s}}(\mathcal{L}_{\boldsymbol{S}}(f[\boldsymbol{s}, \boldsymbol{S}])) - \mathcal{L}_{\boldsymbol{S}}(\mathcal{L}_{\boldsymbol{s}}(f[\boldsymbol{s}, \boldsymbol{S}])) = \dot{s}_j \frac{\partial \dot{S}_i}{\partial s_j}\frac{\partial f[\boldsymbol{s}, \boldsymbol{S}]}{\partial S_i} - \dot{S}_j \frac{\partial \dot{s}_i}{\partial S_j}\frac{\partial f[\boldsymbol{s}, \boldsymbol{S}]}{\partial s_i} \tag{2.43}$$

Since $\dot{\boldsymbol{s}}$ depends on $\boldsymbol{S}$ and $\dot{\boldsymbol{S}}$ depends on $\boldsymbol{s}$, this expression does not vanish for arbitrary functions $f[\boldsymbol{S}, \boldsymbol{s}]$. Hence, the exponential of the sum, is not the product of the exponential of each operator

$$e^{t(\mathcal{L}_{\boldsymbol{s}}+\mathcal{L}_{\boldsymbol{S}})} \neq e^{t\mathcal{L}_{\boldsymbol{s}}}e^{t\mathcal{L}_{\boldsymbol{S}}} \tag{2.44}$$

There is, however, an approximation scheme based on the so-called Magnus expansion [79], which has the appealing property of defining a symplectic/geometric integration scheme. An example is given by

$$e^{t\mathcal{L}} = e^{\frac{t}{2}\mathcal{L}_s} e^{t\mathcal{L}_S} e^{\frac{t}{2}\mathcal{L}_s} + \mathcal{O}(t^3) \tag{2.45}$$

Explicit expressions for the time evolution, defined by this scheme for a precession field, which can vary at each time step, are given in reference [36].

The implementation of this integration scheme consists of several steps.

- We begin by computing the effective field for the first spin. Once this is done, the new orientation for the spin is computed by letting it precess around its effective field for half the integration time step.

- We then proceed to compute the effective field for the other spin. We then, again, compute its dynamics for the time step.

- Finally, we repeat the first step.

This whole procedure is repeated until the chosen final time step. In this way, we manage to compute the dynamics for both spins from the initial time to the final time.

These computations are done for a fixed realization of the noise.

In order to perform an average over the noise, we repeat the whole procedure several times, depending on how many realizations of the noise we want to average over. In order to know whether or not the average is being performed over enough realizations, we study the convergence of this averaging procedure. When having more and more realizations for the averaging no longer significantly enhances precision (*i.e.,* results do not differ much from an average over fewer realizations), we stop increasing the number of realizations.

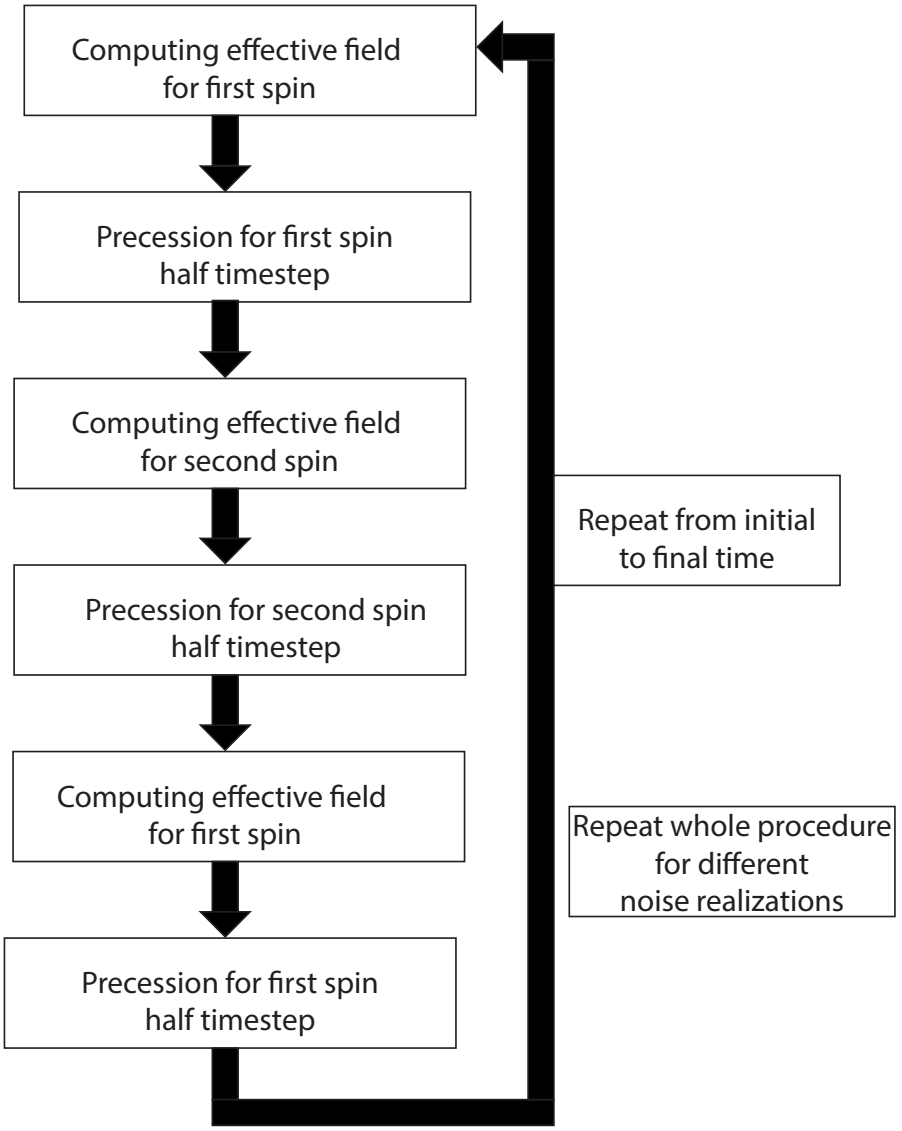

Figure 2.3: Symplectic/geometric integration algorithm. Averaging over the noises to be repeated until convergence is attained

The whole procedure is summarized in Figure 2.3. There are, of course, other methods for integrating Stochastic Differential Equations (SDE) such as the Heun method [80], but these have been shown to present issues such as not preserving the phase space structure or the symmetries of the problem [78, 81].

Finally, because the two operators $\mathcal{L}_{\boldsymbol{s}}$ and $\mathcal{L}_{\boldsymbol{S}}$ do not commute, there are *two* possible ordering schemes for the numerical method:

$$e^{t\mathcal{L}} \approx \begin{cases} e^{t\mathcal{L}_{\boldsymbol{s}}/2} e^{t\mathcal{L}_{\boldsymbol{S}}} e^{t\mathcal{L}_{\boldsymbol{s}}/2} \\ e^{t\mathcal{L}_{\boldsymbol{S}}/2} e^{t\mathcal{L}_{\boldsymbol{s}}} e^{t\mathcal{L}_{\boldsymbol{S}}/2} \end{cases} \tag{2.46}$$

Of course, in the "continuum limit" both should give equivalent results–but, at a finite

time step size, they will not. Therefore, it is of interest to understand, whether one is more efficient/accurate than the other.

This is what we shall discuss in the next section, by providing methods for evaluating the "optimal ordering" of these symplectic operators in the integration scheme.

2.3.1 Optimizing code by symplectic operator ordering

Let us study the operator ordering issue in more detail. The two choices, at least up to order $\mathcal{O}(t^3)$, where t is the time step, can be written as

$$\begin{cases} e^{\frac{t}{2}\mathcal{L}_{\boldsymbol{s}}}\{\boldsymbol{s}(0),\boldsymbol{S}(0)\} = \left\{\boldsymbol{s}\left(\frac{t}{2}\right),\boldsymbol{S}(0)\right\} \\ e^{t\mathcal{L}_{\boldsymbol{S}}}\left\{\boldsymbol{s}\left(\frac{t}{2}\right),\boldsymbol{S}(0)\right\} = \left\{\boldsymbol{s}\left(\frac{t}{2}\right),\boldsymbol{S}(t)\right\} \\ e^{\frac{t}{2}\mathcal{L}_{\boldsymbol{s}}}\left\{\boldsymbol{s}\left(\frac{t}{2}\right),\boldsymbol{S}(t)\right\} = \{\boldsymbol{s}(t),\boldsymbol{S}(t)\} \end{cases} \tag{2.47}$$

(which we shall call light-heavy-light or lhl scheme) and the second possibility is

$$\begin{cases} e^{\frac{t}{2}\mathcal{L}_{\boldsymbol{S}}}\{\boldsymbol{S}(0),\boldsymbol{s}(0)\} = \left\{\boldsymbol{S}\left(\frac{t}{2}\right),\boldsymbol{s}(0)\right\} \\ e^{t\mathcal{L}_{\boldsymbol{s}}}\left\{\boldsymbol{S}\left(\frac{t}{2}\right),\boldsymbol{s}(0)\right\} = \left\{\boldsymbol{S}\left(\frac{t}{2}\right),\boldsymbol{s}(t)\right\} \\ e^{\frac{t}{2}\mathcal{L}_{\boldsymbol{S}}}\left\{\boldsymbol{S}\left(\frac{t}{2}\right),\boldsymbol{s}(t)\right\} = \{\boldsymbol{S}(t),\boldsymbol{s}(t)\} \end{cases} \tag{2.48}$$

(which we shall call heavy-light-heavy or hlh scheme)

The key difference is in the computation of the effective field at each time step. Indeed, once the effective field is computed, both operators act on their respective spin in the same fashion. However, computing the effective field for the heavy spin requires more numerical operations, which means we should avoid algorithms where the heavy spin is evolved more often. But, on the other hand, it might also be that the effective field for the heavy spin is stronger, and thus the computation would be more accurate if this effective field is computed more often. We shall use a test case for both options and average over 10^2, 10^3 and 10^4 realizations of the noise, for each of them. On top of comparing how these schemes converge, depending on the number of noise realizations, we will also check how fast they are by comparing how long each of those schemes takes to produce the plotted data. Results are given in Figures 2.4 and 2.5. Running times for the different schemes and number of realizations are given in Tables 2.1 and 2.2. The results show that, as expected, the first scheme is a little bit faster, but the second scheme converges faster, for the same number of noise realizations. This is why we choose the second scheme for the rest of this chapter, as averaging over a larger number of realizations of the noise is more expensive, computationally, than the additional cost of the second, namely heavy-light-heavy, scheme.

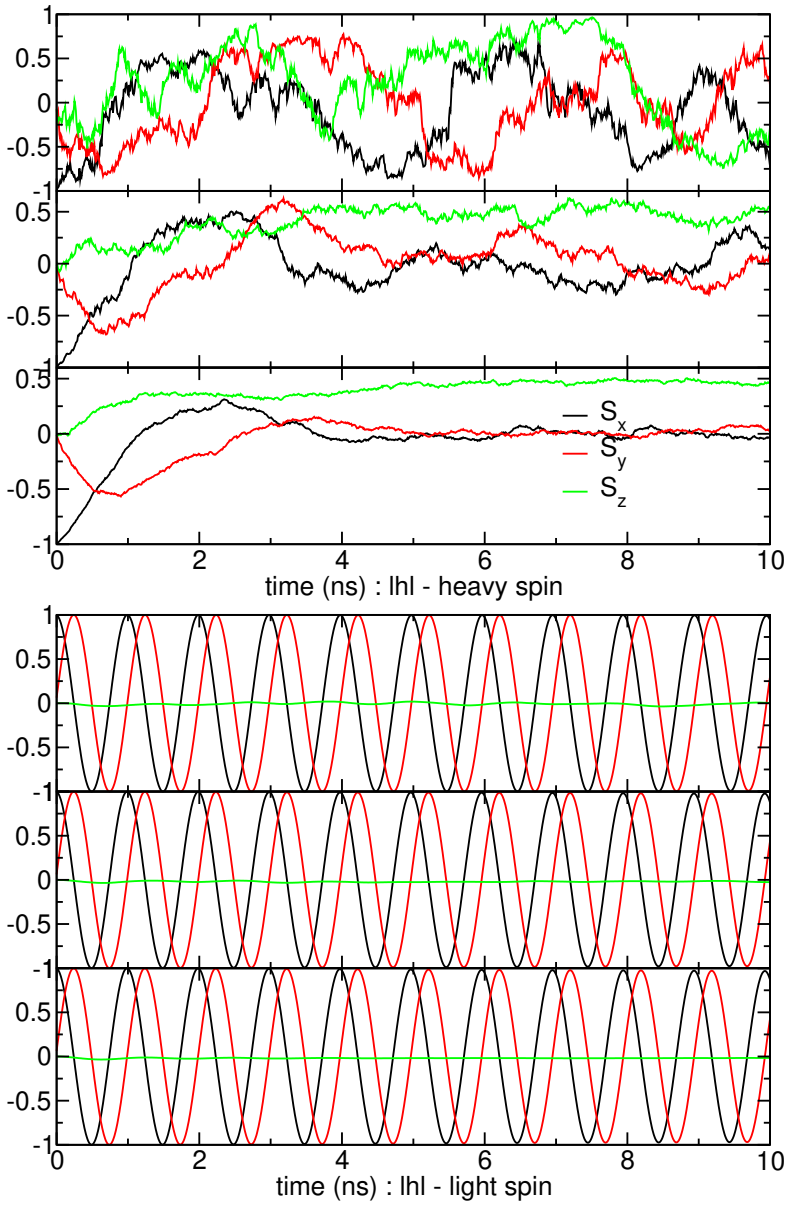

Figure 2.4: Scheme for light-heavy-light spin operators order for (from top to bottom) 10^2, 10^3 and 10^4 realizations of the noise. Conditions: $\{\boldsymbol{s}(0) = \boldsymbol{x}, \boldsymbol{S}(0) = -\boldsymbol{x}, \boldsymbol{\omega} = 2\pi\boldsymbol{z}\,\text{GHz}, \boldsymbol{\Omega} = \frac{\pi}{2}\boldsymbol{z}\,\text{GHz}, J = 0.1\,\text{GHz}, \alpha = 0.3, D = 0.3\,\text{GHz}\}$.

realizations	**runtime**
10^2	1.87s
10^3	21.00s
10^4	3m43.66s

Table 2.1: Running times for 10^2, 10^3 and 10^4 realizations for the l-h-l scheme

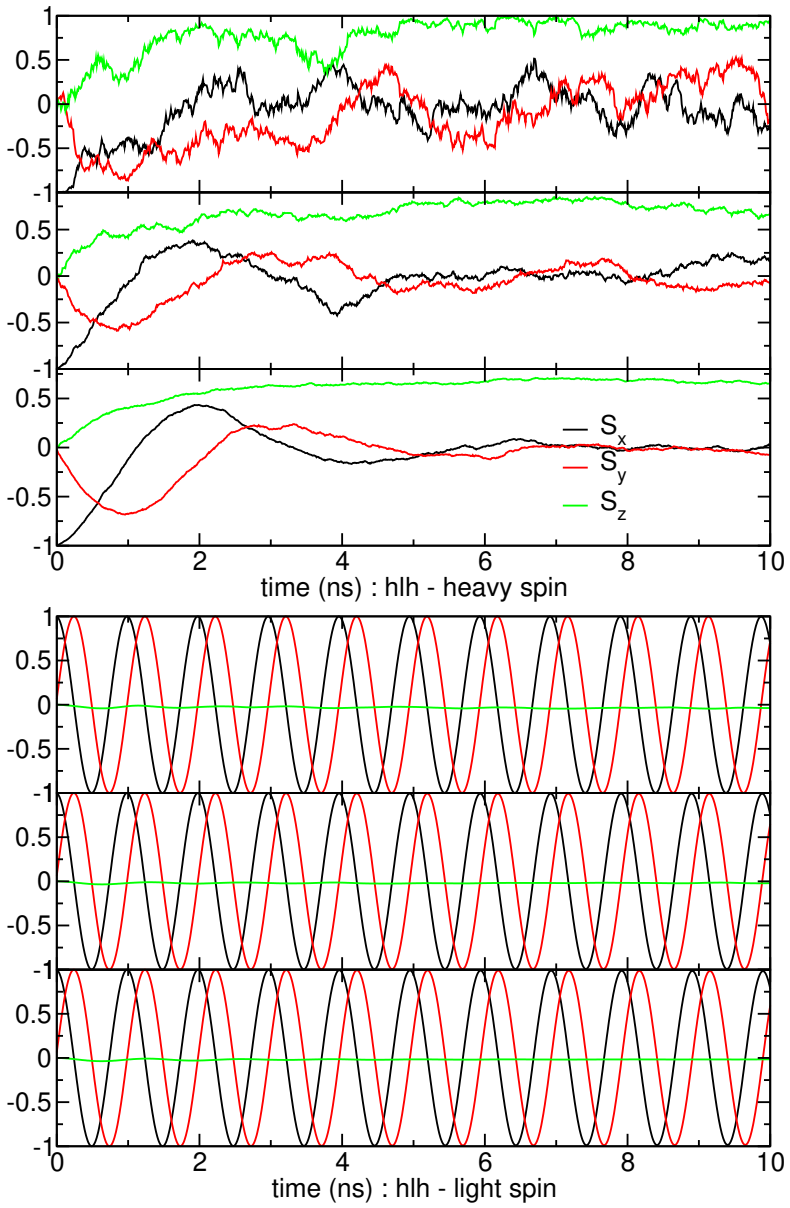

Figure 2.5: Scheme for heavy-light-heavy spin operators order for (from top to bottom) 10^2, 10^3 and 10^4 realizations of the noise. Conditions: $\{\boldsymbol{s}(0) = \boldsymbol{x}, \boldsymbol{S}(0) = -\boldsymbol{x}, \boldsymbol{\Omega} = 2\pi\boldsymbol{z}\,\text{GHz}, \boldsymbol{\omega} = \frac{\pi}{2}\boldsymbol{z}\,\text{GHz}, J = 0.1\,\text{GHz}, \alpha = 0.3, D = 0.3\,\text{GHz}\}$.

realizations	**runtime**
10^2	2.43s
10^3	24.91s
10^4	4m24.42s

Table 2.2: Running times for 10^2, 10^3 and 10^4 realizations for the h-l-h scheme

A useful quality check for our integrator is to monitor the energy of our system over time

$$E \propto \boldsymbol{\omega} \cdot \boldsymbol{s} + \boldsymbol{\Omega} \cdot \boldsymbol{S} + J\boldsymbol{s} \cdot \boldsymbol{S} \tag{2.49}$$

Results for the light-heavy-light scheme are given in Figure 2.6; an estimation of the error is provided by

$$dE = \frac{2\sigma}{\sqrt{N}} \tag{2.50}$$

where σ is the standard deviation about the average for the energy

$$\sigma = \sqrt{\langle E^2 \rangle - \langle E \rangle^2} \tag{2.51}$$

Since we have a symplectic integration scheme, if the system reaches an equilibrium configuration with respect to the noise, then we should see the energy relax towards a "plateau," which is indeed what one can see on the curves. This convergence is not as obvious for 10^2 realizations of the noise but already becomes noticeable for 10^3 realizations. And we can also see that the energy converges towards the same value for 10^4 realizations, which is another consistency check, namely that the convergence, at least after some threshold, does not depend on the number of realizations, only its fluctuations do. In order for the relative error to be below 1% at all times , we choose to average over 10^5 realizations of the noise, for which the energy is plotted by the cyan curve of Figure 2.6.

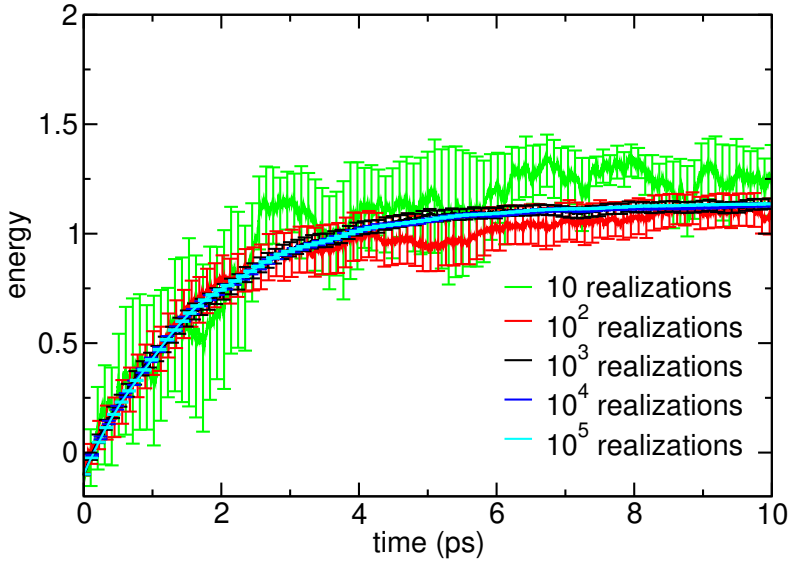

Figure 2.6: Energy convergence (light-heavy-light spin operator order) check for 10^2, 10^3 and 10^4 realizations of the noise. Conditions: $\{\boldsymbol{s}(0) = \boldsymbol{x}, \boldsymbol{S}(0) = -\boldsymbol{x}, \boldsymbol{\Omega} = 2\pi\boldsymbol{z}\,\text{GHz}, \boldsymbol{\omega} = \frac{\pi}{2}\boldsymbol{z}\,\text{GHz}, J = 0.1\,\text{GHz}, \alpha = 0.3, D = 0.3\,\text{GHz}\}$.

Now that we have selected which scheme is most suitable for our problem, *i.e* the heavy-light-heavy integration scheme, we proceed to use it for the dynamics of the first-order moments, for the light and heavy spin, for three test configurations, in order to have a baseline for comparison with the effective model.

2.3.2 Comparing code runs to test configurations

As mentioned in the previous section, we will now proceed to test our stochastic integration scheme on three test cases.

We want to study solutions which relax towards equilibrium, which if the spins both align with an effective field, can be summarized by

$$\dot{\boldsymbol{s}_{\text{eq}}} = \dot{\boldsymbol{S}_{\text{eq}}} = 0 \tag{2.52}$$

Recalling eq. (2.11) we have

$$\begin{cases} \boldsymbol{s}_{\text{eq}} = A\left(\boldsymbol{\omega} + J\boldsymbol{S}_{\text{eq}}\right) \\ \boldsymbol{S}_{\text{eq}} = \dfrac{B}{1+\alpha^2}\left[\left(\boldsymbol{\Omega} + J\boldsymbol{s}_{\text{eq}} + \boldsymbol{\eta}\right) - \alpha\left(\boldsymbol{\Omega} + J\boldsymbol{s}_{\text{eq}}\right) \times \boldsymbol{S}_{\text{eq}}\right] \end{cases} \tag{2.53}$$

where A and B characterize which is the dominant dynamics which rules the final equilibrium. Replacing $\boldsymbol{s}_{\text{eq}}$ in the expression for $\boldsymbol{S}_{\text{eq}}$ in 2.53 we obtain

$$\boldsymbol{S}_{\text{eq}} = \frac{B}{1+\alpha^2}\left[\boldsymbol{\Omega} + JA\boldsymbol{\omega} + J^2A\boldsymbol{S}_{\text{eq}} + \boldsymbol{\eta} - \alpha(\boldsymbol{\Omega} + JA\boldsymbol{\omega} + J^2A\boldsymbol{S}_{\text{eq}}) \times \boldsymbol{S}_{\text{eq}}\right] \tag{2.54}$$

As our assumption is that both spins would relax towards their respective effective field, we will choose $\boldsymbol{\omega}$ and $\boldsymbol{\Omega}$ to be collinear for our numerical studies, this means any cross product between any of the spins and any of the effective field vanishes, once equilibrium is reached, thus yielding

$$\begin{cases} \boldsymbol{s}_{\text{eq}} = A\left(\boldsymbol{\omega} + \dfrac{JB}{1+\alpha^2 - BJ^2A}\left[\boldsymbol{\Omega} + JA\boldsymbol{\omega} + \boldsymbol{\eta}\right]\right) \\ \boldsymbol{S}_{\text{eq}} = \dfrac{B}{1+\alpha^2 - BJ^2A}\left[\boldsymbol{\Omega} + JA\boldsymbol{\omega} + \boldsymbol{\eta}\right] \end{cases} \tag{2.55}$$

Once we average over the noise, we find

$$\begin{cases} \langle \boldsymbol{s}_{\text{eq}} \rangle = A\left[\boldsymbol{\omega} + \dfrac{JB}{1+\alpha^2 - BJ^2A}\left(\boldsymbol{\Omega} + JA\boldsymbol{\omega}\right)\right] \\ \langle \boldsymbol{S}_{\text{eq}} \rangle = \dfrac{B}{1+\alpha^2 - BJ^2A}\left[\boldsymbol{\Omega} + JA\boldsymbol{\omega}\right] \end{cases} \tag{2.56}$$

This means that, for long times, we can expect to find an equilibrium solution, where both spins are aligned with the axis of $\boldsymbol{\Omega}$ and $\boldsymbol{\omega}$. If we take for example, $A = B = 1$, $\alpha = J = 0.01$, $\boldsymbol{\Omega} = -\boldsymbol{\omega} = \boldsymbol{z}$ then we get

$$\begin{cases} \langle \boldsymbol{s}_{\text{eq}} \rangle = 0.9901\boldsymbol{z} \\ \langle \boldsymbol{S}_{\text{eq}} \rangle = -0.99\boldsymbol{z} \end{cases} \tag{2.57}$$

for which both spins indeed align with their external fields with slightly lower norm (both similar) than initially. if we take different values for both fields, *i.e.*, $\boldsymbol{\omega} = -0.5\boldsymbol{z}$ and $\boldsymbol{\Omega} = \boldsymbol{z}$ then we get

$$\begin{cases} \langle \boldsymbol{s}_{\text{eq}} \rangle = -0.49\boldsymbol{z} \\ \\ \langle \boldsymbol{S}_{\text{eq}} \rangle = 0.995\boldsymbol{z} \end{cases} \tag{2.58}$$

Here again both spins align with their external fields with lower than initial norm. The spins thus tend to try and reach the equilibrium given by their respective effective fields.

We will thus take different amplitudes for the external fields in order to determine how they compete, and we will also study how the exchange influences the dynamics, and whether or not this can prevent the system from reaching equilibrium.

Initial conditions for the spins for each case are generated randomly. We choose logarithmic timescales to display long time behavior such that $t_{log} = ln(\frac{t}{t_0})$ and $t_0 = 1\,ps$.

- Our first test configuration will be a softly damped ($\alpha = 0.2$) system with noise amplitude $D = 0.3$ GHz, results and numerical parameters are displayed in Figure 2.7. After some transient period when both spins display very similar behavior, as is

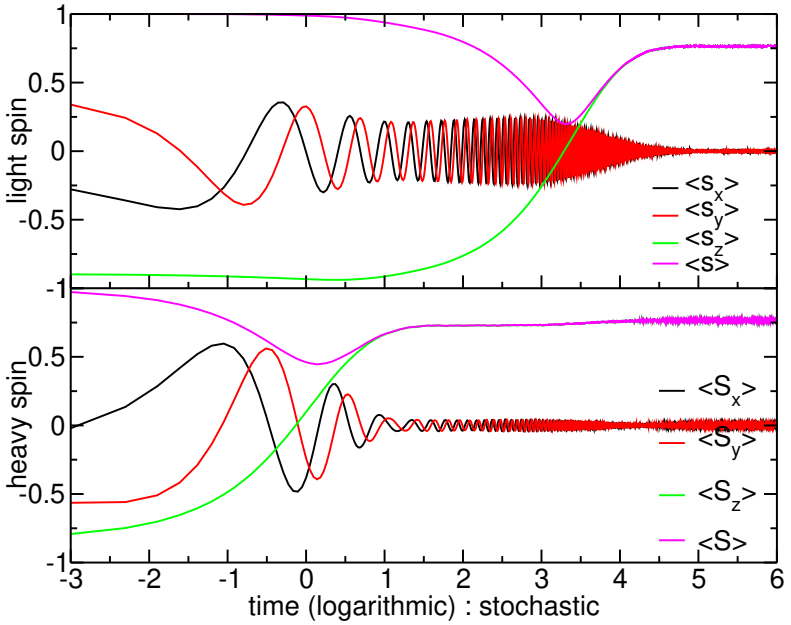

Figure 2.7: Stochastic solutions (10^5 realizations of the noise) with the conditions : $\{s_x(0) = -0.172098,\ s_y(0) = 0.409099,\ s_z(0) = -0.896114,\ S_x(0) = -0.165619,\ S_y(0) = -0.528101,\ S_z(0) = -0.832874,\ D = 0.3$ GHz, $\alpha = 0.2$, $\boldsymbol{\omega} = 2\pi\boldsymbol{z}$ GHz, $\boldsymbol{\Omega} = 2\pi\boldsymbol{z}$ GHz and $J = 0.3$ GHz$\}$

to be expected because $\boldsymbol{\omega} = \boldsymbol{\Omega}$, one can see that the averages for both the heavy and the light spin seem to reach an equilibrium state where the norm of each of them is lower than their initial norm; thus, both systems seem to display longitudinal

damping ($||\langle \boldsymbol{s} \rangle(\infty)|| < ||\langle \boldsymbol{s} \rangle(0)||$), without imposing it *ad hoc*, although there is no explicit coupling to the noise for the light spin, only through exchange with the heavy spin. For reference, this curve has been produced in a little over 10 hours, for 10^5 realizations of the noise. To compare to our analytical simplified model eq. (2.56), the equilibrium can be described by $A \approx 0.115$ and $B \approx 0.120$. These results will serve as a reference case for the next chapter in order to check the differences with the deterministic model.

- In the second test case, we begin by imposing two different external fields, as $\boldsymbol{\omega} = 2\pi \boldsymbol{z}$ GHz and $\boldsymbol{\Omega} = \dfrac{2\pi}{7} \boldsymbol{z}$ GHz. Results are displayed in Figure 2.8. For the heavy spin,

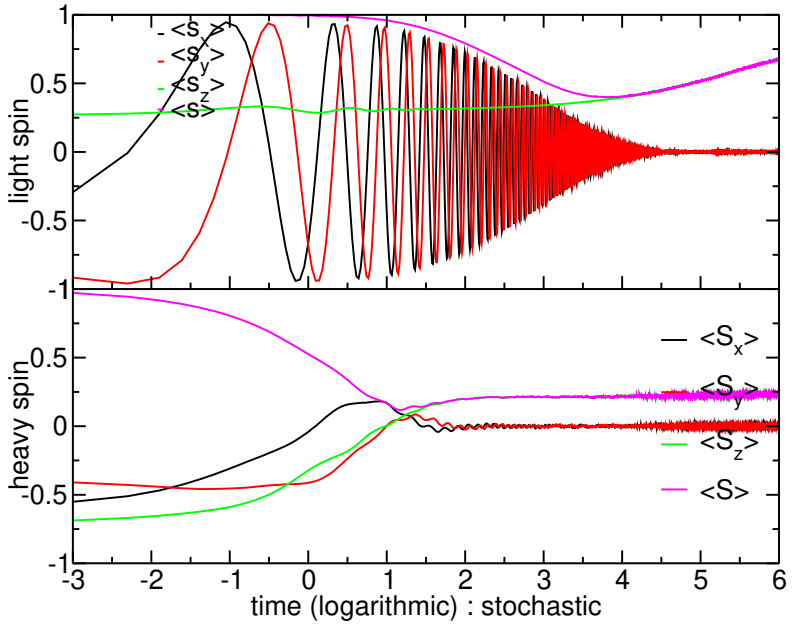

Figure 2.8: Stochastic solutions (10^5 realizations of the noise) with the conditions $\{s_x(0) = -0.551323,\ s_y(0) = -0.790046,\ s_z(0) = 0.268087,\ S_x(0) = -0.589254,\ S_y(0) = -0.385068,\ S_z(0) = -0.710283,\ D = 0.3$ GHz, $\alpha = 0.2$, $\boldsymbol{\omega} = 2\pi \boldsymbol{z}$ GHz, $\boldsymbol{\Omega} = \dfrac{2\pi}{7} \boldsymbol{z}$ GHz and $J = 0.3$ GHz$\}$, On the lower set, effective solutions with the same conditions as on the upper one with $\{\langle s_i s_j \rangle(0) = s_i(0)s_j(0),\ \langle s_i S_j \rangle(0) = s_i(0)S_j(0),\ \langle S_i S_j \rangle(0) = S_i(0)S_j(0)\}$

as in the previous case, we can see that, after some transient period, it reaches an equilibrium with lower norm (for the average). The situation is different for the light spin, however. It seems that no equilibrium is reached within the simulation time. One also notices that the heavy spin's precession frequency progressively becomes equal to that of the light spin, after a short transient period, where one can see a superposition of both frequencies for the heavy spin–i.e., beats.

- For the third test case, displayed in Figure 2.9, a stronger exchange coupling is chosen, as this should result in a situation more difficult to obtain with the effective model, for which Gaussian closure relies (partly) on the fact that the noise amplitude

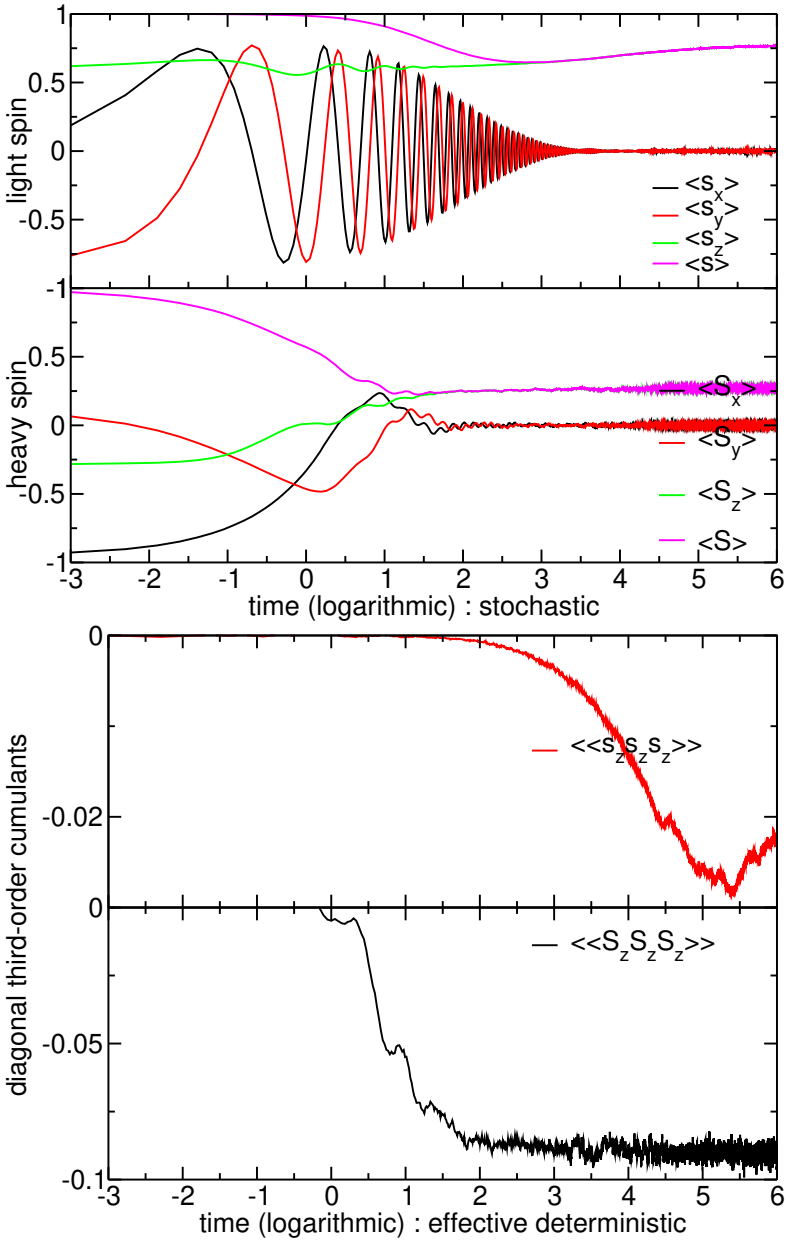

Figure 2.9: On the upper set, stochastic solutions (1.2×10^4 realizations of the noise) with the conditions: $\{s_x(0) = -0.054083,\ s_y(0) = -0.797312,\ s_z(0) = 0.601140,\ S_x(0) = -0.951202,\ S_y(0) = 0.124420,\ S_z(0) = -0.282373,\ D = 0.3$ GHz, $\alpha = 0.2$, $\boldsymbol{\omega} = 2\pi \boldsymbol{z}$ GHz, $\boldsymbol{\Omega} = \dfrac{2\pi}{7}\boldsymbol{z}$ GHz and $J = 0.5$ GHz$\}$. On the bottom set, diagonal third order cumulants for the light and heavy spin distributions are displayed.

is small. This is done in order to probe the limits of this effective model. We also display one of the third order cumulants for both the heavy and light spins, in order to check if, and for how long, the third order vanishing cumulant assumption remains valid. Here, although the two external fields are not the same, as in the second test case, both the light and heavy spin seem to reach an equilibrium state after some transient period. Here again, the analytical simplified model eq. (2.56) provides the same results as the numerical stochastic model, when taking $A \approx 0.118$ and $B \approx 0.231$. One can see, however, that the third order cumulants are growing over time and become noticeably non-zero. The heavy spin third order cumulant grows more and faster than the light spin one, as can be expected from the fact that the heavy spin is directly coupled to the noise. This in turn means, indeed, that we should encounter problems with the effective approach after some time, which makes the long time limit of the Gaussian closure problematic.

Now that we have the stochastic results for our three test cases, we will proceed to evaluate numerical solutions for the moment hierarchy eqs. (2.36) and (2.37). To this end we will discuss the issues pertaining to setting up a numerical integrator for it.

2.4 A numerical integrator for the moment hierarchy

We now proceed to solve the effective system given by eqs. (2.36) and (2.37). This system deals with deterministic quantities and, as such, is different from the stochastic system. Conversely to what has been done in section 2.3.2, instead of the initial stochastic system, which then had to be averaged to obtain the moments, we directly solve the dynamics of the aforementioned moments. This, however, means that we now have to solve a non-linear, coupled ODE system to obtain the aforementioned dynamics. We cannot proceed as in the previous sections as the equations on the moments do not preserve the geometric properties which were preserved for each realization of the stochastic eq. (2.11). As solving this kind of equations is already a vast subject [78, 82, 83], and not the focus of this study, we will use the GSL [84] library as a "black box."

Using the GSL libraries significantly simplifies the task of integrating this system. One just has to code the system of equations and define a set of parameters which are then used by the GSL integration engine. As there are many available choices, we chose an explicit embedded Runge-Kutta Prince-Dormand 8–9 method [85]. We will, thus, proceed to use the code to integrate our effective system and get numerical results for the same three cases studied with the stochastic integration scheme (cf. section 2.3.2).

In this way, we check the validity of our assumptions for the effective system, namely Gaussian closure and small correlation time limits.

- Results for the first case can be found in Figure 2.10. For reference, for the effective solutions the computing time is around a minute, on the exact same computer as for the stochastic solutions. Here the results are very similar to Figure 2.7 for the transient régime (at short times). One can even see what seems to be a first hint of relaxing towards an equilibrium but, as expected, the integration scheme seems to break down, as suddenly the norm grows very quickly. We will check with the

third case whether or not this can be related to the third-order cumulants becoming non-zero. The behavior for the heavy spin is very similar to the stochastic curve for the same case, as we can observe a transient relaxation period towards the same equilibrium. Only after some time, when the light spin solution seems to diverge around $t_{\log} = 3$ (as this is a rather qualitative than quantitative study, it is difficult to define a precise moment when the integration scheme is no longer valid), the heavy spin solution slowly seems to diverge as well, but as the components are much smaller, the effects are less noticeable and do not grow as quickly.

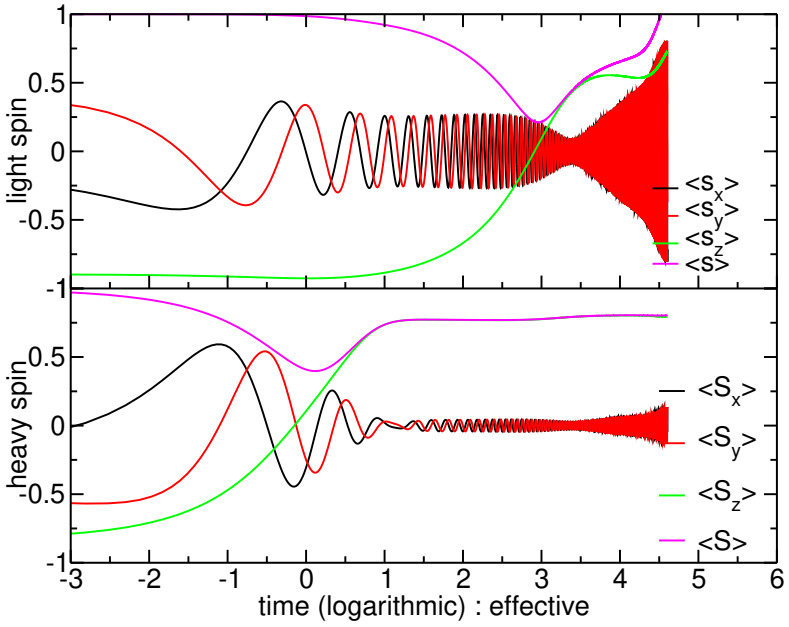

Figure 2.10: Effective solutions with conditions: $\{s_x(0) = -0.172098$, $s_y(0) = 0.409099$, $s_z(0) = -0.896114$, $S_x(0) = -0.165619$, $S_y(0) = -0.528101$, $S_z(0) = -0.832874$, $D = 0.3$ GHz, $\alpha = 0.2$, $\boldsymbol{\omega} = 2\pi \boldsymbol{z}$ GHz, $\boldsymbol{\Omega} = 2\pi \boldsymbol{z}$ GHz and $J = 0.3$ GHz, $\langle s_i s_j \rangle(0) = s_i(0)s_j(0)$, $\langle s_i S_j \rangle(0) = s_i(0)S_j(0)$, $\langle S_i S_j \rangle(0) = S_i(0)S_j(0)\}$

- For the second case, results are displayed in Figure 2.11. Here we can see that as for the stochastic solution, no equilibrium is reached, not even for a short time, but a strange "oscillation" where the norm blows up before becoming smaller again and so forth seems to appear. This could be related to the fact that the external fields are different and would some time act in opposition but we will have to verify if this is also true for the last case. The heavy spin, again, displays very similar behavior to the stochastic case with the notable difference though that the oscillations with the light spin frequency remain visible for a longer time in the effective case before they fade away. It is very likely that the noise averages out those small oscillations, which the effective system displays longer.

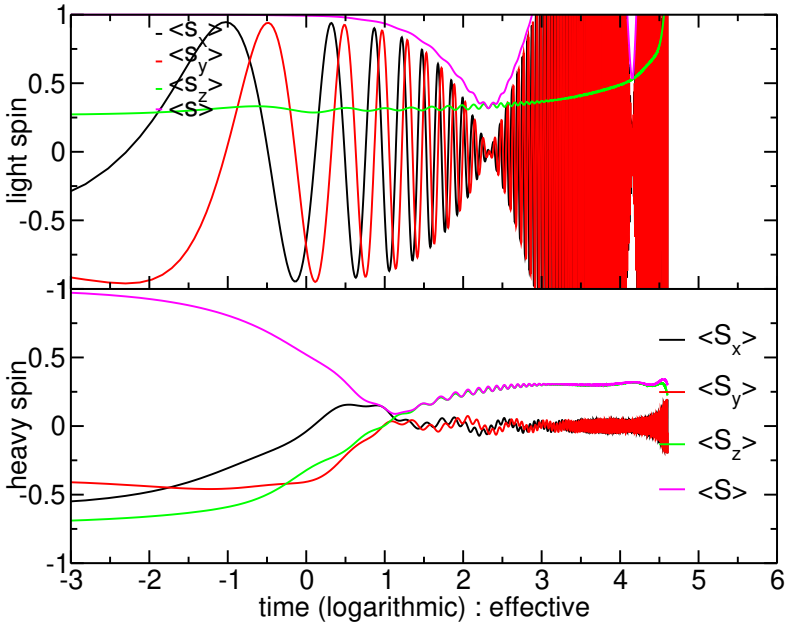

Figure 2.11: Effective solutions with conditions: $\{s_x(0) = -0.551323,\ s_y(0) = -0.790046,\ s_z(0) = 0.268087,\ S_x(0) = -0.589254,\ S_y(0) = -0.385068,\ S_z(0) = -0.710283,\ D = 0.3$ GHz, $\alpha = 0.2$, $\boldsymbol{\omega} = 2\pi \boldsymbol{z}$ GHz, $\boldsymbol{\Omega} = \frac{2\pi}{7}\boldsymbol{z}$ GHz and $J = 0.3$ GHz, $\langle s_i s_j \rangle(0) = s_i(0)s_j(0)$, $\langle s_i S_j \rangle(0) = s_i(0)S_j(0)$, $\langle S_i S_j \rangle(0) = S_i(0)S_j(0)\}$

- The last test case, for which results can be found in Figure 2.12, with a larger coupling constant J seems to reach an equilibrium for the stochastic solution of the light spin but not for the heavy one anymore, this means that the difference in external fields is not what caused this lack of equilibrium state earlier. Also, it seems that here, even the heavy spin effective solution breaks down at the end of the integration window. Of course, the stronger coupling makes the whole system more sensitive to non-linear effects which bring the integration scheme to collapse. Moreover, if we have a look at the third-order cumulants (see Figure 2.9) of the light spin, we can see that the more this cumulant moves away from zero, the less accurate the effective solution becomes, when compared to the stochastic one. For the heavy spin, however, even though this cumulant grows faster and more strongly, the solution seems to remain much more similar to the stochastic case. This can, however, be attributed to the fact that the heavy spin is experiencing a more direct damping, which would quickly erase small differences, whereas the light spin only inherits the damping through the coupling and the averaging.

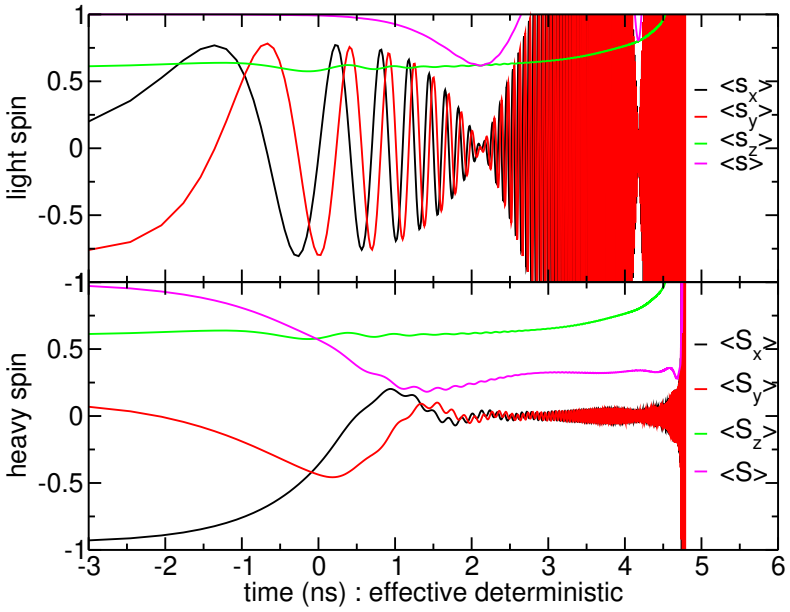

Figure 2.12: Effective solution with conditions: $\{s_x(0) = -0.054083,\ s_y(0) = -0.797312,\ s_z(0) = 0.601140,\ S_x(0) = -0.951202,\ S_y(0) = 0.124420,\ S_z(0) = -0.282373,\ D = 0.3$ GHz, $\alpha = 0.2$, $\boldsymbol{\omega} = 2\pi \boldsymbol{z}$ GHz, $\boldsymbol{\Omega} = \frac{2\pi}{7}\boldsymbol{z}$ GHz and $J = 0.5$ GHz, $\langle s_i s_j \rangle(0) = s_i(0)s_j(0)$, $\langle s_i S_j \rangle(0) = s_i(0)S_j(0)$, $\langle S_i S_j \rangle(0) = S_i(0)S_j(0)\}$.

It is worth noting that although smaller time steps have been investigated, there was no significant change in the plotted curves, even for much smaller integration steps. In order to remain as efficient as possible, we chose to keep a time step of 10^{-5} ps.

To sum up, there are several interesting conclusions that can be drawn.

As long as the Gaussian approximation remains valid, *i.e.,* the third order cumulant can be assumed to vanish, our effective model seems to work pretty well and is wildly more efficient as the 10 hours vs. 1 minute unarguably demonstrate. In both cases, one can see that although the light spin is not directly coupled to the noise, but only indirectly through the heavy spin exchange, it displays not only transverse damping, as does the heavy spin (which includes it explicitly), but also longitudinal damping, as does the heavy spin, without the need for imposing a Bloch-like longitudinal damping term, either on the heavy or on the light spin.

In the stochastic case, on top of the emergence of this longitudinal damping, for some initial conditions and parameters, we can see equilibrated long time solutions where the spins relax to the respective external field's axis with a norm, at equilibrium, which is smaller than the initial norm, thereby describing longitudinal damping.

This particular behavior can be found in magnetostrictive materials where the coupling between magnetic and mechanical degrees of freedom is a possible candidate for such effects [6]. This means that by suitable choice of parameters, for example by choosing the statistical properties of the noise, such an approach should indeed effectively be able to reproduce real magneto-elastic effects.

Now one could argue that these properties of the equilibrium long-time solutions are not as readily deduced from the solutions to the moment hierarchy. Indeed, the non-linearity of the moment equations makes it highly non-trivial to reach long time predictions and one would have to study a variety of initial conditions, in particular for the second-order moments, to detect whether or not it would be possible to effectively reach equilibrium with these, too.

Such considerations provide, however, the motivation and the opportunity for asking more complicated questions such as, which kind of noise distribution would have to be used, in order for different initial conditions to be appropriate and also which kinds of different closure schemes for the hierarchies should be investigated. It seems unavoidable that in order to build the deterministic equivalent model as efficiently as possible, these closing schemes have to be adapted to each family of cases *i.e.*, one has to very carefully check whether or not the hypotheses remain valid and for how long. This makes it a highly efficient approach for very specific cases, but the stochastic approach seems to be much more versatile. One, however, has to have at least one assumption for the stochastic approach which is that the whole system is ergodic [86], namely that it is equivalent to reproduce one experience several times, or to do many experiments just once, before averaging the results. However this approach cannot hope to do more than mimic the behavior of a magneto elastic compound by imposing a statistical distribution for the noise, in order to do so, it would have to be properly "fitted" using an appropriate reference magneto-elastic system. Furthermore, the effects of the mechanical strain are just effectively mimicked by this approach and thus its dynamics is not computed, this means that it does not seem possible to obtain information on the change of shape of a compound from this effective formalism.

As has been covered in the State of the Art, there have been similar approaches [16] where dissipation effects were obtained by introducing the coupling to a noise reservoir of undefined nature. Also, following an inverse approach of ours, the coupling to tensorial elastic degrees of freedom [18] has been investigated through introducing the normal modes expansion of the strain. Some information is lost on the elastic reservoir, but effectively this resembles our approach. The major difference is that in our case, the "microscopic" nature of the noise is not defined and instead of a scalar noise for each equation, we have a vector noise *i.e.*, a spin bath. The spin/spin bath approach is thus interesting and a quite efficient way to simulate thermal or mechanical effects in magnetic materials, as long as one has a method to properly calibrate it beforehand, just as spin dynamics requires other *ab initio* methods such as DFT [87] to be calibrated.

To go further and to study ways to make the interplay between magnetic and mechanical degrees of freedom more transparent, one would need an approach where the parameters and the evolution of both systems can be described on an equal footing. This is why we shall now go on to our next step which is simulating magneto-elasticity through a Lagrangian model.

Summary

- The stochastic model reproduces expected behavior where the system relaxes towards an equilibrium of lower norm for the spin averages of both light and heavy spin, thus indicating longitudinal dissipation
- The effective model displays similar transient behavior but cannot reproduce long time effects, the Gaussian closure assumption seems to break down. They, however, seem to indicate equilibrium solutions before the numerical system becomes unstable.
- Not all configurations relax towards equilibrium, stochastically. This relaxation depends on initial conditions for the spin but also on the external field configuration and on the exchange and noise intensity, as the phase space volume dynamics depends on these quantities.
- Stronger exchange coupling makes the systemic error for the effective model bigger. This is consistent with the fact that the stronger the coupling, the more the coupled effective system should become sensitive to non-linear effects.

Chapter 3

A Lagrangian approach to magnetoelasticity

Résumé

- Nous construisons une théorie de champs pour l'interaction d'un spin et de la déformation mécanique d'un milieu élastique, par une approche Lagrangienne.
- Nous en déduisons les équations du mouvement en prenant soin de définir convenablement la variable de spin.
- Nous proposons un modèle à plusieurs particules en interaction purement magnétique en "colorant" les équations du mouvement précédentes.
- Nous résolvons numériquement les équations obtenues afin de modéliser le retournement du paramètre d'ordre de Néel pour un "modèle jouet" de NiO antiferromagnétique

What is usually done in Lagrangian mechanics is to postulate a Lagrangian density $\mathscr{L}(t, \boldsymbol{q}_i, \dot{\boldsymbol{q}}_i)$, depending on the coordinates $\boldsymbol{q}$ of the system, their time derivatives $\dot{\boldsymbol{q}}$, possibly explicitly on time t and which expresses the symmetries of this system. From the Lagrangian, one defines the action $\mathcal{S}$ as

$$\mathcal{S} = \int \mathscr{L} dt \tag{3.1}$$

which contains more "global" information than the Lagrangian itself.

The equations of motion are obtained by extremizing the action, *i.e.*, from the condition $dS = 0$. These are the Euler-Lagrange equations, which read

$$\frac{\partial \mathscr{L}}{\partial \boldsymbol{q}_i} - \frac{d}{dt}\frac{\partial \mathscr{L}}{\partial \dot{\boldsymbol{q}}_i} = 0 \tag{3.2}$$

It is useful to separate the "potential" (no time derivatives) and "kinetic" (contain time derivatives) contributions, as for example

$$\mathscr{L} = \frac{\dot{\boldsymbol{q}}^2}{2} - V(\boldsymbol{q}) \tag{3.3}$$

In terms of these, the Euler-Lagrange equations of motion take the form

$$\ddot{\boldsymbol{q}} + \frac{\partial V(\boldsymbol{q})}{\partial \boldsymbol{q}} = 0 \tag{3.4}$$

and it is interesting to note that they are of second order in the positions.

What is striking is that this is not the case for Larmor spin ($\boldsymbol{s}$) precession around an external field ($\boldsymbol{\omega}$), which is of first order in the dynamical variable, $\boldsymbol{s}$:

$$\dot{\boldsymbol{s}} = \boldsymbol{\omega} \times \boldsymbol{s} \tag{3.5}$$

and it does not seem useful to define $\boldsymbol{s} \equiv \dot{\boldsymbol{\tau}}$, for instance. There is not any notion of a "position" whose "velocity" would be the spin variable, in the same way as is the case for the "true" position of a particle.

This has the following, interesting, consequence: if the Lagrangian can be expressed as

$$\mathscr{L} = (\dot{\boldsymbol{s}} - \boldsymbol{A}(\boldsymbol{s}))^2 \tag{3.6}$$

where $\boldsymbol{A}(\boldsymbol{s})$ is identified with a "vector potential," that cannot be written as the gradient of a scalar (*i.e.,* the magnetic field is non-zero), then it is obvious that a way to extremize the Action is to note that this Lagrangian vanishes and the action attains its minimum, when

$$\dot{\boldsymbol{s}} = \boldsymbol{A}(\boldsymbol{s}) \tag{3.7}$$

which now indeed is a first order equation of motion. This is, indeed, what is appropriate for an (electrically) charged particle in a magnetic field and is equivalent to the usual equation of motion, that is of second order in the "position."

While there are different ways to obtain first-order EOM, nevertheless it is this feature, which motivated us to search for different Lagrangian formulations for magnetism and for ways to couple magnetic and mechanical DOF through such an approach.

In order to acquire a better understanding of the interplay between magnetic and mechanical degrees of freedom, we have to build a model for their interaction, thereby setting the results of the previous chapter in a broad framework.

Where previous approaches have been dealing with magnetic interactions depending on distances between magnetic particles, such as magnetic molecular dynamics, we shall build the simplest classical field theory to describe the consequences of local interactions between these magnetic and mechanical degrees of freedom in a different fashion. Indeed, the framework of magnetic molecular dynamics imposes that one change each particle's position during the dynamics and compute nearest neighbors at each time step, which is expensive in computational resources. The idea here will be to build two field theories, one for the spin, the other for the lattice, and then build an interaction term in the language of field theory. While this approach is identical to molecular dynamics for the one–particle case, though it provides insight into the symmetries more directly; it proves particularly effective in the many-particle case, since the field equations do not evolve individual particles, but fields, that are superpositions thereof.

This is what we shall now proceed to do by building a Lagrangian model for the spin and the mechanical strain.

3.1 Constructing a Lagrangian model in terms of spin and "local-virtual" mechanical strains

We begin with a simple model, where we have point-like objects, carrying, either, a classical spin vector $\boldsymbol{s}$, or a mechanical strain tensor $\boldsymbol{\epsilon}$; these are the dynamical variables that depend only on time. So, in the simplest case, we have *two* "particles" and we shall apply the rules discussed above to construct the corresponding Lagrangians for the free particles and then, their interaction.

The full Lagrangian $\mathscr{L}$ is, thus, built as a sum of three terms. The magnetic part $\mathscr{L}_s$, the mechanical part $\mathscr{L}_m$, and the coupling term $\mathscr{L}_{sm}$. The magnetic part depends on the spin $\boldsymbol{s}(t)$ and its velocity $\dot{\boldsymbol{s}}(t)$ in such a way that, as is usual, one has a kinetic energy term $\frac{m_{\boldsymbol{s}}}{2}\dot{\boldsymbol{s}}^2$, a potential energy $V_{\boldsymbol{s}}$.

In order to describe precession, what is needed is a "vector potential," mimicking the dynamics of an electrically charged particle in a magnetic field [88, 89], as per eq. (3.6).

The mechanical part $\mathscr{L}_m$ describes the dynamics of the strain tensor $\boldsymbol{\epsilon}(t)$, along with its "velocity" $\dot{\boldsymbol{\epsilon}}(t)$.

It is interesting that a corresponding kinetic term $\frac{m_{\boldsymbol{\epsilon}}}{2}\dot{\boldsymbol{\epsilon}}^2$ and a potential energy $V_{\boldsymbol{\epsilon}}$ [90] can be defined for it. Since the strain tensor is a two–index object, what is implied in these expressions is the trace–in full:

$$\mathscr{L}_m = \mathrm{Tr}\left[\frac{1}{2}\dot{\epsilon}^{\mathrm{T}}\dot{\epsilon} - V(\epsilon^{\mathrm{T}}\epsilon)\right] \tag{3.8}$$

where the notation ϵ^{T} stands for the transposed tensor of ϵ.

In order to keep things simple for the mechanical part, we will take the potential V

to be quadratic in the strain; this describes an extension of Hooke's law to the dynamical case [91].

We can introduce anisotropy and/or inhomogeneity in the medium by writing the potential V as

$$V_\epsilon \equiv \frac{1}{2} C_{ijkl}\epsilon_{ij}\epsilon_{kl} \tag{3.9}$$

where Latin indices range from 1 to 3. Here C is the elastic stiffness tensor. It is possible to define the so-called elastic compliance tensor S [59] through the relation

$$C_{ijkl}S_{ijmn} = \frac{1}{2}\left(\delta_{km}\delta_{ln} + \delta_{kn}\delta_{lm}\right) \tag{3.10}$$

Let us now discuss how symmetry principles constrain the possible interaction terms between the $\boldsymbol{s}(t)$ and the $\epsilon(t)$ "particles."

Since they describe effects that mix magnetism and elasticity, these are more commonly known as "magnetoelastic terms" [6].

Since we want to highlight the fact that the spin satisfies first-order equations of motion, while the strain satisfies second-order equations of motion, this will affect the way the symmetries affect the interactions.

We will, therefore couple spin and strain in a slightly different fashion than what's done in the literature: instead of coupling $\boldsymbol{s}$ and $\boldsymbol{\epsilon}$, we will couple the strain to $\dot{\boldsymbol{s}}$, following, in fact, ref. [23].

We shall, thus, introduce a matrix $\boldsymbol{B}$, such that

$$\mathscr{L}_{\text{sm}} = -\frac{1}{2} B_{ijkl}\dot{s}_i\dot{s}_j\epsilon_{kl}$$

which provides a definition of the magneto-elastic constants.

This trick allows us to write an equation of motion, which is of first order, for the spin.

The full Lagrangian can, therefore, be written as

$$\begin{cases} \mathscr{L}_{\text{s}} = \dfrac{m_s}{2}\dot{s}_i^2 + \dot{s}_i A_i[\boldsymbol{s}] - V_s[\boldsymbol{s}] \\ \mathscr{L}_{\text{m}} = \dfrac{m_\epsilon}{2}\dot{\epsilon}_{ij}^2 - V_\epsilon[\boldsymbol{\epsilon}] \\ \mathscr{L}_{\text{sm}} = -\dfrac{1}{2} B_{ijkl}\dot{s}_i\dot{s}_j\epsilon_{kl} \end{cases} \tag{3.11}$$

where m_s can be interpreted as the gyromagnetic ratio and m_ϵ as an effective inertia for the strain. Thus the total Lagrangian is given by

$$\mathscr{L}_{\text{tot}} = \mathscr{L}_{\text{s}} + \mathscr{L}_{\text{m}} + \mathscr{L}_{\text{sm}} + \frac{dU}{dt} \tag{3.12}$$

where one should recall that any total derivative $\dfrac{dU}{dt}$ added to the Lagrangian will yield exactly the same equations of motion. In the next section, we focus on the equations of motion, that include the interaction terms and discuss the physics they encode.

3.2 Computing the equations of motion in terms of auxiliary variables

Now that we have a Lagrangian system, we can deduce equations of motion for our system. This is done in the usual fashion, namely by identifying them as the Euler-Lagrange equations:

$$\begin{cases} \dfrac{\partial \mathscr{L}_{tot}}{\partial \boldsymbol{s}} - \dfrac{d}{dt}\dfrac{\partial \mathscr{L}_{tot}}{\partial \dot{\boldsymbol{s}}} = 0 \\ \dfrac{\partial \mathscr{L}_{tot}}{\partial \boldsymbol{\epsilon}} - \dfrac{d}{dt}\dfrac{\partial \mathscr{L}_{tot}}{\partial \dot{\boldsymbol{\epsilon}}} = 0 \end{cases} \tag{3.13}$$

Thus the EOM given by the Lagrangian eq. (3.12) read as follows

$$\begin{cases} m_s \ddot{s}_i + \left(\dfrac{\partial A_i}{\partial s_j} - \dfrac{\partial A_j}{\partial s_i}\right)\dot{s}_j + \dfrac{\partial V_s}{\partial s_i} - B_{ijkl}\left(\ddot{s}_j \epsilon_{kl} + \dot{s}_j \dot{\epsilon}_{kl}\right) = 0 \\ m_\epsilon \ddot{\epsilon}_{ij} + \dfrac{\partial V_\epsilon}{\partial \epsilon_{ij}} + \dfrac{1}{2} B_{klij}\dot{s}_k \dot{s}_l = 0 \end{cases} \tag{3.14}$$

As mentioned in section 3.1, the variable we are interested in is $\dot{\boldsymbol{s}}$. By focusing on the time derivative of $\boldsymbol{s}$ instead of $\boldsymbol{s}$ itself, we end up with a first-order ODE for the spin. This introduces some subtleties, especially for the coupling. One could argue that this is not, at least historically, how this coupling has been introduced [6]. The idea is to interpret what we call spin as an "emergent" property, depending on underlying "hidden" variables [22, 92]. Indeed, as $\boldsymbol{s}$ does display hysteresis effects [93], which implies that it depends on its own history, motivates describing this property in terms of a "hidden" variable. Thus we introduce a variable $\boldsymbol{\mu} \equiv \dot{\boldsymbol{s}}$, which we shall call spin as is usually – classically – considered. We would like to insist here that this variable $\boldsymbol{\mu}$ is to be compared to the usual spin, and not the actual time derivative. The reason why we introduce this is simple. The coupling in the case of the charged particle in an electromagnetic field relies on the fact that there are point–like electric charges. There are, however, no magnetic – local – charges, *i.e.,* monopoles. But, by introducing the variable $\boldsymbol{\mu}$ as the velocity of $\boldsymbol{s}$, we introduce exactly what we needed, namely that the variable is nonlocal, thereby describing how $\boldsymbol{s}$ depends on the whole history of $\boldsymbol{\mu}$

$$\boldsymbol{s}(t) - \boldsymbol{s}(0) = \int_0^t \dot{\boldsymbol{s}}(\tau)d\tau \Leftrightarrow \int_0^t \boldsymbol{\mu}(\tau)d\tau \tag{3.15}$$

where $\boldsymbol{s}(0)$ needs to be explicitly given. We will choose $\boldsymbol{s}(0) = 0$ in order not to have to keep track of this constant during the calculations.

A remarkable property of (3.14) is that they remain invariant, if we add the gradient of a function to the "vector potential," *i.e.,* $\mathbf{A}(\mathbf{s}) \to \mathbf{A}(\mathbf{s}) + \partial_{\mathbf{s}} f(\mathbf{s})$. This motivates introducing the antisymmetric Faraday tensor F_{ij} by

$$F_{ij} = \frac{\partial A_i}{\partial s_j} - \frac{\partial A_j}{\partial s_i} \tag{3.16}$$

We can thus rewrite eqs. (3.14) in terms of μ

$$\begin{cases} m_s\dot{\mu}_i + F_{ij}\mu_j + \dfrac{\partial V_s}{\partial s_i} - B_{ijkl}\left(\dot{\mu}_j\epsilon_{kl} + \mu_j\dot{\epsilon}_{kl}\right) = 0 \\ m_\epsilon\ddot{\epsilon}_{ij} + \dfrac{\partial V_\epsilon}{\partial \epsilon_{ij}} + \dfrac{1}{2}B_{klij}\mu_k\mu_l = 0 \end{cases} \tag{3.17}$$

While these equations do describe the consistent interaction of spin and strain, they do not take into account non–conservative effects. Such effects are described by terms that appear on the RHS of the Euler–Lagrange equations and cannot be described by either a scalar or a vector potential. They're of great practical relevance, of course, and describe how the system relaxes to equilibrium. It is possible to describe their effects, without having to specify in detail the microscopic degrees of freedom that define them.

Indeed, magnetic systems can exchange energy with other systems for example either by being driven by an external field, or by radiating thermally. This is why, in the following section, we will introduce the corresponding terms that can describe such dissipative effects and non–conservative terms, more generally.

3.2.1 Introducing dissipation and non-conservative terms through losses and sources

Conventionally, the Lagrangian or equivalently the Hamiltonian framework are – inherently – conservative approaches [94], which means that they cannot describe non–conservative terms, by definition. To describe non–conservative terms requires some care [95]. They are defined by sources.

The expression for the sources, $\mathscr{L}_{\text{sources}}$ can be written as

$$\mathscr{L}_{sources} = -j_i^{\text{ext}}[\boldsymbol{s}]\dot{s}_i - \sigma_{ij}^{\text{ext}}\epsilon_{ij} \tag{3.18}$$

since these are the only terms that are linear in the dynamical variables and invariant under rotations. Further properties reflect the dynamics.

Here j_i^{ext} is a conserved – magnetic – current, which does not give rise to spin transfer torque and σ_{ij}^{ext} is an external, spatially uniform and instantaneous mechanical stress tensor. We do not consider cases of non-instantaneous or non-uniform sources in this study.

For the losses, it is, still, a non–trivial problem to write down the corresponding terms in full generality, except for Rayleigh damping. To overcome this issue, we choose to define the losses and sources through their derivatives as

$$\begin{cases} \dfrac{\partial\mathscr{L}_{\text{losses}}}{\partial\dot{\mu}_i} = \dfrac{\partial\mathscr{L}_{\text{losses}}}{\partial\ddot{s}_i} = \alpha\varepsilon_{ijk}\dot{s}_j\ddot{s}_k + J(\dot{s}_i\dot{s}_j p_j - p_i\dot{s}_j\dot{s}_j) \\ \dfrac{\partial\mathscr{L}_{\text{losses}}}{\partial\dot{\epsilon}_{ij}} = \gamma\dot{\epsilon}_{ij} \end{cases} \tag{3.19}$$

These terms turn out to have a clear physical interpretation: α is the Gilbert damping coefficient, J is the Spin Transfer Torque (STT) intensity and $\boldsymbol{p}$ is the STT direction.

Here we introduce this STT as an external source, thus anticipating on later sections where this external torque will serve as a trigger for the switching of the magnetization. The coefficient γ is a mechanical damping parameter. This term is necessary in order for the mechanical system not to oscillate infinitely but rather to relax towards an equilibrium position.

Therefore, the EOM, including the dissipative – non-conservative [95] – parts read as follows

$$\begin{cases} \dfrac{\partial \mathscr{L}}{\partial s_i} - \dfrac{d}{dt}\left(\dfrac{\partial \mathscr{L}}{\partial \dot{s}_i}\right) = \dfrac{\partial \mathscr{L}_{sources}}{\partial \dot{s}_i} + \dfrac{\partial \mathscr{L}_{losses}}{\partial \ddot{s}_i} \\ \dfrac{\partial \mathscr{L}}{\partial \epsilon_{ij}} - \dfrac{d}{dt}\left(\dfrac{\partial \mathscr{L}}{\partial \dot{\epsilon}_{ij}}\right) = \dfrac{\partial \mathscr{L}_{sources}}{\partial \epsilon_{ij}} + \dfrac{\partial \mathscr{L}_{losses}}{\partial \dot{\epsilon}_{ij}} \end{cases} \tag{3.20}$$

More explicitly:

$$\begin{cases} m_s \dot{\mu}_i + F_{ij}\mu_j + \dfrac{\partial V_s}{\partial s_i} - B_{ijkl}\left(\dot{\mu}_j \epsilon_{kl} + \mu_j \dot{\epsilon}_{kl}\right) = j_i \\ m_\epsilon \ddot{\epsilon}_{ij} + \dfrac{\partial V_\epsilon}{\partial \epsilon_{ij}} + \dfrac{1}{2} B_{klij}\mu_k \mu_l = \sigma_{ij} \end{cases} \tag{3.21}$$

where $j_i = j_i^{\text{ext}} + \alpha \varepsilon_{ijk}\mu_j \dot{\mu}_k + J(\mu_i \mu_j p_j - p_i \mu_j \mu_j)$ and $\sigma_{ij} = \sigma_{ij}^{\text{ext}} - \gamma \dot{\epsilon}_{ij}$.

For the simplest case *i.e.*, $V_s = 0$, $B = 0$ and $\boldsymbol{j} = 0$ and $F_{ij} = \varepsilon_{ijk}\omega_k$, we recover a precession equation for the magnetic system $\boldsymbol{\mu}$ as

$$m_s \dot{\boldsymbol{\mu}} = \boldsymbol{\omega} \times \boldsymbol{\mu} \tag{3.22}$$

and if we also have $V_\epsilon = 0$ and σ_{ij} constant, then

$$m_\epsilon \ddot{\epsilon}_{ij} = \sigma_{ij} \tag{3.23}$$

which describes a set of harmonic oscillators for the mechanical system $\boldsymbol{\epsilon}$. Now, one can compute the variation of the phase space volume by computing

$$\frac{\partial \dot{\mu}_i}{\partial \mu_i} + \frac{\partial \dot{\epsilon}_{ij}}{\partial \epsilon_{ij}} = \frac{1}{m_s}(2J\mu_j p_j + B_{jjkl}\dot{\epsilon}_{kl}) - \frac{\gamma}{m_\epsilon} \tag{3.24}$$

where repeated indices are summed over. This means that over time, the volume of our phase space is not conserved. If this variation is negative, then we should move towards a stable equilibrium state. If it is positive, however, then our system may "run away" and never reach a definite equilibrium state. Whether it may reach a "strange attractor" remains a possibility. This will have to be kept in mind in the following sections. One should also recall that as our systems are respectively first and second order ODE for the spin and for the strain, in order to solve these, one must provide initial conditions for $\boldsymbol{\mu}(0)$, $\epsilon_{ij}(0)$ and $\dot{\epsilon}_{ij}(0)$.

Now that we have the EOM for a single particle system, we need to implement the description to larger – many particles – objects. One way to do this is through a magnetic exchange interaction.

3.3 Extending the model to multi-particle systems through a magnetic exchange interaction

In order to describe larger systems, we will define several domains with uniform magnetic and mechanical properties by introducing several particle-like sites. Hence, we will describe this collection of domains by a "colored" set of equations, by introducing a label, L, that takes values 1 to N, in the expressions (3.21).

$$\begin{cases} m_s^L \dot{\mu}_i^L + F_{ij}\mu_j^L + \dfrac{\partial V_s}{\partial s_i^L} - B_{ijkl}\left(\dot{\mu}_j^L \epsilon_{kl}^L + \mu_j^L \dot{\epsilon}_{kl}^L\right) = j_i^L \\ m_\epsilon^L \ddot{\epsilon}_{ij}^L + \dfrac{\partial V_\epsilon}{\partial \epsilon_{ij}^L} + \dfrac{1}{2} B_{klij}\mu_k^L \mu_l^L = \sigma_{ij}^L \end{cases} \tag{3.25}$$

as well as initial conditions for $\boldsymbol{\mu}^{(L)}(0)$, $\epsilon_{ij}^{(L)}(0)$ and $\dot{\epsilon}_{ij}^{(L)}(0)$.

The way the "particles," labeled by L, interact can be described as follows:

As the main aspect we are interested in is the magnetic behavior, we shall introduce a simple coupling through a magnetic exchange given by

$$\boldsymbol{\omega}_{\text{eff}}^L = \boldsymbol{\omega}^L + \omega_E^L \sum_{P \in NN} \boldsymbol{s}^P - \omega_a^L \boldsymbol{n}^L \left(\boldsymbol{n}^L . \boldsymbol{s}\right) \tag{3.26}$$

where ω_E^L is the exchange frequency and $P \in NN$ stands for the sum over all nearest neighbors. And we have also introduced a global magnetic anisotropy with frequency ω_a^L and direction $\boldsymbol{n}^L$ in order to favor relaxation towards a given local easy-axis and equilibrium solutions. Here we made a non-trivial choice, namely having an ultra-local mechanical interaction, having only a self-interaction on each site through the mechanical potential. This is a simplifying assumption as this would introduce much more complicated features such as Edwards field theories and granular field theories [96] for non-local strains and stresses correlations.

Now that we have constructed a – multi-particle – interacting model, we shall go on to study the simplest case, that of two particles, *i.e.,* $L = 2$. This case is relevant for describing the switching behavior for the magnetization for a toy model of an antiferromagnet, namely NiO, that's driven by an external STT. This STT can be for example generated by a spin polarized current (not a "simple" electric current), which acts on a given magnetic moment as a torque term. Though this is a simple, mean field model, that describes an antiferromagnet by two subdomains of opposite magnetization, it, nonetheless, captures the salient features of the physics and is based on the Néel model[97].

3.4 The switching of magnetization of a toy model AF for NiO through an external STT

As mentioned in section 3.3, we shall describe here a test case where $L = 2$, as this is the simplest case for an antiferromagnet, with two magnetic sublattices. As a further

simplification, we chose to study cases where the spin potential does not act on each lattice site and there is not any external magnetic current *i.e.*

$$\begin{cases} \dfrac{\partial V_s}{\partial s_i^L} = 0 \\ \\ \boldsymbol{j}^{\text{ext}} = \mathbf{0} \end{cases} \tag{3.27}$$

We shall also define, for convenience, for the magnetic part, the net magnetization $\boldsymbol{m}$ as

$$\boldsymbol{m} \equiv \frac{1}{2}\left(\boldsymbol{\mu}^1 + \boldsymbol{\mu}^2\right) \tag{3.28}$$

and the Néel order parameter $\boldsymbol{l}$ [98–101], as

$$\boldsymbol{l} \equiv \frac{1}{2}\left(\boldsymbol{\mu}^1 - \boldsymbol{\mu}^2\right) \tag{3.29}$$

For the mechanical part, we shall define the ferromagnetic "net strain" matrix ϵ_{ij}

$$\epsilon_{ij} \equiv \frac{1}{2}\left(\epsilon_{ij}^1 + \epsilon_{ij}^2\right) \tag{3.30}$$

As for the magnetic part, one could also define the antiferromagnetic Néel strain matrix η_{ij}

$$\eta_{ij} \equiv \frac{1}{2}\left(\epsilon_{ij}^1 - \epsilon_{ij}^2\right) \tag{3.31}$$

Now in order to make the precession effects easier to see, we can write down the spin part of eq. (3.21) in the Landau-Lifshitz-Gilbert-Slonczewski form as

$$M_{ij}^L \dot{\mu}_j^L + D_{ij}^L \mu_j^l = j_i^L \tag{3.32}$$

with $M_{ij}^L \equiv \delta_{ij} m_s^L - B_{ijkl}\epsilon_{kl}^L$ and $D_{ij}^L \equiv F_{ij} - B_{ijkl}\dot{\epsilon}_{kl}^L$. If B vanishes, then D_{ij}^L is totally antisymmetric, and when $\boldsymbol{j} = \mathbf{0}$, we recover the usual spin precession equation. If the medium under study is isotropic, then we can express C – the elastic stiffness tensor – and B – the magnetoelastic constants – using only two independent material constants for each: [6]

$$\begin{cases} B_{ijkl} &= B_0\delta_{ij}\delta_{kl} + B_1(\delta_{ik}\delta_{jl} + \delta_{il}\delta_{jk}) \\ C_{ijkl} &= C_0\delta_{ij}\delta_{kl} + C_1(\delta_{ik}\delta_{jl} + \delta_{il}\delta_{jk}) \end{cases} \tag{3.33}$$

Here C_0 and C_1 are more commonly known as the Lamé coefficients [59]. Consequently, these relations hold for a material with spherically symmetric elastic properties. These constants can be recast in more familiar form as

$$\begin{cases} C_0 + \dfrac{2C_1}{3} \equiv \kappa \text{ bulk modulus} \\ \\ C_1 \equiv G \text{ shear modulus} \\ \\ \dfrac{C_1(3C_0 + 2C_1)}{C_0 + C_1} \equiv E \text{ Young modulus} \end{cases} \tag{3.34}$$

These quantities are usually derived either by ab initio methods or experimentally. In order for these quantities to be dimensionless, we divide σ_{ij}^{ext}, B_0, B_1, C_0 and C_1 by $\mu_0 M_s^2$ – where M_s is the saturation magnetization – . To sum up, we get the following expression

$$\begin{cases} \dfrac{\partial V_\epsilon}{\partial \epsilon_{ij}} = 2C_{ijkl}\epsilon_{kl} = C_0\delta_{ij}\epsilon_{kk} + 2C_1\epsilon_{ij} \\ B_{ijkl}\left(\dot{\mu}_j^L\epsilon_{kl}^L + \mu_j^L\dot{\epsilon}_{kl}^L\right) = B_0\left(\dot{\mu}_i\epsilon_{kk} + \mu_i\dot{\epsilon_{kk}}\right) + 2B_1\left(\dot{\mu}_k\epsilon_{ik} + 2B_1\mu_k\dot{\epsilon_{ik}}\right) \\ B_{klij}\mu_k\mu_l = B_0\delta_{ij}\mu_k\mu_k + 2B_1\mu_i\mu_j \end{cases} \tag{3.35}$$

And given these expressions the final system we will consider is

$$\begin{cases} m_s\dot{\mu}_i^L + F_{ij}\mu_j^L - \left[B_0\left(\dot{\mu}_i^L\epsilon_{kk}^L + \mu_i^L\dot{\epsilon}_{kk}^L\right) + 2B_1\left(\dot{\mu}_k^L\epsilon_{ik}^L + 2B_1\mu_k^L\dot{\epsilon}_{ik}^L\right)\right] \\ \qquad = \alpha\varepsilon_{ijk}\mu_j^L\dot{\mu}_k^L + J(\mu_i^L\mu_j^L p_j - p_i\mu_j^L\mu_j^L) \\ m_\epsilon\ddot{\epsilon}_{ij}^L + C_0\delta_{ij}\epsilon_{kk}^L + 2C_1\epsilon_{ij}^L + \dfrac{B_0}{2}\delta_{ij}\mu_k^L\mu_k^L + B_1\mu_i^L\mu_j^L = \sigma_{ij}^{\text{ext}} - \gamma\dot{\epsilon}_{ij}^L \end{cases} \tag{3.36}$$

Where $L = \{1, 2\}$ for the two sub lattices. Now that we have the final form for the EOM, we want to study how the magnetization switches in this system, due to the spin transfer torque. Indeed, as eq. (3.24) shows, the STT provides a way to enlarge the phase space. The new states describe configurations, where both spins are no longer aligned with the easy axis. Once the STT pulse is over, however, the spins may relax towards alignment with the easy axis again, but in the opposite direction. This is called switching.

We will study the magnetization switching by numerical integration of the coupled EOM.

3.4.1 Studying the magnetization switching by numerical integration of the coupled EOM

We now proceed with the numerical integration of the equations of motion. We start with the simplest antiferromagnetic (AF) model, with two spins. They are coupled by an AF exchange and both have the same easy axis so as to favor the same direction, but the opposite sign for the magnetization. As a further simplification, we chose the strain inertia $m_\epsilon = 0$, so as to prevent the mechanical system from oscillating. Indeed, we are only interested in the relaxation of the mechanical system and its influence on the magnetization.

We now proceed with the description of the numerical integration scheme.

We use a Runge-Kutta 4-5 order integration scheme with adaptive time step. We checked higher order integration schemes as well, in order to verify the validity of the numerical results. The results were virtually identical as is illustrated by Figure 3.1, thus we used the lower order scheme for efficiency.

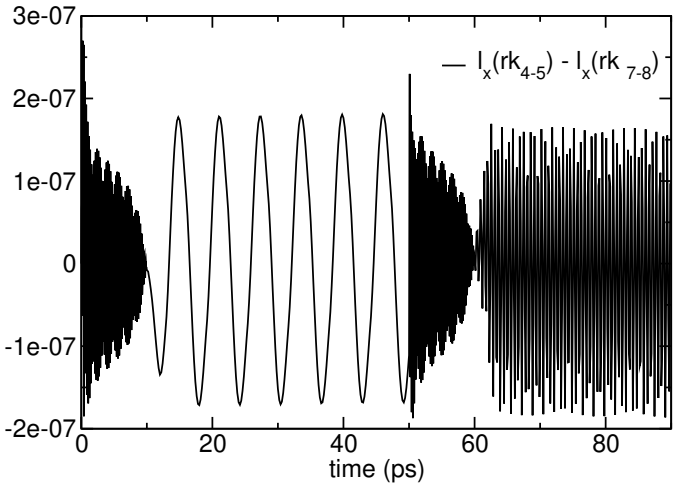

Figure 3.1: Difference between l_x computed with the Runge-Kutta 4-5 order ($l_x(rk_{4-5})$) and the 7-8 order ($l_x(rk_{7-8})$) methods.

How the switching appears is illustrated in Figure 3.2.

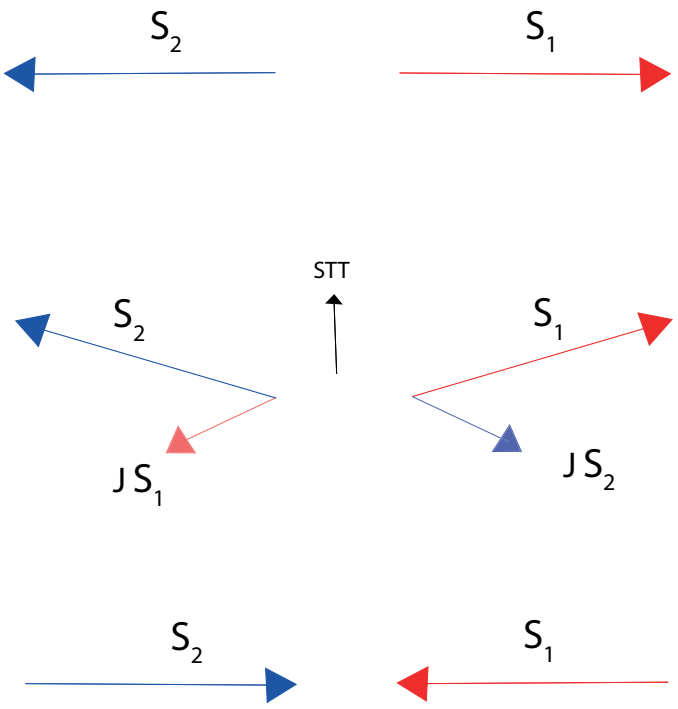

Figure 3.2: How the switching appears, for the AF NiO, by an external STT. At first, the two sublattices have opposite magnetization. Then the STT pushes the magnetization out of the ($\boldsymbol{x}$, $\boldsymbol{y}$) plane. Due to the strong AF exchange, the magnetization for both sublattices precesses and if the STT is timed correctly, both magnetization vectors return to the easy-axis opposite to their initial orientation.

We begin by studying the purely magnetic case *i.e.,* with $B_0 = B_1 = 0$ and compare it to the coupled case by choosing B_0 and B_1 such that they to describe the magnetoelastic coupling for NiO.

Polycrystalline NiO has been investigated as a candidate for antiferromagnetic switching in ref. [101]. The idea is to try and switch the Néel order parameter $\boldsymbol{l}$ by an electric STT pulse. To show that this is possible in our model, we plot the Néel order parameter along the easy axis $\boldsymbol{n}$, and the net magnetization along the STT pulse direction $\boldsymbol{p}$. Results – which are identical to [101] – are displayed in Figure 3.3, on the black curve, for an STT pulse along the $\boldsymbol{z}$-axis.

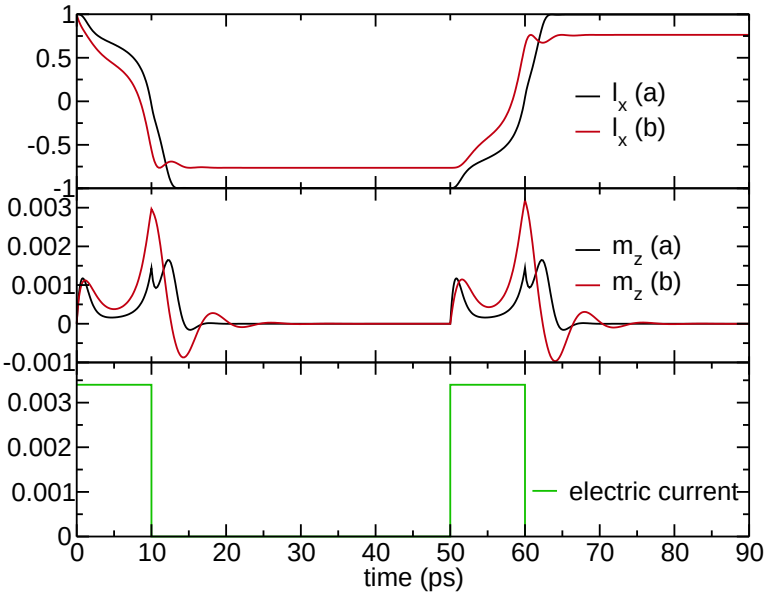

Figure 3.3: Out-of-plane magnetization m_z, Néel order parameter l_x (along the easy axis) and STT pulse along the z-axis as functions of time. $\{m_s = 1,\ m_\epsilon = 0,\ C_0 = 5.1 \times 10^5,\ C_1 = 3.5{\times}10^5$, for (a) $B_0 = B_1 = 0$ and for (b) $B_0 = 7.7,\ B_1 = -23,\ \gamma = 2{\times}10^6,\ \alpha = 0.005,\ J = 0.0034$rad.THz, $\omega_a = 2\pi$rad.GHz, ω_E=172.16 rad.THz, $M_s = 5.10^5$A.m$^{-1}\}$. Initial conditions: $\boldsymbol{s}_1(0) = -\boldsymbol{s}_2(0) = \hat{\boldsymbol{x}}$. (a) is the uncoupled situation and (b) is coupled with $\sigma_{11}^{\text{ext(b)}} = \sigma_{22}^{\text{ext(b)}} = \sigma_{33}^{\text{ext(b)}} = 3 \times 10^4$.

One can see that the Néel order parameter indeed switches within 12ps for a 10ps pulse duration, and, as can be expected, there is a noticeable spin accumulation along the pulse's direction. On the red curve, we have enabled magneto-elastic coupling and imposed a homogeneous isostatic pressure stress. The result is that the switching, for the same pulse, seems to happen more quickly, now within 10ps. One can also see that, when the medium is compressed, the spin accumulation is about twice as strong. For both curves, we also apply the same pulse again, in order to understand, whether or not the system is symmetric under time-reversal symmetry. The main difference one notices, apart from how fast the switching is, is that the Néel order parameter relaxes towards a lower value, along the $\boldsymbol{x}$-axis. In both cases, the STT acts as a strong damping, thus forcing

the magnetization to move from the easy axis; but including the magnetoelastic coupling and imposing an external pressure seems to make the system more sensitive to this torque term.

The next step is to focus on the mechanical part. Thus, in order to evaluate the constants C_0 and C_1, we used references [59, 102, 103]. One can also relate the constants B_0 and B_1 to the more traditional magnetostriction coefficients which are defined by

$$\lambda_s = \beta_i \epsilon_{ij} \beta_j, \tag{3.37}$$

where $\boldsymbol{\beta}$ is the unit vector along which the strain is projected. If one takes only the magnetoelastic coupling into account for the equilibrated strain equations (*i.e.*, $\dot{\epsilon^{\text{eq}}}_{ij} = \ddot{\epsilon^{\text{eq}}}_{ij} = 0$) then one has

$$C_{ijkl}\epsilon^{\text{eq}}_{kl} \approx -\frac{B_{klij}}{2}\mu^{\text{eq}}_k \mu^{\text{eq}}_l \tag{3.38}$$

By recalling the definition of the stiffness tensor S_{ijkl} as the inverse of the elastic constants C_{ijkl} and considering only the mechanical constants (C_0, C_1), we have

$$S_{ijkl} = \frac{-C_0}{2C_1(3C_0 + 2C_1)}\delta_{ij}\delta_{kl} + \frac{1}{4C_1}(\delta_{ik}\delta_{jl} + \delta_{il}\delta_{jk}) \tag{3.39}$$

Inverting this relation thus yields

$$\epsilon^{\text{eq}}_{kl} \approx -S_{ijuv}\frac{B_{kluv}}{2}\mu^{\text{eq}}_k \mu^{\text{eq}}_l \tag{3.40}$$

and now, keeping only the magnetoelastic constants (B_0, B_1), one can express the equilibrium strain components as

$$\epsilon^{\text{eq}}_{ij} \approx \frac{\frac{1}{2}\left(\frac{C_0 B_1}{C_1} - B_0\right)}{3C_0 + 2C_1}\delta_{ij} - \frac{B_1}{2C_1}\mu^{\text{eq}}_i \mu^{\text{eq}}_j \tag{3.41}$$

if the sample is magnetically saturated along the $\boldsymbol{x}$-axis (i.e., $\mu^{\text{eq}}_x = 1$ and $\mu^{\text{eq}}_y = \mu^{\text{eq}}_z = 0$), then we find

$$\begin{cases} \lambda^L_s = \epsilon^{\text{eq}}_{xx} \approx \dfrac{\frac{1}{2}\left(\frac{C_0 B_1}{C_1} - B_0\right)}{3C_0 + 2C_1} - \dfrac{B_1}{2C_1} \\ \lambda^T_s = \lambda^L_s + \dfrac{B_1}{2C_1} \end{cases} \tag{3.42}$$

Where λ^L_s is the longitudinal magnetostriction and λ^T_s is the transverse magnetostriction. These relations can be inverted so as to find expressions for B_0 and B_1 such that

$$\begin{cases} B_0 = \dfrac{C_0\left(2C_1(\lambda^T_s + \lambda^L_s)\right)}{C_1} - \left(\lambda^L_s + \dfrac{2C_1(\lambda^T_s + \lambda^L_s)}{2C_1}\right)(6C_0 + 4C_1) \\ B_1 = 2C_1(\lambda^T_s + \lambda^L_s) \end{cases} \tag{3.43}$$

If the magnetoelastic coupling is neglected, then the new equilibrium strain is given by

$$\epsilon^{\text{eq}}_{ij} = \frac{\sigma^{\text{ext}}_{ij}}{3C_0 + 2C_1} \tag{3.44}$$

or, as expected, in terms of the bulk modulus κ

$$\epsilon_{ij}^{\text{eq}} = \frac{1}{3\kappa}\sigma_{ij}^{\text{ext}} \tag{3.45}$$

as the magnetoelastic constants are much smaller than the mechanical ones, this equilibrium strain should be a good approximation of the computed one, displayed in Figure 3.4.

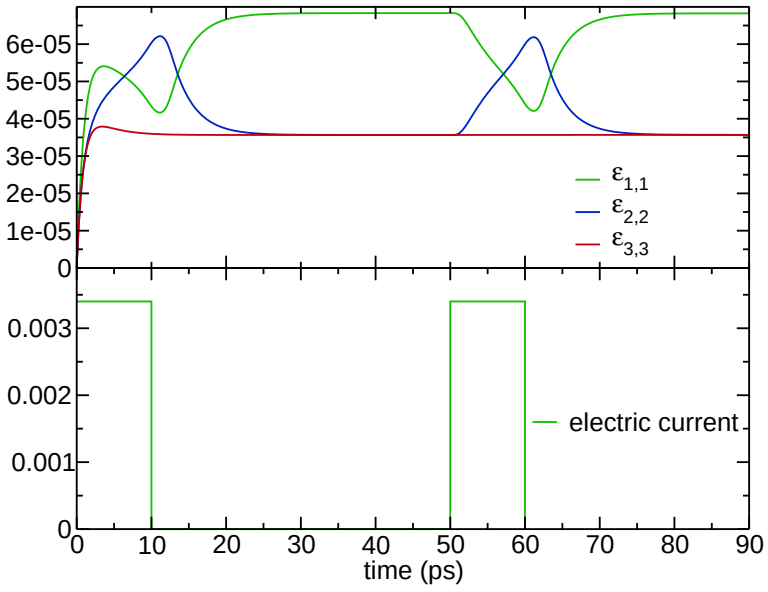

Figure 3.4: Diagonal strain components as functions of time. Conditions are identical to Figure 3.3(a).

Indeed, as can be derived from eq. (3.44), the strain components are of order 10^{-5}. One can see the reaction of the elastic medium to the STT pulse, even though the strains are quite small. This, however, can be understood by the fact that polycrystalline NiO is known for being only weakly magnetostrictive. Thus the response of the mechanical system is not as strong as what can be expected in materials where magnetostriction is stronger. One can, however, already see that the coupling between mechanical and magnetic degrees of freedom changes the equilibrium for the mechanical system, as the $\epsilon_{1,1}$ component converges to a different value than the two other ones displayed. Moreover, one can see that the STT tries to push the mechanical strains away from equilibrium, towards which they relax, as soon as the pulse is over. Conversely to the Néel parameter, the dynamics for the strain remains very similar for both pulse except the initial very fast relaxation towards equilibrium. Now something interesting happens if we consider shear instead of tensile stress, as is displayed in Figure 3.5.

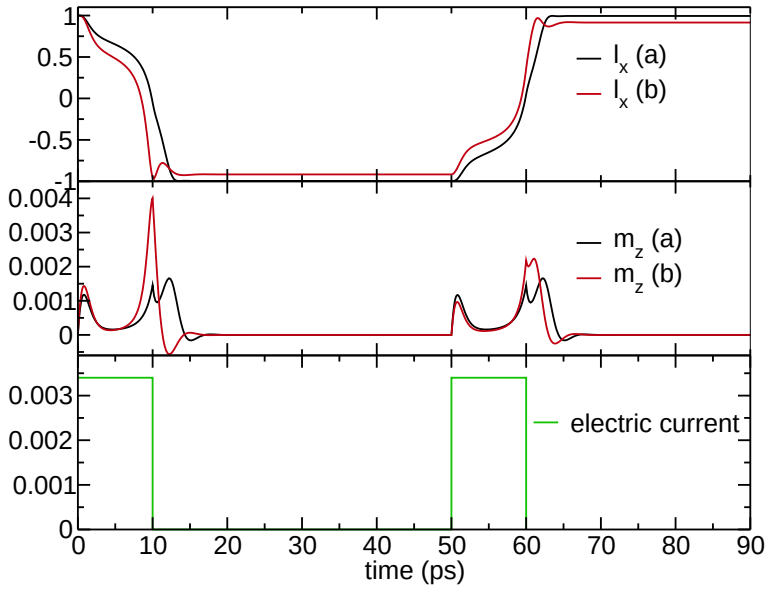

Figure 3.5: Out-of-plane magnetization m_z, Néel order parameter l_x (along the easy axis) and STT pulse (along the z-axis) as functions of time. Numerical constants are identical to Figure 3.3 except for the external stress where non-zero components are $\sigma_{12}^{\mathrm{ext}(a)} = \sigma_{21}^{\mathrm{ext}(a)} = 100$ for (a) and $\sigma_{12}^{\mathrm{ext}(b)} = \sigma_{21}^{\mathrm{ext}(b)} = 5000$ for (b).

Here one can see that the switching is indeed quicker for the red curve, as it was the case in Figure 3.3 but the required threshold for the shear stress is much lower than for the compression. Indeed for Figure 3.3 we had σ_{ii} components of 3.10^4 which corresponds to an external pressure of 30GPa. For Figure 3.5 we have $\sigma_{12} = \sigma_{21} = 5.10^3$. This seems to indicate that this system is less sensitive to tensile or compressive stresses than to shear stresses which can make the switching faster with a much smaller applied external stress. Obviously, materials with much stronger magnetoelastic coupling – such as galfenol [104, 105] – should be investigated but they require much more complicated mechanical and magnetic structures than our simple model with only two spins representing two magnetic sublattices of opposite magnetization [26].

If we sum up, this approach enables us to describe magnetoelastic compounds, at least simple ones, in a way, that's complementary to usual approaches. Indeed, what is usually considered is simply effective anisotropy fields due to shape or mechanical structure. Our approach goes beyond that, even though it needs several parameters which have to be previously determined such as mechanical and magnetoelastic constants. This approach could be complementary to molecular dynamics, or even magnetic molecular dynamics to numerically compute these constants.

Hence we have built a model which allows tracking the intricate dynamics of magnetic and mechanical degrees of freedom without encoding these in the distances between neighbors as does magnetic molecular dynamics. This means that, for larger simulations, one does not have to compute distances to nearest neighbors at each step, as this step is

replaced by the coupling term in the field theory formalism. On top of this, conversely to what most models coupling magnetism and mechanics do, our model allows for a back reaction of the mechanical strain on the magnetic DOF. Unfortunately, the Lagrangian approach does not easily allow implementing coupling to baths and interpretation of physically relevant temperatures related to these baths [106]. This is why in the following section, we will focus on simpler magnetic systems and especially on the coupling to baths and their influence on these systems. Furthermore, we shall see that precessional motion can more naturally be described by an extension of Hamiltonian dynamics, known as Nambu dynamics. Thus we will try a novel approach and build a generalization of Nambu mechanics, that incorporates stochastic and, more particularly, dissipative effects.

Summary

- The vector potential which is coupled to the spin to induce precession depends – non-locally – on the variable which we relabeled spin, $\mu \equiv \dot{s}$.
- We were able to numerically produce the switching of the Néel order parameter for a toy model AF NiO.
- The magnetoelastic coupling enables enhancing of the switching of this parameter for compression and shear stress.
- Shear stress seems to be more efficient than compression in order to accelerate the switching process, although it breaks – even if only slightly – the time reversal symmetric behavior which was noticed in the case of a compression.

Chapter 4

The influence of noise on a magnetic system within stochastic and dissipative generalizations of Nambu mechanics

Résumé

- Nous construisons une généralisation de la dynamique de Nambu afin de décrire la précession amortie d'un spin dans un champ magnétique.
- Nous introduisons dans ce modèle un couplage à un bain thermique et discutons dans quelle mesure ceci décrit un bruit additif ou un bruit multiplicatif.
- Nous construisons à partir des systèmes stochastiques des modèles effectifs, déterministes pour les moments de leur distributions, à partir d'hypothèses pour la fermeture des hiérarchies obtenues.
- Nous simulons les cas de bruits additifs et multiplicatifs à travers les propriétés des modèles stochastiques et déterministes correspondants.

As mentioned in section 3.4.1, we now study the evolution of the magnetization, within the context of Nambu mechanics, a generalization of Hamiltonian mechanics. In Nambu mechanics, there are no longer one, but several Hamiltonians.

More precisely, for Hamiltonian mechanics, one can write the evolution equation for a variable x and its canonically conjugate partner, p, as

$$\begin{cases} \dot{x} &= \{x, \mathcal{H}\} \\ \dot{p} &= \{p, \mathcal{H}\} \end{cases} \tag{4.1}$$

which implies that any function, $f(x, p)$ evolves according to

$$\dot{f} = \{f, H\} \tag{4.2}$$

This has as consequence that $\dot{H} = \{H, H\} = 0$.

This formalism requires that every dynamical variable has a conjugate partner, thus imposing an even number of DOF for the phase-space of Hamiltonian systems.

There are, however, examples [107] of mechanical systems which can be difficult to describe in the Hamiltonian framework–notably, those with constraints.

Indeed the Euler rigid-body equations

$$\begin{cases} I_1\dot{\Omega}_1 = (I_2 - I_3)\Omega_2\Omega_3 \\ I_2\dot{\Omega}_2 = (I_3 - I_1)\Omega_3\Omega_1 \\ I_3\dot{\Omega}_3 = (I_1 - I_2)\Omega_1\Omega_2 \end{cases} \tag{4.3}$$

where $\boldsymbol{\Omega}$ is the body's angular velocity and $\boldsymbol{I}$ are constants (moments of inertia) which depend on the shape and mass distribution of the body. One can see that this system presents an odd number of equations, as such it cannot be put into canonical Hamiltonian form. There are however ways to cast this problem into a Hamiltonian (or equivalently Lagrangian) form by describing its motion in terms of the Euler angles (θ, ϕ, ψ) and their respective velocities $(\dot{\theta}, \dot{\phi}, \dot{\psi})$, thus recovering an even number of DOF for the phase space. Hence, an odd number of degrees of freedom does not necessarily imply that one cannot use Hamiltonian dynamics. However, as presented in section 1.5, there are more convenient ways to generalize the Hamiltonian framework, in particular to phase spaces of odd numbers of DOF.

And as there is no quantity conjugate to spin, this proves to be particularly useful for describing its phase-space. Moreover, Nambu dynamics more naturally implements the constraints which are inherent to vector (*i.e.*, an odd number of) DOF.

The simplest case for the equations of motion for Nambu dynamics [45, 108], is given by an expression similar to (4.1), and for a variable $\boldsymbol{s}$ they read as follows

$$\dot{\boldsymbol{s}} = \{\boldsymbol{s}, H_1, H_2\} \tag{4.4}$$

where now H_1 and H_2 are the two Hamiltonians of the system and the three-legged bracket is the Nambu bracket presented in section 1.5. In this fashion, one can easily describe the precession of a magnetic moment – or classical spin – $\boldsymbol{s}$ where the two Hamiltonians are

given by

$$\begin{cases} H_1 = \frac{1}{\hbar}\boldsymbol{\omega} \cdot \boldsymbol{s} \\ H_2 = \frac{\boldsymbol{s}^2}{2} \end{cases} \tag{4.5}$$

as both of these quantities H_1 and H_2 are conserved (indeed, $\{H_1, H_1, H_2\} = \{H_2, H_1, H_2\} = 0$), we indeed recover a precession around the axis of $\boldsymbol{\omega}$. We would like to emphasize that the bracket is homogeneous to an action, which is illustrated by the $\frac{1}{\hbar}$ factor present in H_1. If we chose $\boldsymbol{\omega}$ aligned with the $\boldsymbol{z}$-axis, then the phase space of this magnetic moment $\boldsymbol{s}$ can be represented by the intersection between the sphere or radius $||\boldsymbol{s}||$ and the plane normal to $\boldsymbol{\omega}$ at $z = \boldsymbol{\omega} \cdot \boldsymbol{s}$. This is illustrated in Figure 4.1

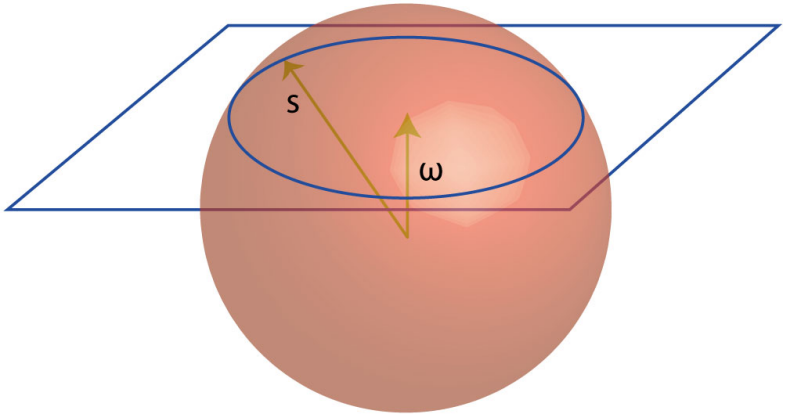

Figure 4.1: Spin of radius $||\boldsymbol{s}||$ cut by the plane defined by $\boldsymbol{\omega} \cdot \boldsymbol{s}$, illustrating the spin precession in the framework of Nambu dynamics.

It should be stressed, however, that the appearance of $\hbar$ here is, solely, for dimensional reasons–it is just a convenient name for a quantity that has the dimensions of angular momentum and has, unfortunately, been used in the literature. It does not describe any quantum effects whatsoever.

Equation (4.4) describes the spin precession equation

$$\dot{\boldsymbol{s}} = \boldsymbol{\omega} \times \boldsymbol{s} \tag{4.6}$$

This formulation, by construction is, of course, consistent with the usual conservation laws, as one can, immediately, remark that

$$\frac{\partial \dot{s}_i}{\partial s_i} = 0 \tag{4.7}$$

hence, the phase-space velocity is divergenceless, which is consistent with Liouville's theorem. This serves as an intuition as to why one can identify $\dot{\boldsymbol{s}}$ with the Nambu bracket on the RHS of eq. (4.4).

This, however, implies that is not possible to describe an experimentally very well-established property of magnetic systems, namely damped precession towards the dominant magnetic field.

This is why, in the next section, we will investigate how to introduce dissipation.

4.1 Building a dissipative extension to Nambu mechanics

Indeed, our aim is to describe damped magnetic motion through a damped precession. As Nambu mechanics is inherently a conservative framework, it is not possible to use it without modifications to describe dissipative motion, as it is, even though it is tempting to simply change the Hamiltonian $\boldsymbol{\omega} \cdot \boldsymbol{s}$, by imposing for example that $\boldsymbol{\omega} \equiv \boldsymbol{\omega}(t)$, thus simply shifting this plane upward until its intersection with the sphere comprises only a single point, this is shown in figure 4.2.

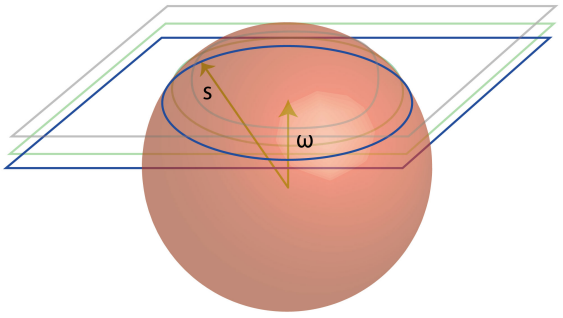

Figure 4.2: The plane $\boldsymbol{\omega} \cdot \boldsymbol{s}$ shifts up, as does the intersection with the sphere

While one might think that this indeed describes the motion represented in Figure 4.3, in fact, it does not, since $(\boldsymbol{\omega}(t) \times \boldsymbol{s}) \cdot \boldsymbol{s} = 0$, whatever the time dependence, as long as $\boldsymbol{\omega}(t)$ does not change direction. What the time dependence achieves is modifying the density on the circle, not its position.

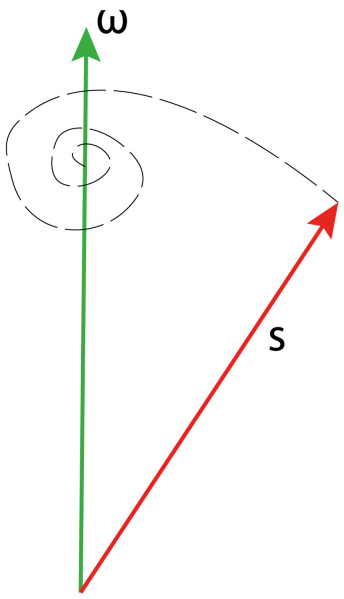

Figure 4.3: Schematic view of a magnetic moment's $\boldsymbol{s}$ damped precession towards an effective field $\boldsymbol{\omega}$

Similarly as what occurs in Hamiltonian mechanics, we need to find terms that cannot be reabsorbed by a redefinition of the bracket, whether Poisson or Nambu. The key observation is that the bracket defines a divergence–less vector field and dissipation is described by the non–zero divergence of a vector field. So we shall generalize the Clebsch-Monge/Helmholtz/Hodge decomposition of a vector field into a curl (that's locally divergence-free) and a gradient (that's, locally, curl–free).

4.1.1 Using the Helmholtz and Monge gauge so as to find out how to plug in a dissipative term

In three dimensions, there are several ways to decompose a given vector field $\boldsymbol{V}(\boldsymbol{s})$, two of which can be understood as special cases of Hodge decomposition [109]. The first one, is the Helmholtz representation [107] such that

$$V_i \equiv \varepsilon_{ijk}\frac{\partial A_j}{\partial s_k} + \frac{\partial \phi}{\partial s_i} \tag{4.8}$$

which is unique, up to a gradient of an "arbitrary" function ψ and any constant term ϕ_0 such that $\boldsymbol{A} \to \boldsymbol{A} + \boldsymbol{\nabla}_s\boldsymbol{\psi}$ and $\phi \to \phi + \phi_0$. In this representation, the vector field $\boldsymbol{V}$ is decomposed into a purely rotational part and a purely gradient part. Thus $\boldsymbol{A}$ is a vector potential and ϕ is a scalar potential.

The second – less-common – representation, is the Monge representation, [110] such that

$$V_i \equiv \frac{\partial C_1}{\partial s_i} + C_2\frac{\partial C_3}{\partial s_i} \tag{4.9}$$

Where C_1, C_2 and C_3 are the so–called Clebsch-Monge Potentials. This decomposition is not unique, either, [111], and equation (4.9) is known as the Lamb form.

Another example is the Keller form

$$v_i \equiv \frac{\partial C_1}{\partial s_i} + \frac{1}{2}\left(C_2\frac{\partial C_3}{\partial s_i} - C_3\frac{\partial C_2}{\partial s_i}\right) \tag{4.10}$$

If we identify these potentials as $C_1 = D$, $C_2 = H_1$ and $C_3 = H_2$

$$V_i = \frac{\partial D}{\partial s_i} + H_1\frac{\partial H_2}{\partial s_i} \tag{4.11}$$

Because $\boldsymbol{A}$ is also a vector field, we express it using the Monge (Lamb) representation (4.9). Furthermore, we express $\dot{\boldsymbol{s}}$ using the Helmholtz decomposition (4.8)

$$\begin{aligned} \dot{s}_i &= \varepsilon_{ijk}\frac{\partial}{\partial s_j}\left(\frac{\partial D}{\partial s_k} + H_1\frac{\partial H_2}{\partial s_k}\right) + \frac{\partial \phi}{\partial s_i} \\ \Rightarrow \dot{s}_i &= \varepsilon_{ijk}\frac{\partial H_1}{\partial s_j}\frac{\partial H_2}{\partial s_k} + \frac{\partial \phi}{\partial s_i} \end{aligned} \tag{4.12}$$

which can be shown to hold for both the Lamb (eq. (4.9)) and Keller (eq. (4.10)) choices of Monge decomposition. This last expression is equivalent to

$$\dot{\boldsymbol{s}} = \{\boldsymbol{s}, H_1, H_2\} + \boldsymbol{\nabla}_s\phi \tag{4.13}$$

This means that what can be added to the Nambu formalism if we want to be able to describe dissipation, is the second term of the RHS of (4.13), namely $\boldsymbol{\nabla}_s\phi$. In a more general fashion [51, 112] the evolution equation for any function $F(\boldsymbol{s})$ can be deduced from

$$\frac{dF}{dt} = \frac{\partial F}{\partial s_i}\dot{s}_i = \frac{\partial F}{\partial s_i}\{s_i, H_1, H_2\} + \frac{\partial \phi}{\partial s_i}\frac{\partial F}{\partial s_i} \tag{4.14}$$

which leads to the expression

$$\dot{F} = \{F, H_1, H_2\} + \frac{\partial \phi}{\partial s_i}\frac{\partial F}{\partial s_i} \tag{4.15}$$

Now that we have managed to find out how any vector can be related to an extended Nambu description, we will introduce a plausible candidate for the damping.

4.1.2 Introducing LLG damping as a fitting candidate for the model

As we remarked, above, it's not enough for the frequency to be time–dependent, unless its direction, also, changes. Such a change in direction can be described by a dependence on the magnetization itself $\boldsymbol{\omega} \equiv \boldsymbol{\omega}[\boldsymbol{s}]$ [72] such that

$$\dot{\boldsymbol{s}} = \boldsymbol{\omega}[\boldsymbol{s}] \times \boldsymbol{s} \tag{4.16}$$

While such an *Ansatz* does preserve the norm, since $\boldsymbol{s}\cdot\dot{\boldsymbol{s}} = 0$, this does not mean that damping does not occur, since the sphere need not be uniformly sampled.

It is interesting that this expression contains, as a special case, the Landau-Lifshitz (LL) equation

$$\dot{\boldsymbol{s}} = \boldsymbol{\omega} \times \boldsymbol{s} + \alpha \left(\boldsymbol{s} \times (\boldsymbol{\omega} \times \boldsymbol{s}) \right) \tag{4.17}$$

simply by taking $\boldsymbol{\omega} \to \boldsymbol{\omega} - \alpha \boldsymbol{\omega} \times \boldsymbol{s}$.

Another special case is the so-called Landau-Lifshitz-Gilbert (LLG) equation, originally proposed for strongly damped systems:

$$\dot{\boldsymbol{s}} = \boldsymbol{\omega} \times \boldsymbol{s} + \alpha \left(\boldsymbol{s} \times \dot{\boldsymbol{s}} \right) \tag{4.18}$$

This equation seems quite complicated, the complication, however, is illusory.

It can be recast into a LL form as

$$\dot{\boldsymbol{s}} = \frac{1}{1+\alpha^2} \left(\boldsymbol{\omega} \times \boldsymbol{s} \right) + \frac{\alpha}{1+\alpha^2} \left(\boldsymbol{s} \times (\boldsymbol{\omega} \times \boldsymbol{s}) \right) \tag{4.19}$$

Let us now define two "damping" terms $D_\perp$ and $D_\parallel$ such that

$$\dot{s}_i = \{ s_i, H_1 + D_\perp, H_2 \} + \frac{\partial D_\parallel}{\partial s_i} \tag{4.20}$$

then, using the linearity of the bracket, we have

$$\dot{s}_i = \{ s_i, H_1, H_2 \} + \{ s_i, D_\perp, H_2 \} + \frac{\partial D_\parallel}{\partial s_i} \tag{4.21}$$

Thus in what follows, we will identify the extension of the Nambu expression to this dissipation term

$$\boldsymbol{\nabla}_s \phi \to \frac{\alpha}{1+\alpha^2} \left(\boldsymbol{s} \times (\boldsymbol{\omega} \times \boldsymbol{s}) \right) \tag{4.22}$$

where one can show that the two terms on the RHS can be identified with the Gilbert damping, namely, as

$$\{ s_i, D_\perp, H_2 \} + \frac{\partial D_\parallel}{\partial s_i} \equiv \frac{1}{1+\alpha^2} \left(\boldsymbol{\omega} \times \boldsymbol{s} \right) \tag{4.23}$$

We would like to stress that any form $\{ s_i, H_1 + D_\perp^{(1)}, H_2 + D_\perp^{(2)} \}$ would be relevant as well, which is why we do not want to focus on the exact expression for these terms. Concerning the regular precession part, we simply choose

$$\{ \boldsymbol{s}, H_1, H_2 \} \equiv \frac{1}{1+\alpha^2} \left(\boldsymbol{\omega} \times \boldsymbol{s} \right) \tag{4.24}$$

Now that we have managed to extend our Nambu description of this system so as to include dissipation, the next question which flows from this is how to describe the fluctuations, as the fluctuation dissipation theorem imposes that any dissipating system must also be subjected to fluctuations.

To this end it is useful to recall the geometry of the problem, namely the tip of the magnetization vector is a particle that explores a sphere, which is a curved surface. Motion on such a surface involves describing its geometry in parametric form, in particular, in order to allow it to fluctuate. The most straightforward way to realize this is through the so–called noise-vielbein.

4.2 Introducing stochastic effects through a vielbein-noise coupling

In this section we will couple (4.19) linearly to a stochastic process $\boldsymbol{\eta}(t)$ with a given law of probability,$P(\boldsymbol{\eta})$.

The evolution equation for the spin, $\boldsymbol{s}(t)$, can be written as a Langevin equation,

$$\dot{\boldsymbol{s}} = \frac{1}{1+\alpha^2}\left(\boldsymbol{\omega}\times\boldsymbol{s}\right) + \frac{\alpha}{1+\alpha^2}\left(\boldsymbol{s}\times\left(\boldsymbol{\omega}\times\boldsymbol{s}\right)\right) + e_{ij}(\boldsymbol{s})\eta_j(t) \tag{4.25}$$

where $e_{ij}(\boldsymbol{s})$ is the vielbein [113] on a manifold described by the dynamical variables $\boldsymbol{s}$. Here the latin indices are coordinate indices (not lattice sites). Because $\boldsymbol{s}(t)$ is now defined by equation (4.25), it becomes a stochastic process for which we can define the conditional probability $P_\eta(\boldsymbol{s},t;\boldsymbol{s}_0,t_0)$ which corresponds to the probability of finding a state $\boldsymbol{s}$ at a time t, knowing that one started from a state $\boldsymbol{s}_0$ at time t_0 for one realization of the noise $\boldsymbol{\eta}(t)$ (*i.e.*, a particular trajectory in phase space). One often omits the initial conditions by writing $P(\boldsymbol{s},t)$, defined by

$$P(\boldsymbol{s},t) = \int \left[\mathscr{D}\boldsymbol{\eta}(t)\right] P(\boldsymbol{\eta}) \underbrace{\delta\left(\boldsymbol{s}-\boldsymbol{s}_\eta(t)\right)}_{P_\eta(\boldsymbol{s},t)} \tag{4.26}$$

where $\boldsymbol{s}_\eta(t)$ denotes a solution of (4.25), corresponding to the realization, $\{\boldsymbol{\eta}(t)\}$, of the noise. One can show that it satisfies a continuity equation in configuration space.

$$\frac{\partial P_\eta(\boldsymbol{s},t)}{\partial t} + \frac{\partial\left(\dot{s}_i P_\eta(\boldsymbol{s},t)\right)}{\partial s_i} = 0. \tag{4.27}$$

To be specific, we consider an Ornstein-Uhlenbeck process [114] of intensity Δ and auto-correlation time τ

$$\begin{cases} \langle\eta_i(t)\rangle = 0 \\ \langle\eta_i(t)\eta_j(t')\rangle = \dfrac{\Delta}{\tau}\delta_{ij}e^{-\frac{|t-t'|}{\tau}} \end{cases} \tag{4.28}$$

and higher-order correlation functions are given by Wick's theorem. Now that we have introduced how to implement stochasticity, we will compare additive and multiplicative noise couplings.

In this framework, the first difference between additive and multiplicative noises is the form taken by the vielbein e_{ij}. For the additive noise, it can be identified as $e_{ij} \equiv \dfrac{\delta_{ij}}{1+\alpha^2}$ (we would like to stress that, in particular, it should not be a function of $\boldsymbol{s}$). If one takes the white noise limit for the Ornstein-Uhlenbeck process *i.e.* $\tau \to 0$, then one can take advantage of the Shapiro-Loginov theorem [39] and (4.27) in order to express mixed

moments of the noise and the probability distribution as

$$\begin{aligned}\frac{d}{dt}\left\langle \eta_i(t)P_\eta(\boldsymbol{s},t)\right\rangle &= \left\langle \eta_i(t)\frac{\partial P_\eta(\boldsymbol{s},t)}{\partial t}\right\rangle - \frac{1}{\tau}\left\langle \eta_i(t)P_\eta(\boldsymbol{s},t)\right\rangle \\ &= -\left\langle \eta_i(t)\frac{\partial(\dot{s}_j P_\eta(\boldsymbol{s},t))}{\partial s_j}\right\rangle - \frac{1}{\tau}\left\langle \eta_i(t)P_\eta(\boldsymbol{s},t)\right\rangle \\ &= -\left\langle \eta_i(t)\dot{s}_j(t)\frac{\partial P_\eta(\boldsymbol{s},t)}{\partial s_j}\right\rangle - \left\langle \eta_i(t)P_\eta(\boldsymbol{s},t)\frac{\partial \dot{s}_j(t)}{\partial s_j}\right\rangle - \frac{1}{\tau}\left\langle \eta_i(t)P_\eta(\boldsymbol{s},t)\right\rangle\end{aligned} \tag{4.29}$$

assuming Gaussian closure, *i.e.*, that third order moments can be expressed in terms of first and second order moments as

$$\begin{aligned}\left\langle f_1(\eta)f_2(\eta)f_3(\eta)\right\rangle = \left\langle f_1(\eta)f_2(\eta)\right\rangle\left\langle f_3(\eta)\right\rangle + \left\langle f_1(\eta)f_3(\eta)\right\rangle\left\langle f_2(\eta)\right\rangle + \\ \left\langle f_2(\eta)f_3(\eta)\right\rangle\left\langle f_1(\eta)\right\rangle - 2\left\langle f_1(\eta)\right\rangle\left\langle f_2(\eta)\right\rangle\left\langle f_3(\eta)\right\rangle\end{aligned} \tag{4.30}$$

where $f_1(\eta)$, $f_2(\eta)$ and $f_3(\eta)$ are functions of the noise, we have (keeping only terms which can lead to a factor $\frac{1}{\tau}$ (*i.e.*, linear in the noise) and replacing $\boldsymbol{s}_j(t)$ by the corresponding term in (4.25))

$$\begin{aligned}-\left\langle \eta_i(t)\dot{s}_j(t)\frac{\partial P_\eta(\boldsymbol{s},t)}{\partial s_j}\right\rangle &= -\left\langle \eta_i(t)\dot{s}_j(t)\right\rangle\left\langle \frac{\partial P_\eta(\boldsymbol{s},t)}{\partial s_j}\right\rangle + \mathcal{O}(\tau^n) \\ &= -\left\langle \eta_i(t)e_{jl}(\boldsymbol{s})\eta_l(t)\right\rangle\left\langle \frac{\partial P_\eta(\boldsymbol{s},t)}{\partial s_j}\right\rangle + \mathcal{O}(\tau^n)\end{aligned} \tag{4.31}$$

where n is any positive integer (including 0), as we omit all terms which do not lead to a factor $\frac{1}{\tau}$. Here, by recalling $e_{jl} \equiv \frac{\delta_{jl}}{1+\alpha^2}$ we get

$$\begin{aligned}-\left\langle \eta_i(t)e_{jl}(\boldsymbol{s})\eta_l(t)\right\rangle\left\langle \frac{\partial P_\eta(\boldsymbol{s},t)}{\partial s_j}\right\rangle &= -\frac{1}{1+\alpha^2}\left\langle \eta_i(t)\eta_j(t)\right\rangle\left\langle \frac{\partial P_\eta(\boldsymbol{s},t)}{\partial s_j}\right\rangle + \mathcal{O}(\tau^n) \\ &= -\frac{\Delta}{\tau(1+\alpha^2)}\frac{\partial P(\boldsymbol{s},t)}{\partial s_i} + \mathcal{O}(\tau^n)\end{aligned} \tag{4.32}$$

returning to (4.29) and keeping only terms with a factor $\frac{1}{\tau}$ for the RHS, we get the following expression

$$\frac{d}{dt}\left\langle \eta_i(t)P_\eta(\boldsymbol{s},t)\right\rangle = -\frac{\Delta}{\tau(1+\alpha^2)}\frac{\partial P(\boldsymbol{s},t)}{\partial s_i} - \frac{1}{\tau}\left\langle \eta_i(t)P_\eta(\boldsymbol{s},t)\right\rangle + \mathcal{O}(\tau^n) \tag{4.33}$$

now multiplying both sides of (4.33) by τ and taking the limit $\tau \to 0$ yields

$$\left\langle \eta_i(t)P_\eta(\boldsymbol{s},t)\right\rangle = -\tilde{\Delta}\frac{\partial P(\boldsymbol{s},t)}{\partial s_i} \tag{4.34}$$

where each tilde in the notation stands for a $\frac{1}{1+\alpha^2}$ factor (*i.e.*, $\tilde{\Delta} = \frac{\Delta}{1+\alpha^2}$). Now by defining the damped current vector $\boldsymbol{J}$ as

$$\boldsymbol{J} \equiv \frac{1}{1+\alpha^2}(\boldsymbol{\omega}\times\boldsymbol{s}) + \frac{\alpha}{1+\alpha^2}(\boldsymbol{s}\times(\boldsymbol{\omega}\times\boldsymbol{s})) \tag{4.35}$$

and including (4.25) in (4.27), one gets the following expression for $P(\boldsymbol{s},t)$

$$\frac{\partial P(\boldsymbol{s},t)}{\partial t}+\frac{\partial}{\partial s_i}(J_iP(\boldsymbol{s},t))-\tilde{\tilde{\Delta}}\frac{\partial^2 P(\boldsymbol{s},t)}{\partial s_i\partial s_i}=0 \tag{4.36}$$

which is of the Fokker-Planck form [115] as has initially been remarked by Walton [116] when introducing additive noise into an LLG equation. We recall that each tilde stands for a factor $\dfrac{1}{1+\alpha^2}$, as such $\tilde{\tilde{\Delta}}=\dfrac{\Delta}{(1+\alpha^2)^2}$. The average value, $\langle s_i\rangle$ is expressed in terms pf $P(\boldsymbol{s},t)$ by the expression

$$\frac{d\langle s_i\rangle}{dt}=-\int d\boldsymbol{s}\, s_i\frac{\partial P(\boldsymbol{s},t)}{\partial t}=\langle J_i\rangle\,. \tag{4.37}$$

In a similar fashion

$$\frac{d\langle s_is_j\rangle}{dt}=-\int d\boldsymbol{s}\, s_is_j\frac{\partial P(\boldsymbol{s},t)}{\partial t} \tag{4.38}$$

which implies that

$$\frac{d\langle s_is_j\rangle}{dt}=\langle\dot{s}_is_j\rangle+\langle s_i\dot{s}_j\rangle \tag{4.39}$$

For the LLG equation in a field $\boldsymbol{B}$ or equivalently a frequency $\boldsymbol{\omega}=\gamma\boldsymbol{B}$ this yields the following equations for the first and second order moments for the spin

$$\begin{cases}\dfrac{d}{dt}\langle s_i\rangle=\varepsilon_{ijk}\tilde{\omega}_j\langle s_k\rangle+\alpha[\tilde{\omega}_i\langle s_js_j\rangle-\tilde{\omega}_j\langle s_js_i\rangle]\\ \dfrac{d}{dt}\langle s_is_j\rangle=\tilde{\omega}_l\left(\epsilon_{ilk}\langle s_ks_j\rangle+\epsilon_{jlk}\langle s_ks_i\rangle\right)+\alpha\left[\tilde{\omega}_i\langle s_ls_ls_j\rangle+\tilde{\omega}_j\langle s_ls_ls_i\rangle-2\tilde{\omega}_l\langle s_ls_is_j\rangle\right]-2\tilde{\tilde{\Delta}}\delta_{ij}\end{cases} \tag{4.40}$$

In order to close the system (4.40), we shall impose Gaussian closure *i.e.* $\langle\!\langle s_is_js_k\rangle\!\rangle=0$. Under this condition, the third-order moments can be expressed in terms of the first and second order moments of the spin distribution as

$$\langle s_is_js_k\rangle=\langle s_is_j\rangle\langle s_k\rangle+\langle s_is_k\rangle\langle s_j\rangle+\langle s_js_k\rangle\langle s_i\rangle-2\langle s_i\rangle\langle s_j\rangle\langle s_k\rangle \tag{4.41}$$

This yields the following effective system of the first and second order moments of the spin coupled to an additive noise

$$\begin{cases}\dfrac{d}{dt}\langle s_i\rangle=\varepsilon_{ijk}\tilde{\omega}_j\langle s_k\rangle+\alpha[\tilde{\omega}_i\langle s_js_j\rangle-\tilde{\omega}_j\langle s_js_i\rangle]\\ \dfrac{d}{dt}\langle s_is_j\rangle=\tilde{\omega}_l\left(\epsilon_{ilk}\langle s_ks_j\rangle+\epsilon_{jlk}\langle s_ks_i\rangle\right)+\alpha\Big[\tilde{\omega}_i\left(\langle s_ls_l\rangle\langle s_j\rangle+\langle s_ls_j\rangle\langle s_l\rangle+\langle s_ls_j\rangle\langle s_l\rangle-2\langle s_l\rangle\langle s_l\rangle\langle s_j\rangle\right)\\ \qquad+\tilde{\omega}_j\left(\langle s_ls_l\rangle\langle s_i\rangle+\langle s_ls_i\rangle\langle s_l\rangle+\langle s_ls_i\rangle\langle s_l\rangle-2\langle s_l\rangle\langle s_l\rangle\langle s_i\rangle\right)-2\tilde{\omega}_l\Big(\langle s_ls_i\rangle\langle s_j\rangle\\ \qquad+\langle s_ls_j\rangle\langle s_i\rangle+\langle s_is_j\rangle\langle s_l\rangle-2\langle s_l\rangle\langle s_i\rangle\langle s_j\rangle\Big)\Big]+2\tilde{\tilde{\Delta}}\delta_{ij}\end{cases} \tag{4.42}$$

Now for the case of a multiplicative noise, the first non-trivial proposition was made by Brown [30] for the LLG equation in the form

$$e_{ij}(\boldsymbol{s}) = \varepsilon_{ijk}\frac{s_k}{1+\alpha^2} \tag{4.43}$$

where it is of interest to note that it is present even if $\alpha = 0$ *i.e.* without Gilbert damping. Furthermore, this vielbein is not invertible, but what does matter is that it preserves the norm of the spin, given that the dissipation term ϕ is also chosen to preserve this property (which is the case for LLG) in the same – white-noise – limit, we now have

$$\langle \eta_i P_\eta(\boldsymbol{s},t)\rangle = -\tilde{\Delta}\frac{\partial}{\partial s_j}\left(e_{ji}P(\boldsymbol{s},t)\right), \tag{4.44}$$

which transforms the final equation for $P(\boldsymbol{s},t)$ into

$$\frac{\partial P(\boldsymbol{s},t)}{\partial t} + \frac{\partial}{\partial s_i}(J_i P(\boldsymbol{s},t)) - \tilde{\tilde{\Delta}}\frac{\partial}{\partial s_i}\left(e_{ij}\frac{\partial}{\partial s_k}\left(e_{kj}P(\boldsymbol{s},t)\right)\right) = 0. \tag{4.45}$$

this yields the following expression for the time evolution of the averaged spin

$$\frac{d\langle s_i\rangle}{dt} = \langle J_i\rangle + \tilde{\tilde{\Delta}}\left\langle \frac{\partial e_{il}}{\partial s_k}e_{kl}\right\rangle. \tag{4.46}$$

To be more specific, for the vielbein proposed by Brown, and a constant external field, we have, for the first and second order moments

$$\begin{cases} \dfrac{d\langle s_i\rangle}{dt} = \varepsilon_{ijk}\tilde{\omega}_j\langle s_k\rangle + \alpha\left(\tilde{\omega}_i\langle s_j s_j\rangle - \tilde{\omega}_j\langle s_j s_i\rangle\right) - 2\tilde{\tilde{\Delta}}\langle s_i\rangle. \\ \dfrac{d\langle s_i s_p\rangle}{dt} = \varepsilon_{ijk}\left(\tilde{\omega}_j\langle s_k s_p\rangle + \tilde{\tilde{\Delta}}\left(\varepsilon_{kjm}\langle s_m\rangle\langle s_p\rangle + \varepsilon_{pjm}\langle s_m\rangle\langle s_k\rangle\right) + \varepsilon_{klm}\tilde{\omega}_l\langle s_m s_j s_p\rangle\right) \\ \qquad + \varepsilon_{pjk}\Big(\tilde{\omega}_j\langle s_k s_i\rangle + \tilde{\tilde{\Delta}}\left(\varepsilon_{kjm}\langle s_m\rangle\langle s_i\rangle + \varepsilon_{ijm}\langle s_m\rangle\langle s_k\rangle\right) + \varepsilon_{klm}\tilde{\omega}_l\langle s_m s_j s_i\rangle\Big) \end{cases} \tag{4.47}$$

Under the same closing assumptions as for the additive case, *i.e.* $\langle\!\langle s_i s_j s_k\rangle\!\rangle = 0$

$$\begin{cases} \dfrac{d\langle s_i\rangle}{dt} = \varepsilon_{ijk}\tilde{\omega}_j\langle s_k\rangle + \alpha\left(\tilde{\omega}_i\langle s_j s_j\rangle - \tilde{\omega}_j\langle s_j s_i\rangle\right) - 2\tilde{\tilde{\Delta}}\langle s_i\rangle. \\ \dfrac{d\langle s_i s_p\rangle}{dt} = \varepsilon_{ijk}\Bigg(\tilde{\omega}_j\langle s_k s_p\rangle + \tilde{\tilde{\Delta}}\left(\varepsilon_{kjm}\langle s_m\rangle\langle s_p\rangle + \varepsilon_{pjm}\langle s_m\rangle\langle s_k\rangle\right) \\ \qquad + \varepsilon_{klm}\tilde{\omega}_l\Big(\langle s_m s_j\rangle\langle s_p\rangle + \langle s_m s_p\rangle\langle s_j\rangle + \langle s_j s_p\rangle\langle s_m\rangle - 2\langle s_m\rangle\langle s_j\rangle\langle s_p\rangle\Big)\Bigg) \\ \qquad + \varepsilon_{pjk}\Bigg(\tilde{\omega}_j\langle s_k s_i\rangle + \tilde{\tilde{\Delta}}\left(\varepsilon_{kjm}\langle s_m\rangle\langle s_i\rangle + \varepsilon_{ijm}\langle s_m\rangle\langle s_k\rangle\right) \\ \qquad + \varepsilon_{klm}\tilde{\omega}_l\Big(\langle s_m s_j\rangle\langle s_i\rangle + \langle s_m s_i\rangle\langle s_j\rangle + \langle s_j s_i\rangle\langle s_m\rangle - 2\langle s_m\rangle\langle s_j\rangle\langle s_i\rangle\Big)\Bigg) \end{cases} \tag{4.48}$$

We, therefore have a closed system of equations for the flow of the moments of magnetization, in presence of additive or multiplicative noise. In the next section, we shall proceed to study the properties of their solutions and, in particular, compare the results of the moment equations, with those of the stochastic equations.

4.3 Comparing effective and stochastic models by simulating additive and multiplicative noise

In the previous section we have focused on computing the equations of motion for the stochastic systems and their deterministic counterparts, which we obtained by imposing several closing assumptions on the hierarchy of moments. We shall now proceed to integrate them, numerically, in the same fashion as in the previous chapters, both for the stochastic systems and the effective systems.

4.3.1 The case of additive noise

We start by simulating the case, when the noise is additive, as described by equations (4.42) for the deterministic model, and (4.25) and $e_{ij} \equiv \dfrac{\delta_{ij}}{1+\alpha^2}$.

Our first simulation results are given in Figure 4.4. As we have chosen an additive noise here, the norm of the spin is not conserved for each realization of the noise. Indeed by taking the scalar product of (4.25) with $\boldsymbol{s}$, we have

$$\frac{1}{2}\frac{d\boldsymbol{s}^2}{dt} = \boldsymbol{s}\cdot\dot{\boldsymbol{s}} = \frac{\boldsymbol{s}\cdot\boldsymbol{\eta}}{1+\alpha^2} \tag{4.49}$$

which has no particular reason to vanish at all times. The averaging procedure tends to smooth out the effects of this variation of the norm but only for short times and low values of the noise intensity Δ. Thus in Figure 4.4, where both the stochastic and deterministic models are in quite good agreement, as the simulation time is short and the noise intensity small, the norm remains within reasonable bounds and its variation is barely noticeable on the curves. It is however, slightly more noticeable on the deterministic curves (b) where the z-component of the spin grows beyond the value of 1. Obviously the difference between these curves grows for larger values of the noise intensity, as the arguments for the closing assumptions are no longer valid.

However as shown in reference [38] one can work around this by changing the closing relations and by imposing, for example $\langle\langle s_i s_j s_k \rangle\rangle = C_{ijk}(\Delta)$.

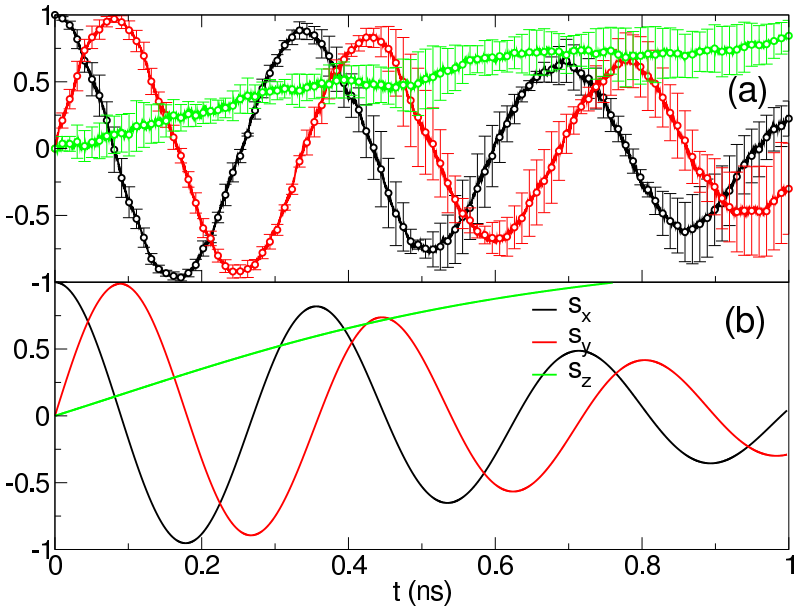

Figure 4.4: Magnetization dynamics of a paramagnetic spin in a constant magnetic field, connected to an additive noise. The upper graphs (a) plot some of the first–order moments of the averaged magnetization vector over 10^2 realizations of the noise, when the lower graphs (b) plot the associated model closed to the third-order cumulant (see text). Parameters of the simulations : $\{\Delta = 0.13$ rad.GHz; $\alpha = 0.1$; $\boldsymbol{\omega} = (0, 0, 18)$ rad.GHz; timestep $\Delta t = 10^{-4}$ ns$\}$. Initial conditions: $\boldsymbol{s}(0) = (1, 0, 0)$, $\langle s_i(0)s_j(0)\rangle = 0$ but $\langle s_1(0)s_1(0)\rangle = 1$.

What is of more direct interest to us is the influence of the initial conditions. In Figure 4.5 we chose a non-zero component along the external field axis, however of opposite sign as $\boldsymbol{s}(0) = (1/\sqrt{2}, 0, -1/\sqrt{2})$ and by taking all the initial correlations accordingly

$$\langle s_i(0)s_j(0)\rangle = \begin{pmatrix} \frac{1}{2} & 0 & -\frac{1}{2} \\ 0 & 0 & 0 \\ -\frac{1}{2} & 0 & \frac{1}{2} \end{pmatrix} \tag{4.50}$$

We also chose a larger time-window so as to demonstrate the issue with the conservation of the norm. One can see more easily here, that the norm tends to diverge slowly, which is not in agreement with experiment. This holds for both the stochastic and deterministic models. Indeed in the case of additive noise one can write the time derivative of the averaged norm of the spin as

$$\frac{d}{dt}\left\langle \boldsymbol{s}^2 \right\rangle = \frac{2\langle s_i \eta_i \rangle}{1+\alpha^2}. \tag{4.51}$$

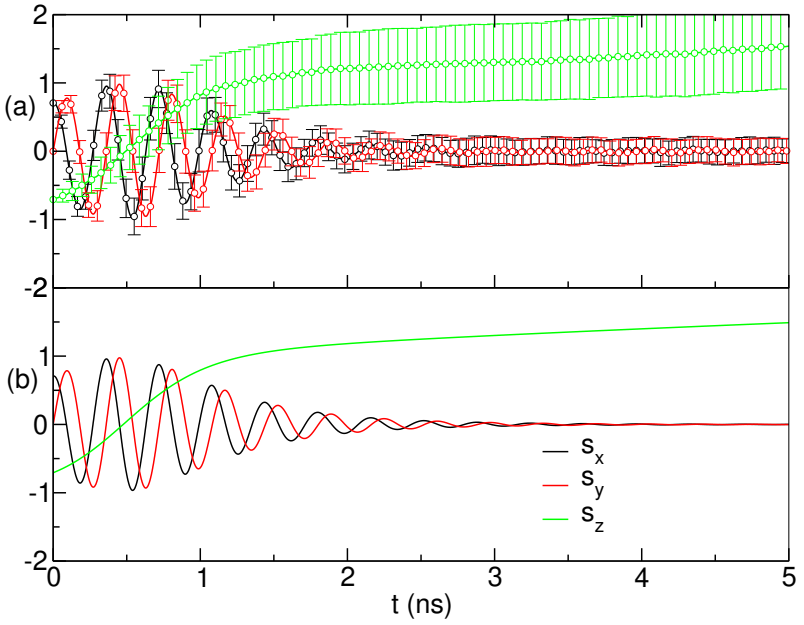

Figure 4.5: Magnetization dynamics of a paramagnetic spin in a constant magnetic field, connected to an additive noise. The upper graphs (a) plot some of the first–order moments of the averaged magnetization vector over 10^3 realizations of the noise, when the lower graphs (b) plot the associated model closed to the third-order cumulant (see text). Parameters of the simulations : $\{\Delta = 0.0655$ rad.GHz; $\alpha = 0.1$; $\boldsymbol{\omega} = (0, 0, 18)$ rad.GHz; timestep $\Delta t = 10^{-4}$ ns, $\boldsymbol{s}(0) = \langle \boldsymbol{s}(0) \rangle = (1/\sqrt{2}, 0, -1/\sqrt{2})$, $\langle s_i s_j \rangle(0) = 0$ except for (11)=1/2, (13)=(31)=-1/2, (33)=1/2 $\}$.

In the white noise limit, using the Shapiro-Loginov formula in the same fashion as in previous chapters, one gets

$$\frac{d}{dt}\langle s_i s_i \rangle = 6\tilde{\tilde{\Delta}} \tag{4.52}$$

which yields the following relation for the value of the norm over time

$$\left\langle \boldsymbol{s}^2(t) \right\rangle = \boldsymbol{s}^2(0) + 6\tilde{\tilde{\Delta}} t, \tag{4.53}$$

This is clearly in agreement with Figure 4.6 where increasing the number of realizations implies that the variation of the norm becomes closer and closer to the expected diffusion regime.

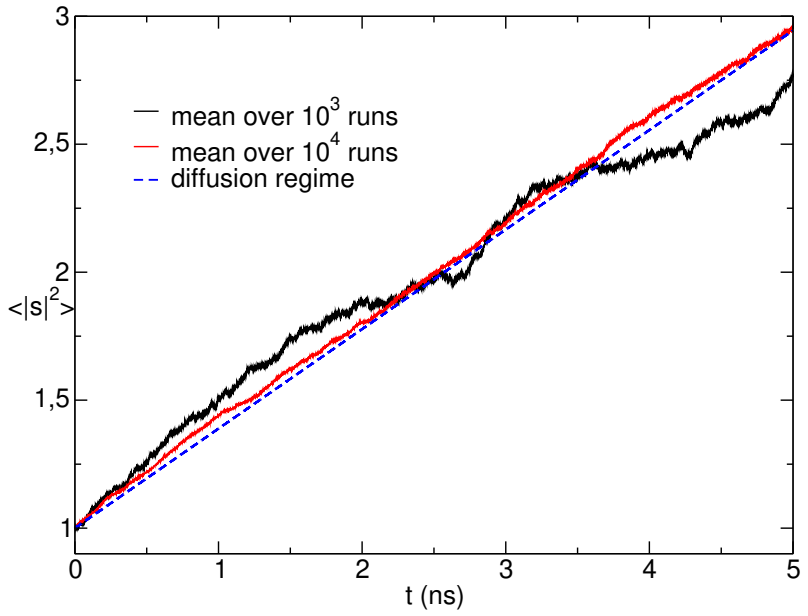

Figure 4.6: Mean square norm of the spin in the additive white noise case for the following conditions: integration step of 10^{-4}ns; $\Delta = 0.0655$ rad.GHz; $\boldsymbol{s}(0) = (0, 1, 0)$; $\alpha = 0.1$; $\boldsymbol{\omega} = (0, 0, 18)$ rad.GHz compared to the expected diffusion regime (see text).

In summary, we have seen that coupling our damped Nambu system to an additive noise can describe the precession of magnetic moments for small noise intensities and over short periods of time and the effective – deterministic – model, as does the stochastic averaged model, but faster, can describe the dynamics of this damped and fluctuating system. However for larger time-windows or noise intensities, this additive noise coupling cannot be chosen to describe magnetic systems as it inherently implies a diffusion regime on the norm of the magnetic moment which is simply not in agreement with experimental observations. In order to evaluate whether or not a different noise coupling is more appropriate to describe magnetic systems, we shall now proceed to investigate the multiplicative noise coupling by simulating, again, the corresponding stochastic model and the effective – deterministic – one.

4.3.2 The case of multiplicative noise

We now consider multiplicative noise [30], with again, both respectively the deterministic and stochastic models provided by equations (4.48) and (4.25) with the multiplicative vielbein $e_{ij} \equiv \frac{\varepsilon_{ijk} s_k}{1+\alpha^2}$.

If we keep only the first order moment of the hierarchy, or equivalently only small fluctuations so as to keep the distribution of the spin Gaussian ($\langle\langle s_i s_j \rangle\rangle = 0$), we can deduce from (4.48) that there is a longitudinal relaxation time τ_L described by the term $2\tilde{\tilde{\Delta}}$

$$\tau_L = \frac{(1+\alpha^2)^2}{2\Delta} \tag{4.54}$$

Indeed, as can be seen in Figure 4.7 and conversely to what was observed in the additive noise case, here we can see that, even though the norm of the spin is not necessarily conserved, it converges to an equilibrium value. As the noise intensity is small, the convergence is indeed in agreement with the relaxation time τ_L. What is also remarkable is that, although the dynamics of both cases are quite similar, qualitatively, they differ quite a lot quantitatively.

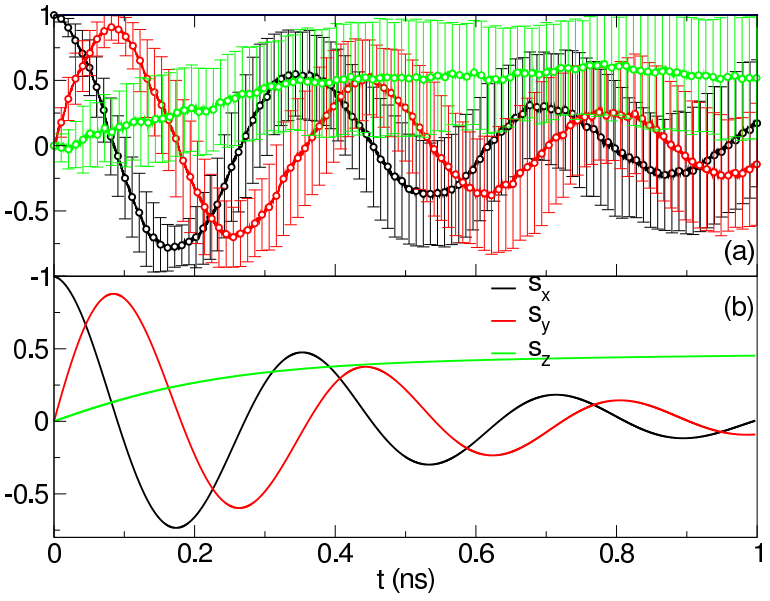

Figure 4.7: Magnetization dynamics of a paramagnetic spin in a constant magnetic field, connected to a multiplicative noise. The upper graphs (a) plot some of the first–order moments of the averaged magnetization vector over 10^2 realizations of the noise, when the lower graphs (b) plot the associated model closed to the third-order cumulant (see text). Parameters of the simulations : $\{\Delta = 0.65$ rad.GHz; $\alpha = 0.1$; $\boldsymbol{\omega} = (0, 0, 18)$ rad.GHz; timestep $\Delta t = 10^{-4}$ ns$\}$. Initial conditions: $\boldsymbol{s}(0) = (1, 0, 0)$, $\langle s_i(0)s_j(0)\rangle = 0$ but $\langle s_x(0)s_x(0)\rangle = 1$.

This becomes more obvious in Figure 4.8 where simulations over longer times have been performed, for different initial conditions. Here we can see that the spin becomes aligned with the external field and the z-component of the spin is lower than 1, even though the initial conditions have a non zero z-component as in Figure 4.5. The root mean square errors (error bars) are also much larger for the multiplicative noise than for additive noise [1]. This is expected as the noise dependence is much more intricate in the multiplicative noise case, which explains that one requires more realizations for the average to be as accurate as in the additive case.

[1] In a similar fashion to subsection 2.3.1, the convergence of this model depending on the number of realizations N can be checked, by using another error estimator, such as $\frac{\sigma}{\sqrt{N}}$

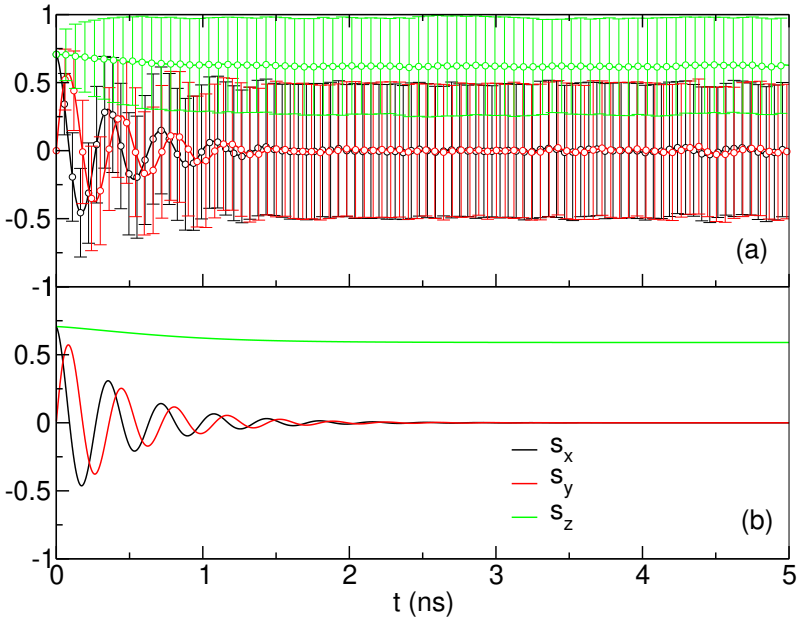

Figure 4.8: Magnetization dynamics of a paramagnetic spin in a constant magnetic field, connected to a multiplicative noise. The upper graphs (a) plot some of the first–order moments of the averaged magnetization vector over 10^4 realizations of the noise, when the lower graphs (b) plot the associated model closed to the third-order cumulant (see text). Parameters of the simulations : $\{\Delta = 0.65$ rad.GHz; $\alpha = 0.1$; $\boldsymbol{\omega} = (0, 0, 18)$ rad.GHz; timestep $\Delta t = 10^{-4}$ ns$\}$. Initial conditions: $\boldsymbol{s}(0) = \left(1/\sqrt{2}, 0, 1/\sqrt{2}\right)$, $\langle s_i(0)s_j(0)\rangle = 0$ except for $\langle s_1(0)s_1(0)\rangle = \langle s_1(0)s_3(0)\rangle = \langle s_3(0)s_3(0)\rangle = 1/2$.

We have thus shown that, it is possible to describe dissipation in magnetic systems, by an extension of Nambu mechanics. The fluctuations, however, are consistently described only using multiplicative noise, as the additive noise coupling induces a diffusion regime where the norm of the spin grows (positively or negatively, according to the sign of the intensity) indefinitely. The coupling of the magnetization to multiplicative noise can be schematized in the following way. As the external field $\boldsymbol{\omega}$ is supplemented by the noise $\boldsymbol{\eta}$, it behaves as if the Nambu phase space, which in the non dissipating case is built by the intersection of the two surfaces described in the Figure 4.1, was now constructed by the intersection of the sphere described by H_2 and a "fuzzy"-plane describe by H_1. In the case where the norm of the spin is conserved, the intersection of the "fuzzy"-plane and the sphere can, while remaining on the sphere, travel up and down, as if the plane was vibrating up and down. This illustrates how fluctuations can imply transverse dissipation for this description of magnetic systems. If now we also allow the sphere to be "fuzzy" then this description can transform constant angle precession as described by the Larmor equation, into longitudinally and transversely damped precession as described by stochastic-LLG equation.

Now that we have a better understanding of how dissipating and fluctuating magnetic systems can emerge from our framework, we can take into account the mechanical degrees of freedom. Indeed, one issue we have remarked upon, in previous sections, when describing

spin degrees of freedom, was the emergence of non-local quantities. When dealing with non-local quantities, especially with spins, there are two ways to proceed. Either indeed, work with non-local quantities and commuting variables, or work with local quantities but *non-commuting* variables. This is why in the next chapter, we will build a coupled model for magnetic and elastic degrees of freedom, through a Hamiltonian approach using anticommuting and commuting variables.

Summary

- An extension for Nambu dynamics to include dissipative phenomena is constructed, for the special case of magnetic systems whose time evolution is given by the LLG equation.
- The geometry is described by a linear noise vielbein, corresponding to the case of additive and/or multiplicative noise and a system of equations for the moments of the distribution are deduced for both cases.
- The hierarchies of the moments for both cases are truncated by closure assumptions, so as to obtain effective deterministic systems, which describe the dynamics of the moments of the distributions.
- Both the effective – deterministic – and stochastic models are simulated, both for additive and multiplicative noise couplings. The multiplicative noise is more suitable for describing the dissipation and fluctuations of magnetic systems and its consistent description can be provided within Nambu mechanics.

Chapter 5

A Hamiltonian approach for magnetoelasticity, combining anticommuting and commuting variables

Résumé

- Nous employons des variables commutantes et anticommutantes pour réinterpréter la précession d'un moment magnétique et construire un crochet de Poisson pour un système magnétoélastique.
- Nous définissons un Hamiltonien, cohérent avec ce crochet et en déduisons les équations du mouvement qui décrivent la dynamique couplée des degrés de liberté magnétiques et mécaniques.
- Nous étendons ce modèle–à une particule–au cas de plusieurs particules, en interaction, pour pouvoir décrire des systèmes magnétiques plus intéressants, tels que les antiferromagnétiques
- Nous étudions numériquement le retournement de l'aimantation d'un modèle jouet d'AF NiO par couple de transfert de spin

In the previous chapters, we have presented several methods for describing the dynamics of magnetic degrees of freedom, either for undamped precessional motion of a single moment, or for a collection of interacting magnetic moments, that satisfy appropriate generalizations of the LLG equation. Our approach amounts to building an effective model for the coupling of a spin to a "spin bath" in chapter 2, a Lagrangian model in chapter 3 and a generalization of Nambu dynamics, in chapter 4.

The Lagrangian approach, which described the coupling to the mechanical DOF most explicitly, however, implies a nonlocal description in terms of the magnetic moments – or spin – variables themselves, that satisfy the commutation relations of the rotation group.

In this chapter we will review that this non–locality can be expressed using anticommuting variables (in terms of which the spin degrees of freedom satisfy the expected, commutation relations of the rotation group). To this end we will begin by introducing a model for describing precessional motion through anticommuting variables. This was proposed by Berezin and Marinov in the 1970s [22]. There was, also, considerable activity in formal developments by the Firenze group [21]. What, however, remained dormant all these years, is putting these insights into use for describing effects in real materials–in particular regarding dissipation. This is the focus of this chapter and of the paper [117].

5.1 Interpreting precession using Poisson brackets and their generalizations for anticommuting variables

In section section 1.1, we have reviewed, how (classical) precession motion for the spin can emerge from quantum mechanics. Within non–relativistic quantum mechanics, the dynamics of spin must be described separately from that of the mechanical degrees of freedom, that carry it, since there isn't any spin–statistics relation in this case. In particular, while spin can take integer and half–integer values only, as a consequence of the properties of the rotation group, there does not seem to be any constraint on the value of the spin.

When relativistic effects become significant, the situation changes dramatically and consistent interactions, for spinning degrees of freedom, can be formulated, in terms of particles, only for spin 0, spin 1/2, 1, 3/2 and 2. For higher values of spin, that were encountered in the experiments in hadronic physics in the 1960s [118] the consistent formulation turned out to involve extended objects, namely strings–and the absence of a massless resonance of spin 2 became the motivation for reinterpreting the string theory for hadronic resonances as a theory of gravity, since the graviton is a massless particle of spin 2.

While this effort is, still, a work in progress, what has happened, much more recently, is that it has become possible to control the spin degrees of freedom at the scale of atoms and molecules in condensed matter systems with a precision that has surpassed all expectations–and this has proved crucial to imagining and developing new materials and new phases thereof. This has led to "spintronics," in particular [119, 120].

This has made the theoretical developments of the 1970s and 1980s [121, 122] in particular regarding the Hamiltonian description of spinning particles [123], very topical for

practical applications to new materials. In this framework, what is fascinating is that the "relativistic" features are "emergent" at the scale where baths are relevant, but their constituents cannot be resolved.

Let us, therefore, recall that one example, describing the dynamics of spin ½ variables are spinors, in the context of the Dirac equation [124].

Another one, which proves to be particularly useful for coupling magnetic to mechanical DOF, as we have seen in section section 1.7, is the description in terms of Majorana fermions [125], in which the spin variable $\boldsymbol{S}$

$$S_I = \frac{-\imath}{2}\varepsilon_{IJK}\xi_I\xi_J \tag{5.1}$$

in terms of a set of three anticommuting variables ξ_I such that

$$\xi_I\xi_J + \xi_J\xi_I = 2\delta_{IJ} \tag{5.2}$$

The ξ_I thus generate a Clifford algebra.

Interestingly, this spin, even though constructed using anticommuting variables, satisfies

$$[S_I, S_J] = \imath\varepsilon_{IJK}S_K \tag{5.3}$$

and can thus be understood to define a representation of the Lie group of SU(2). An interpretation of this representation is that the spin $\boldsymbol{S}$ is in fact a composite object whose underlying "fundamental" building blocks are the $\boldsymbol{\xi}$. The motivation behind this [92] is similar to section 3.1 where we introduced $\boldsymbol{\mu} = \dot{\boldsymbol{s}}$; indeed the notion of hidden variables in this specific context was proposed by [22] as we have seen in section 1.7.

An interesting question is whether it is possible to work with the ξ and the usual, commuting, positions and momenta in phase space, in a unified way, thereby enlarging the phase space into a supermanifold. The answer is, indeed, affirmative, as was shown in [126]. The appropriate generalization of the Poisson brackets turns out to be graded Poisson brackets of functions f and g of $\boldsymbol{\xi}$ that satisfy a relation of the following kind

$$\{f(\boldsymbol{\xi}), g(\boldsymbol{\xi})\}_{PB} \equiv \frac{\imath}{\hbar} f(\boldsymbol{\xi}) \frac{\overleftarrow{\partial}}{\partial\xi_K} \frac{\overrightarrow{\partial}}{\partial\xi_K} g(\boldsymbol{\xi}), \tag{5.4}$$

where the left derivation $\overleftarrow{\partial}$ simply means that one applies the derivation operator from the left to the right $\overrightarrow{\partial}$ and conversely for the right derivation. This bracket satisfies all relevant properties with a generalization of the Jacobi identity as a graded Jacobi identity [127]. Applying this bracket to the spin variables defined by eq. (5.1) yields the following relation

$$\{S_I, S_J\} = \frac{1}{\hbar}\varepsilon_{IJK}S_K \tag{5.5}$$

Now the fact that the $\boldsymbol{\xi}$ anticommute implies that any function of them can only be, at most, quadratic.

It should be stressed at this point that the appearance of $\hbar$ in this–and the following–relation(s) is purely of dimensional origin and does not imply that any quantum effects are present.

If we chose f and g, as functions of $\boldsymbol{\xi}$, to have vanishing linear part – *i.e.,* to be expressed only as functions of the $\boldsymbol{S}$ – then one can rewrite the bracket eq. (5.4) as

$$\begin{aligned}\{f(\boldsymbol{S}), g(\boldsymbol{S})\}_{PB} &= \frac{\imath}{\hbar}\frac{\partial f}{\partial S_I} S_I \frac{\overleftarrow{\partial}}{\partial \xi_K}\frac{\overrightarrow{\partial}}{\partial \xi_K} S_J \frac{\partial g}{\partial S_J} \\ &= \{S_I, S_J\}_{PB}\frac{\partial f}{\partial S_I}\frac{\partial g}{\partial S_J} = \frac{1}{\hbar}\varepsilon_{IJK} S_K \frac{\partial f}{\partial S_I}\frac{\partial g}{\partial S_J},\end{aligned} \tag{5.6}$$

This bracket can clearly be identified with the "spinning part" of the Poisson bracket proposed by Yang and Hirschfelder [19] and Ruijgrok and Van der Vlist [20] in the context of magnetized fluid dynamics

$$\{A, B\}_{PB} \equiv \frac{\partial A}{\partial q_I}\frac{\partial B}{\partial p_I} - \frac{\partial A}{\partial p_I}\frac{\partial B}{\partial q_I} - \frac{1}{\hbar}\varepsilon_{IJK} S_I \frac{\partial A}{\partial S_J}\frac{\partial B}{\partial S_K}. \tag{5.7}$$

where q_I are the position and p_I are the conjugate momenta of the moving particles. The spin part of this bracket enforces the constraint that the spin be on a sphere, of fixed radius. Indeed, by recalling section 1.5 and chapter 3 one can see that, if we define $H_2 = \frac{1}{2}S_K^2$, we can write

$$\{A, B, H_2\}_{NB} = \frac{1}{\hbar}\varepsilon_{IJK}\frac{\partial A}{\partial S_I}\frac{\partial B}{\partial S_J}\frac{\partial C_2}{\partial S_K} = -\{A, B\}_{PB} \tag{5.8}$$

where $\{A, B, H_2\}_{NB}$ is the Nambu bracket, which preserves H_2.

In order for this bracket to describe the intricate dynamics between mechanical and spin degrees of freedom, one must, therefore, construct a new bracket, that combines the properties of the "spinning" bracket, just reviewed with those of the, usual, Poisson bracket. This can be achieved as follows:

$$\begin{aligned}\{A, B\}_{PB} \equiv \frac{\partial A}{\partial \epsilon_{IJ}}\frac{\partial B}{\partial \pi_{IJ}} - \frac{\partial A}{\partial \pi_{IJ}}\frac{\partial B}{\partial \epsilon_{IJ}} \\ + \frac{1}{\hbar}\varepsilon_{IJK} S_I \frac{\partial A}{\partial S_J}\frac{\partial B}{\partial S_K},\end{aligned} \tag{5.9}$$

This is possible because ϵ_{IJ} and π_{IJ} can be identified with the position and momentum of a "particle," whose dynamics captures the elastic degrees of freedom, where the magnetic moment is embedded.

π_{ij}, the canonically conjugate variable to the strain tensor ϵ_{ij}, can be, indeed, understood– as expected, through the relation

$$\pi_{IJ} = \frac{\partial \mathcal{L}}{\partial \dot{\epsilon}_{IJ}} \tag{5.10}$$

where $\mathcal{L}$ is the Lagrangian of this system, an example being found in chapter 3. For $\boldsymbol{\epsilon}$ and $\boldsymbol{\pi}$ the bracket satisfies the following relations

$$\{\epsilon_{IJ}, \pi_{KL}\}_{PB} = \delta_{IJKL}, \tag{5.11}$$

$$\{\epsilon_{IJ}, \epsilon_{KL}\}_{PB} = \{\pi_{IJ}, \pi_{KL}\}_{PB} = 0 \tag{5.12}$$

where the notation δ_{IJKL} can be understood as

$$\delta_{IJKL} = \begin{cases} \delta_{IJ}\delta_{KL} \\ \delta_{IJ}\delta_{LK} \\ \delta_{JI}\delta_{LK} \\ \delta_{JI}\delta_{KL} \end{cases} \tag{5.13}$$

The definition of a canonical bracket for such tensors is, of course, by no means unique; the canonical transformations, that these define have been studied in [128–130], for instance.

Using this Poisson bracket, one can now obtain the EOM for the full phase space variables in the usual form as

$$\begin{aligned} \dot{\epsilon}_{IJ} &= \{\epsilon_{IJ}, \mathcal{H}\}_{PB} = \frac{\partial \mathcal{H}}{\partial \pi_{IJ}} \\ \dot{\pi}_{IJ} &= \{\pi_{IJ}, \mathcal{H}\}_{PB} = -\frac{\partial \mathcal{H}}{\partial \epsilon_{IJ}} \\ \dot{S}_I &= \{S_I, \mathcal{H}\}_{PB} = \frac{1}{\hbar}\varepsilon_{IJK} S_J \frac{\partial \mathcal{H}}{\partial S_K} \end{aligned} \tag{5.14}$$

where $\mathcal{H}$ is the Hamiltonian, which is a function of $\boldsymbol{\epsilon}$, $\boldsymbol{\pi}$ and $\boldsymbol{S}$ only.

Now that the Poisson bracket has been defined for the commuting alter ego $\boldsymbol{S}$ of the anticommuting, underlying variables $\boldsymbol{\xi}$ and for the mechanical strain tensor $\boldsymbol{\epsilon}$ (and its conjugate momenta $\boldsymbol{\pi}$), we need to construct an appropriate Hamiltonian for the magnetoelastic system that can capture its dynamics.

5.2 Constructing the Hamiltonian for a magnetoelastic system.

The Hamiltonian of the magnetoelastic system will be expressed in terms of the magnetic – $\boldsymbol{S}$ – and mechanical – $\boldsymbol{\epsilon}$ and $\boldsymbol{\pi}$ – variables. We will begin by building the free parts, *i.e.,* that describe the magnetic and mechanical parts without any interaction.

5.2.1 Defining the free Hamiltonian

The first contribution for the purely magnetic part of our system [1] is the Zeeman term:

$$\mathcal{H}_z = -\hbar\omega_I S_I \tag{5.15}$$

This term represents the magnetic energy of the system. In fact, the effective frequency $\boldsymbol{\omega}$, in this expression, can be a function of $\boldsymbol{S}$, thereby generalizing the purely Zeeman expression, where it is a constant.

The next term is the internal mechanical energy [131, 132], for which we keep only the lowest, non-trivial, *i.e.,* quadratic terms

$$\mathcal{H}_{\text{mech}} = \frac{V_0}{2} C_{IJKL}\epsilon_{IJ}\epsilon_{KL} \tag{5.16}$$

The C_{IJKL} are the elastic constants of the material, that are packaged in a $3 \times 3 \times 3 \times 3$ tensor, which is consistent with the Bravais symmetries, and V_0 is a reference volume, so that the expression for the Hamiltonian scales like an energy. For a homogeneous medium, the elastic constants can be expressed in terms of the two Lamé parameters [133] (C_0, C_1). In Cartesian coordinates these are related as

$$C_{IJKL} = C_0 \delta_{IJ} \delta_{KL} + C_1 \left(\delta_{IK} \delta_{JL} + \delta_{IL} \delta_{JK} \right) \tag{5.17}$$

As we have introduced π_{IJ} as the canonically conjugate "momenta" to the strain tensor ϵ_{IJ}, we also define a kinetic term for the mechanical system as

$$\mathcal{H}_{\text{kinetic}} = \frac{1}{2} \pi_{IJ} M^{-1}_{IJKL} \pi_{KL} \tag{5.18}$$

In this expression, the M_{IJKL} is a $3 \times 3 \times 3 \times 3$ mass tensor which verifies

$$M_{IJKL} = M_{KLIJ} = M_{JIKL} = M_{IJLK} \tag{5.19}$$

and describes the inertia of the mechanical response. Again, for isotropic media, we will assume a Lamé-like form, given by

$$M_{IJKL} = M_0 \delta_{IJ} \delta_{KL} + M_1 \left(\delta_{IK} \delta_{JL} + \delta_{IL} \delta_{JK} \right) \tag{5.20}$$

Here, M_0 is the effective inertia for the frequency of longitudinal waves and M_1 the effective inertia for the frequency of transverse waves, when the description is generalized to an extended medium, described by more than one "particle," carrying the mechanical and spin DOF.

We shall use the inverse of M, M^{-1}, further on; it can be computed from the relation

$$M_{IJKL} M^{-1}_{IJMN} = \frac{1}{2} \left(\delta_{KM} \delta_{LN} + \delta_{KN} \delta_{LM} \right) \tag{5.21}$$

in a similar fashion as the elastic compliances tensor [133] can be deduced from the elastic constants tensor (cf. chapter 3). This yields the following expression for the components of M^{-1}

$$\begin{aligned} M^{-1}_{IJKL} = & \frac{-M_0}{2M_1(3M_0 + 2M_1)} \delta_{IJ} \delta_{KL} \\ & + \frac{1}{4M_1} \left(\delta_{IK} \delta_{JL} + \delta_{IL} \delta_{JK} \right) \end{aligned} \tag{5.22}$$

We will also add a mechanical source term that describes an external (uniform in space and time) stress σ^{ext}_{IJ} to the Hamiltonian, *viz.*

$$\mathcal{H}_{\text{ext}} = -V_0 \sigma^{\text{ext}}_{IJ} \epsilon_{JI}. \tag{5.23}$$

Together, eqs. (5.16), (5.23) and (5.18) represent the total mechanical energy of our system, in the absence of interactions, in particular, between the mechanical and magnetic parts. Since we do want to study their intricate/coupled dynamics, we have to introduce an interaction term in the Hamiltonian, in a way that's consistent with the symmetries.

5.2.2 Local, magnetoelastic interactions

Now we proceed with the last step, which is to construct the interaction Hamiltonian. It must, of course, contain both $\boldsymbol{\epsilon}$ and $\boldsymbol{S}$. Of course, this, simply, represents a choice of coordinates in phase space, since it isn't possible to invariantly distinguish the canonically conjugate variables from each other.

Experiments show that only the axis and the intensity–but not the direction–of the magnetic field affect how it controls magnetostrictive behavior [6]. Thus the interaction Hamiltonian must be an even function of the magnetization $\boldsymbol{S}$.

To lowest order, we can, therefore, keep only the quadratic terms for the magnetization (as long as we can neglect morphic effects, which can arise in experiments, but are described by higher order terms [6]).

For the strain, on the other hand, no symmetry arguments impose that the interaction Hamiltonian be an even function thereof.

This implies that the lowest order magnetoelastic interaction term is given by

$$\mathcal{H}_{\text{me}} = B_{IJKL}\epsilon_{IJ}S_K S_L \tag{5.24}$$

where B_{IJKL} are the components of the $3 \times 3 \times 3 \times 3$ tensor of magnetoelastic constants . This is the usual form which has been considered in the literature on models of magnetoelasticity [134–136].

The main difference here is that $\boldsymbol{\epsilon}$ and $\boldsymbol{S}$ are variables which have a non–trivial time dependence.

Again, if the system is isotropic these can be written as

$$B_{IJKL} = B_0\delta_{IJ}\delta_{KL} + B_1\left(\delta_{IK}\delta_{JL} + \delta_{IL}\delta_{JK}\right) \tag{5.25}$$

We now face a problem. The equation (5.1) imposes that $S_I S_J = 0$, or a constant, since the ξ generate a Clifford algebra. However for lattice dynamics, or more precisely, Atomistic Spin Dynamics (ASD) the physical interpretation for the magnetization on each site depends on the spatial scale in the simulation–whether it represents a single magnetic moment, or the average over a domain. Usually, the magnetization S_I^{eff} at each *simulation* site I is an average over the magnetization of several "physical" sites i, to which is associated a local magnetization vector S_I^i. This can formally be written as

$$S_I^{\text{eff}} = \langle S_I^i \rangle_i \tag{5.26}$$

Since the ξ_I on *different* sites span a much larger space, their anticommutation relations allow a correspondingly larger number of multilinears, before triviality sets in. So, the S_I^{eff}, even though they represent one site, are, in fact, averages over several sites. This in turn means that the $S_I^{\text{eff}}S_J^{\text{eff}}$ no longer require to vanish identically (or be constants). Equation (5.24) can, in fact, be identified with the expression over two sites, as introduced by [137].

We have thus defined all the terms in our Hamiltonian and with the Poisson bracket (5.9)

we can write the equations of motion for our system which read

$$\begin{cases} \dot{\epsilon}_{IJ} = M^{-1}_{IJKL}\pi_{KL} \\ \dot{\pi}_{IJ} = -V_0 C_{IJKL}\epsilon_{KL} + V_0\sigma^{\text{ext}}_{IJ} - B_{IJKL}S_K S_L \\ \dot{S}_I = \varepsilon_{IJK}\left(\omega_J - \frac{2}{\hbar}B_{ABJC}\epsilon_{AB}S_C\right)S_K \end{cases} \tag{5.27}$$

where remarkably, the last equation still is a precession equation for the spin, where the precession frequency is modified by the magnetoelastic coupling. By construction, this is a Hamiltonian dynamical system which preserves the extended phase space volume as one can show by checking

$$\frac{\partial \dot{\epsilon}_{IJ}}{\partial \epsilon_{IJ}} + \frac{\partial \dot{\pi}_{IJ}}{\partial \pi_{IJ}} + \frac{\partial \dot{S}_I}{\partial S_I} = 0 \tag{5.28}$$

Now this system only describes a single domain, carrying both the magnetic moment $\boldsymbol{S}$ and the strain and conjugate tensors $\{\epsilon_{IJ}, \pi_{IJ}\}$ depicted in Figure 5.1. Schematically, $\boldsymbol{\pi}$ can be thought of as the reciprocal volume of $\boldsymbol{\epsilon}$.

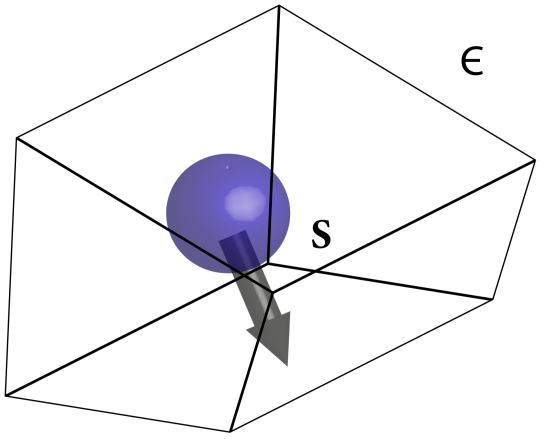

Figure 5.1: Schematic representation of the coupled strain and magnetization for a finite volume V_0 magnetoelastic solid

Therefore, the description presented here describes single domains and cannot capture phenomena that involve exchange interactions between domains, for example. In order to describe such larger systems, we thus need to extend this model to take into account the fact that sites need not be equivalent. This, in particular, will allow us to describe how sublattices can interact, which is useful for antiferromagnets.

5.3 Extending the model to multi-particle magneto-elastic solids

The first step towards a multi–domain and, therefore, "multi–particle" description is to introduce a label, for each lattice site: $i = 1..N$ in (5.27).

We have decided not to "decorate" the constants M, C and B, which appear in this system, so as to keep things simple; but this would not cause any conceptual issues. Despite this simplification, this framework, nonetheless, allows the quantitative study of materials with homogeneous properties. In equations:

$$\begin{cases} \dot{\epsilon}^i_{IJ} = M^{-1}_{IJKL}\pi^i_{KL} \\ \dot{\pi}^i_{IJ} = -V_0 C_{IJKL}\epsilon^i_{KL} + V_0\sigma^{\text{ext}}_{IJ} - B_{IJKL}S^i_K S^i_L \\ \dot{S}^i_I = \varepsilon_{IJK}\left(\omega^i_J + \dfrac{\partial\omega^i_I}{\partial S^i_L}S^i_L - \dfrac{2}{\hbar}B_{ABJC}\epsilon^i_{AB}S^i_C\right)S^i_K \end{cases} \tag{5.29}$$

where one has to add the term $\dfrac{\partial\omega^i_I}{\partial S^i_L}S^i_L$, to take into account possible dependence of the field $\boldsymbol{\omega}^i$ on $\boldsymbol{S}^i$.

This system describes a set of non-interacting particles, evolving according to the same EOM.

In order for this new set to describe interacting particles, we need to introduce a way for having different labels.

We choose to encode the interaction through an effective frequency, $\boldsymbol{\omega}^i_{\text{eff}}$, by adding a purely magnetic exchange term over the nearest neighbors j :

$$\omega^i_{\text{eff}\,I} = \frac{1}{\hbar}\sum_{j\in nn} J^{ij}S^j_I \tag{5.30}$$

where J^{ij} is the exchange matrix for the different sites, and is assumed to be symmetric (*i.e.*, symmetric exchange). We chose not to implement a mechanical interaction between different sites as we want to focus rather on how the magnetic response is modified by the coupling to the mechanical system. Generalizations of this formalism for taking into account such "back reaction" effects have, however, been explored in [138] and [139].

We have now generalized our model in a way that is appropriate for describing the dynamics of interacting, multi-"particle" systems, consisting of lattice sites, each carrying a magnetic moment $\boldsymbol{S}$ and the conjugate mechanical variables $\{\epsilon_{IJ}, \pi_{IJ}\}$. The sites can now interact through a magnetic exchange interaction. In this fashion we can therefore hope to describe more complex magnetic systems such as ferromagnets or antiferromagnets. As the latter, in particular, have recently drawn a lot of interest in the quest for developing fast spintronic devices [140, 141], in the next section we will show how to use our framework to understand magnetoelastically coupled antiferromagnets.

5.4 The magnetoelasticity of antiferromagnets

In section 5.3 we have introduced a magnetic exchange interaction between sites of a lattice. A particularly interesting application is to systems, whose magnetic degrees of freedom can display antiferromagnetic order. The simplest AF system consists of two sites, interacting through AF exchange and thus of opposite local magnetization, along the same axis.

A practical application is to the case of NiO.

In this case we need, also, to introduce a local easy axis, by adding an anisotropy term to the effective frequency

$$\omega^i_{\text{eff}\,I} = \frac{1}{\hbar}\sum_{j\in nn} J^{ij} S^j_I + \frac{K}{\hbar} n_J n_I S^i_J \tag{5.31}$$

In this expression, $\boldsymbol{n}$ describes the orientation of the easy axis and K is the uniaxial anisotropy constant. In this fashion, we can define a toy model for an AF NiO-like solid by studying a $N = 2$ sites, where the sites now are to be identified with the sublattices of NiO. This model is depicted in Figure 5.2.

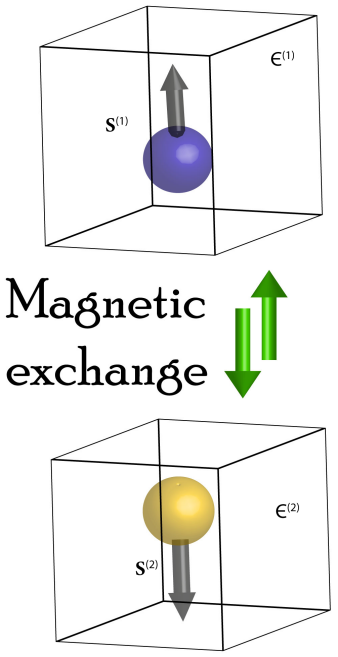

Figure 5.2: Schematic representation for an AF NiO like toy model, magnetoelastically coupled.

At this point, our system is defined by the following set of EOM.

$$\begin{cases} \dot{\epsilon}^i_{IJ} = M^{-1}_{IJKL}\pi^i_{KL} \\ \dot{\pi}^i_{IJ} = -V_0 C_{IJKL}\epsilon^i_{KL} + V_0\sigma^{\text{ext}}_{IJ} - B_{IJKL}S^i_K S^i_L \\ \dot{S}^i_I = \varepsilon_{IJK}\left(\frac{1}{\hbar}\sum_{j\in nn} J^{ij}S^j_J + \frac{K}{\hbar}n_K n_J S^i_K - \frac{2}{\hbar}B_{ABJC}\epsilon^i_{AB}S^i_C\right)S^i_K \end{cases} \tag{5.32}$$

The dynamics described by eq. (5.32) is elucidated by solving these equations numerically. As we have done in the chapter 3, we will set up a symplectic integration scheme for the coupled system.

5.4.1 A symplectic integration scheme for the magneto-elastically coupled dynamics

We proceed to the numerical integration of eq. (5.32). The method is similar to chapter 3 but there is one key difference, which is the appearance of the strain-rate tensor π_{IJ}, since we are using a Hamiltonian formalism (recall that the spin DOF is self–conjugate).

The first step, as usual, is to write eq. (5.32) in terms of Liouville operators – $\mathcal{L}$ – that act on the phase-space variables as

$$\begin{aligned} \dot{\boldsymbol{\epsilon}} &= \mathcal{L}_{\boldsymbol{\epsilon}}\boldsymbol{\epsilon}, \\ \dot{\boldsymbol{\pi}} &= \mathcal{L}_{\boldsymbol{\pi}}\boldsymbol{\pi}, \\ \dot{\boldsymbol{S}} &= \mathcal{L}_{\boldsymbol{S}}\boldsymbol{S}. \end{aligned} \tag{5.33}$$

These Liouville operators are defined for any phase space variable x through

$$\mathcal{L}_x = \dot{x}\frac{\partial}{\partial x} \tag{5.34}$$

Applying such an operator to the variable x yields

$$[\mathcal{L}_x]\, x = \dot{x} \tag{5.35}$$

as expected. Hence, for any function $f \equiv f(\boldsymbol{s}(t), \boldsymbol{\epsilon}(t), \boldsymbol{\pi}(t))$ the total derivative (which we shall write by the dot notation) can be expressed as

$$\begin{aligned} \dot{f} &= \dot{\epsilon}_{IJ}\frac{\partial f}{\partial \epsilon_{IJ}} + \dot{\pi}_{IJ}\frac{\partial f}{\partial \pi_{IJ}} + \dot{S}_I\frac{\partial f}{\partial S_I} \\ &\equiv [\mathcal{L}]f. \end{aligned} \tag{5.36}$$

where we have defined the (total) Liouville operator $\mathcal{L}$ by

$$\mathcal{L} = \dot{\epsilon}_{IJ}\frac{\partial}{\partial \epsilon_{IJ}} + \dot{\pi}_{IJ}\frac{\partial}{\partial \pi_{IJ}} + \dot{S}_I\frac{\partial}{\partial S_I} = \mathcal{L}_{\boldsymbol{\epsilon}} + \mathcal{L}_{\boldsymbol{\pi}} + \mathcal{L}_{\boldsymbol{S}} \tag{5.37}$$

The solutions of eq. (5.33) can, at least formally, be given at any time by

$$f(\boldsymbol{\epsilon}(t), \boldsymbol{\pi}(t), \boldsymbol{S}(t)) = e^{\mathcal{L}t} f(\boldsymbol{\epsilon}(0), \boldsymbol{\pi}(0), \boldsymbol{S}(0)). \tag{5.38}$$

There is, however, an issue with the exponentiation of operators. Indeed, if these operators do not commute

$$e^{\mathcal{L}t} = e^{\mathcal{L}_{\boldsymbol{\epsilon}}t+\mathcal{L}_{\boldsymbol{\pi}}t+\mathcal{L}_{\boldsymbol{S}}t} \neq e^{\mathcal{L}_{\boldsymbol{\epsilon}}t}e^{\mathcal{L}_{\boldsymbol{\pi}}t}e^{\mathcal{L}_{\boldsymbol{S}}t}. \tag{5.39}$$

One can easily show that this is, in fact, the case for $\mathcal{L}_{\boldsymbol{\epsilon}}$ and $\mathcal{L}_{\boldsymbol{S}}$

$$[\mathcal{L}_{\boldsymbol{S}}, \mathcal{L}_{\boldsymbol{\epsilon}}] = \dot{S}_I \frac{\partial \dot{\epsilon}_{AB}}{\partial S_I} \frac{\partial}{\partial \epsilon_{AB}} - \dot{\epsilon}_{AB} \frac{\partial \dot{S}_I}{\partial \epsilon_{AB}} \frac{\partial}{\partial S_I} \neq 0 \tag{5.40}$$

and for $\mathcal{L}_{\boldsymbol{\epsilon}}$ and $\mathcal{L}_{\boldsymbol{\pi}}$

$$[\mathcal{L}_{\boldsymbol{\epsilon}}, \mathcal{L}_{\boldsymbol{\pi}}] = \dot{\epsilon}_{AB} \frac{\partial \dot{\pi}_{CD}}{\partial \epsilon_{AB}} \frac{\partial}{\partial \pi_{CD}} - \dot{\pi}_{CD} \frac{\partial \dot{\epsilon}_{AB}}{\partial \pi_{CD}} \frac{\partial}{\partial \epsilon_{AB}} \neq 0 \tag{5.41}$$

An example of the consequences of non-commutativity of operators can be given by the rotations around different axis. An illustration is found in Figure 5.3.

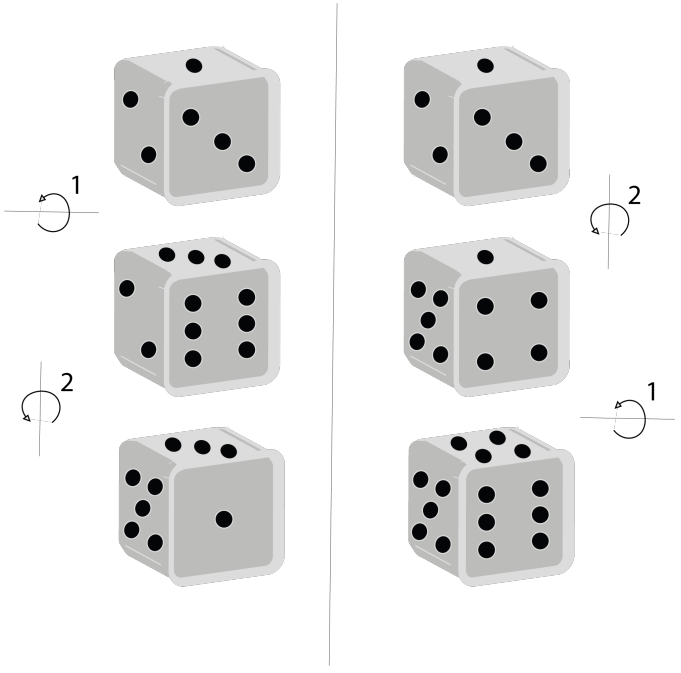

Figure 5.3: Example of non-commuting rotations for a 6 faced dice

One can see that indeed, the result of the combination of two rotations depends on the ordering of these rotations.

Now we would like to be able to act with the individual exponentials of the Liouville operators, since these act "simply" on the phase space variables. Since we are, anyway, interested in a numerical treatment, we would like to use a scheme that allows us this flexibility. Such schemes can be constructed using the Magnus expansion [79].

This expansion allows us, in particular, to express any operator as a product of its "parts" in powers of the time step, according to the splitting-method presented, for instance, in [78]. This has the virtue of preserving the phase space volume. For a time step

τ, one has

$$e^{\mathcal{L}\tau} = e^{\mathcal{L}_{\boldsymbol{S}}\frac{\tau}{4}} e^{\mathcal{L}_{\boldsymbol{\pi}}\frac{\tau}{2}} e^{\mathcal{L}_{\boldsymbol{S}}\frac{\tau}{4}} e^{\mathcal{L}_{\boldsymbol{\epsilon}}\tau} e^{\mathcal{L}_{\boldsymbol{S}}\frac{\tau}{4}} e^{\mathcal{L}_{\boldsymbol{\pi}}\frac{\tau}{2}} e^{\mathcal{L}_{\boldsymbol{S}}\frac{\tau}{4}} + \mathcal{O}(\tau^3), \tag{5.42}$$

What is of practical interest, now, is that there are several possibilities for the decomposition, that allow the same error at any given order; a list of those that allow for the same $\mathcal{O}(\tau^3)$ error, for instance, is presented in Table 5.1

A	$\frac{\tau}{4}$	$\frac{\tau}{2}$	$\frac{\tau}{4}$	τ	$\frac{\tau}{4}$	$\frac{\tau}{2}$	$\frac{\tau}{4}$
1	$\boldsymbol{S}$	$\boldsymbol{\pi}$	$\boldsymbol{S}$	$\boldsymbol{\epsilon}$	$\boldsymbol{S}$	$\boldsymbol{\pi}$	$\boldsymbol{S}$
2	$\boldsymbol{S}$	$\boldsymbol{\epsilon}$	$\boldsymbol{S}$	$\boldsymbol{\pi}$	$\boldsymbol{S}$	$\boldsymbol{\epsilon}$	$\boldsymbol{S}$
3	$\boldsymbol{\pi}$	$\boldsymbol{\epsilon}$	$\boldsymbol{\pi}$	$\boldsymbol{S}$	$\boldsymbol{\pi}$	$\boldsymbol{\epsilon}$	$\boldsymbol{\pi}$
4	$\boldsymbol{\pi}$	$\boldsymbol{S}$	$\boldsymbol{\pi}$	$\boldsymbol{\epsilon}$	$\boldsymbol{\pi}$	$\boldsymbol{S}$	$\boldsymbol{\pi}$
5	$\boldsymbol{\epsilon}$	$\boldsymbol{\pi}$	$\boldsymbol{\epsilon}$	$\boldsymbol{S}$	$\boldsymbol{\epsilon}$	$\boldsymbol{\pi}$	$\boldsymbol{\epsilon}$
6	$\boldsymbol{\epsilon}$	$\boldsymbol{S}$	$\boldsymbol{\epsilon}$	$\boldsymbol{\pi}$	$\boldsymbol{\epsilon}$	$\boldsymbol{S}$	$\boldsymbol{\epsilon}$

Table 5.1: Decomposition table of symplectic integrators

The choice of the ordering will have consequences on how often a particular effective field is computed during the integration process, which in practice, should be adapted to its amplitude. Because of the Poisson bracket we introduced, the one–step evolution operators for $\boldsymbol{\epsilon}$ and $\boldsymbol{\pi}$ are shifts of their tensor components, whereas the one–step evolution operator for $\boldsymbol{S}$ describes rotations.

Thus applying these operators on the phase space for any given time τ yields

$$e^{\mathcal{L}_{\epsilon}\tau}(\boldsymbol{\epsilon}(t), \boldsymbol{\pi}(t), \boldsymbol{S}(t)) = (\boldsymbol{\epsilon}(t) + \tau\dot{\boldsymbol{\epsilon}}(t), \boldsymbol{\pi}(t), \boldsymbol{S}(t)) \tag{5.43}$$

$$e^{\mathcal{L}_{\pi}\tau}(\boldsymbol{\epsilon}(t), \boldsymbol{\pi}(t), \boldsymbol{S}(0)) = (\boldsymbol{\epsilon}(t), \boldsymbol{\pi}(t) + \tau\dot{\boldsymbol{\pi}}(t), \boldsymbol{S}(t)) \tag{5.44}$$

$$e^{\mathcal{L}_{S}\tau}(\boldsymbol{\epsilon}(t), \boldsymbol{\pi}(t), \boldsymbol{S}(t)) = (\boldsymbol{\epsilon}(t), \boldsymbol{\pi}(t), \underbrace{\boldsymbol{S}(t+\tau)}_{R(\tau)\boldsymbol{S}(t)}) \tag{5.45}$$

and $\boldsymbol{S}(t+\tau) = R(\tau)\boldsymbol{S}(t)$ is expressed by the Rodrigues rotation formula [36, 142, 143] for a spin vector around a given precession vector $\boldsymbol{\omega}_{\text{eff}}(t)$.

Here we should briefly recall that as we study the $N = 2$ case, we have two spins for which the operators do not commute, as

$$[\mathcal{L}_{\boldsymbol{S}^{(1)}}, \mathcal{L}_{\boldsymbol{S}^{(2)}}] = \dot{S}_I^{(1)} \frac{\partial S_J^{(2)}}{\partial S_I^{(1)}} \frac{\partial}{\partial S_J^{(2)}} - \dot{S}_J^{(2)} \frac{\partial S_I^{(1)}}{\partial S_J^{(2)}} \frac{\partial}{\partial S_I^{(1)}} \tag{5.46}$$

because the effective field $\boldsymbol{\omega}_{\text{eff}}^i$ depends on the other spin through the exchange interaction. This means that here, as well, we have to approximate the exponentiation of the $\mathcal{L}_S$ operator as

$$e^{\mathcal{L}_S\tau} = e^{\mathcal{L}_{S^{(1)}}\frac{\tau}{2}} e^{\mathcal{L}_{S^{(2)}}\tau} e^{\mathcal{L}_{S^{(1)}}\frac{\tau}{2}} + \mathcal{O}(\tau^3) \tag{5.47}$$

where we define the (total) spin Liouville operator $\mathcal{L}_S = \mathcal{L}_{S^{(1)}} + \mathcal{L}_{S^{(2)}}$. As the evolution equations for ϵ_{IJ}^i and π_{IJ}^i do not explicitly depend on each other, their Liouville operators

commute and can simply be factorized as

$$\begin{cases} e^{\mathcal{L}_\epsilon \tau} &= e^{\mathcal{L}_{\epsilon^{(1)}} \tau} e^{\mathcal{L}_{\epsilon^{(2)}} \tau} \\ e^{\mathcal{L}_\pi \tau} &= e^{\mathcal{L}_{\pi^{(1)}} \tau} e^{\mathcal{L}_{\pi^{(2)}} \tau} \end{cases} \tag{5.48}$$

where we define the (total) strain Liouville operator $\mathcal{L}_\epsilon = \mathcal{L}_{\epsilon^{(1)}} + \mathcal{L}_{\epsilon^{(2)}}$ and $\mathcal{L}_\epsilon = \mathcal{L}_{\pi^{(1)}} + \mathcal{L}_{\pi^{(2)}}$.

In order to adapt the time step of the integration to the required precision, we also implement a variable time step for the integration by implementing a quality factor Q. To do this, we verify that at each time step when computing the effective precession fields $\boldsymbol{\omega}^i_{\text{eff}}$, the time step for the current integration step, corresponds to $\frac{1}{Q}$ of the period of the largest effective precession field

$$\frac{\tau}{Q} = \min\left(\frac{1}{||\boldsymbol{\omega}^i_{\text{eff}}||}\right) \tag{5.49}$$

Now, we just need to choose a decomposition and apply it for each time step to the phase space variables $\{\epsilon^i_{IJ}, \pi^i_{IJ}, \boldsymbol{S}^i\}$.

As a test of our approach, we simulate the switching of magnetization of a NiO AF toy model through an external STT.

5.4.2 Simulating switching of the magnetization in a NiO AF through an external STT

In the previous section we have set up a framework for simulating the coupled dynamics of magnetoelastic materials, described by magnetization $\boldsymbol{S}$, strain $\boldsymbol{\epsilon}$ and strain-rate $\boldsymbol{\pi}$. In order to check the quality of the framework, we shall apply it to the simulation of the switching of the magnetization in two–sublattice model, that's appropriate for NiO.

Specifically, we will simulate how the Néel vector of the magnetization switches orientation, under an external stress, that's generated by an external STT pulse. This pulse can experimentally be realized, for example, by a laser pulse, that produces a field-induced STT. This simulation is illustrated in Figure 5.4.

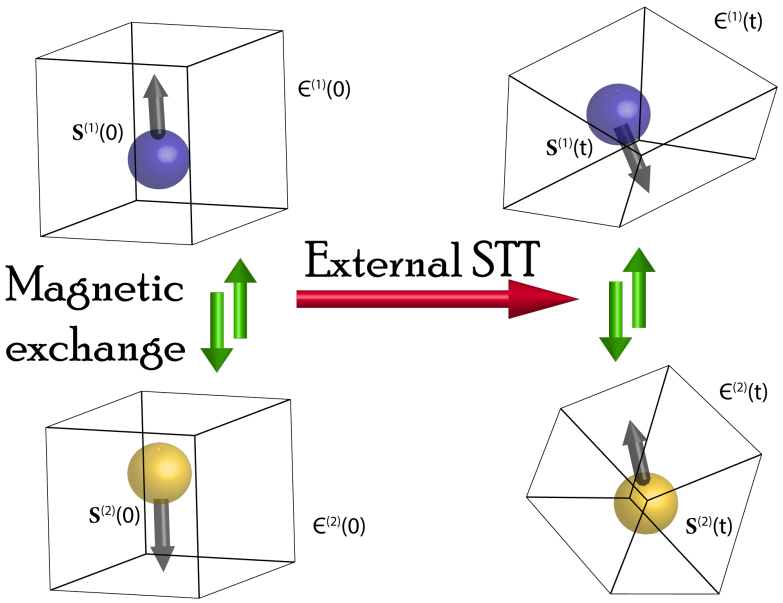

Figure 5.4: Schematic representation of the spin transfer torque magnetization switching for the antiferromagnetic NiO toy model. The two different colors represent the two opposite magnetizations of the sub-lattices and the box represent the localized strains and their time evolution.

It is possible to gain some physical insights, by realizing that there are two factors at work here: The strong exchange interaction in AFs, along with the anisotropy. Their combination gives rise to an effective inertia, that produces a time scale, for the response, significantly longer than the pulse itself. After the pulse, the magnetization of each sub-lattice follows a natural path, slightly out of the easy plane, and relaxes to other, more favorable, magnetic configurations.

This results in the switching of the magnetization of the two sub-lattices, in the opposite direction. This is known as ultrafast AF switching [101]. During this switching phenomena, the AF acquires a small–net–magnetization, generally in the direction of the STT. This "spin-accumulation," can be transferred to a magnetic material to produce a spin current via scattering of electrons. The innovation here is to consider an external stress, that can enhance–or inhibit–this switching.

In order to compare our results to chapter 3 and to introduce the STT into our model, we will add a torque term $\boldsymbol{T}$, consisting of a "damping-like" STT term and a damping term for the magnetic part, *viz.*

$$T_I^i = \alpha \varepsilon_{IJK} S_J^i \dot{S}_K^i + G\left(S_I^i S_J^i p_J - p_I S_J^i S_J^i\right) \tag{5.50}$$

Thus the final form for the EOM is given by inserting eq. (5.50) into eq. (5.32), yielding

$$\begin{cases} \dot{\epsilon}^i_{IJ} = M^{-1}_{IJKL}\pi^i_{KL} \\ \dot{\pi}^i_{IJ} = -V_0 C_{IJKL}\epsilon^i_{KL} + V_0\sigma^{\text{ext}}_{IJ} - B_{IJKL}S^i_K S^i_L \\ \dot{S}^i_I = \varepsilon_{IJK}\left(\frac{1}{\hbar}\sum_{j\in nn} J^{ij}S^j_J + \frac{K}{\hbar}n_K n_J S^i_K - \frac{2}{\hbar}B_{ABJC}\epsilon^i_{AB}S^i_C\right)S^i_K + T^i_I \end{cases} \tag{5.51}$$

These are the equations which are being solved hereafter, by using the approach detailed in the previous section. It is useful to remark that T^i_I can also be recast into an additional contribution for the effective precession frequency as

$$T^i_I = -\varepsilon_{IJK}\left(\alpha\dot{S}_J + G\varepsilon_{JLM}S_L p_M\right)S_K \tag{5.52}$$

so that

$$\begin{aligned} \dot{S}^i_I &= \varepsilon_{IJK}\Bigg(\frac{1}{\hbar}\sum_{j\in nn} J^{ij}S^j_J + \frac{K}{\hbar}n_K n_J S^i_K \\ &- \frac{2}{\hbar}B_{ABJC}\epsilon^i_{AB}S^i_C - \varepsilon_{IJK}\left(\alpha\dot{S}_J + G\varepsilon_{JLM}S_L p_M\right)\Bigg)S^i_K \end{aligned} \tag{5.53}$$

As in chapter 3, for the magnetization, we plot the average magnetization $\boldsymbol{m} = \frac{1}{2}\left(S^1 + S^2\right)$ and the Néel vector $\boldsymbol{l} = \frac{1}{2}\left(S^1 - S^2\right)$; the latter is the quantity that describes the switching.

Results for the uncoupled, *i.e.,* purely magnetic problem, are given in Figure 5.5.

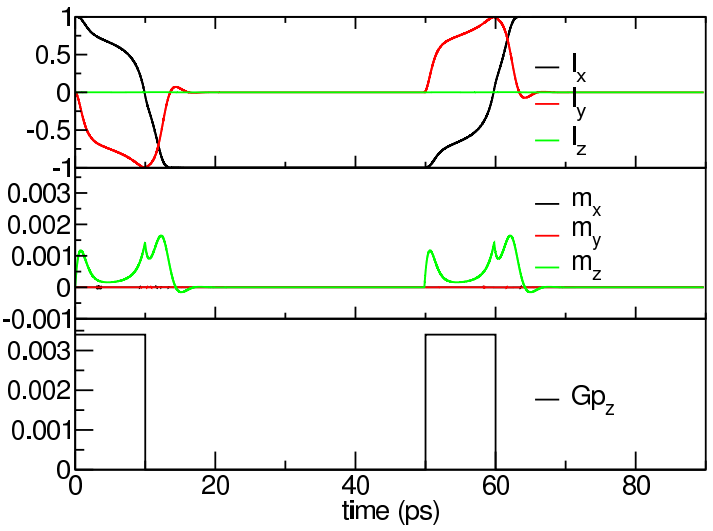

Figure 5.5: Average magnetization (upper panel) and Néel order parameter components (middle panel) for uncoupled switching with parameters : $\{\alpha = 0.5,\ K = 2\pi$rad.GHz, J=172.16 rad.THz, $M_s = 5.10^5$A.m$^{-1}\}$. Initial conditions: $\{\boldsymbol{S}^1(0) = -\boldsymbol{S}^2(0) = \hat{\boldsymbol{x}}\}$. The lower panel displays the STT pulses. The figures agree with the reference [101] because the magnetoelastic constants are set to zero.

Here the results are identical to reference [101] and subsection 3.4.1 in Figure 3.3 for the uncoupled curves. The only notable difference is that all the components are plotted, both for the Néel vector and the average magnetization. This is a first consistency check of our framework. Now in the coupled case, results are different and can be found in Figure 5.6.

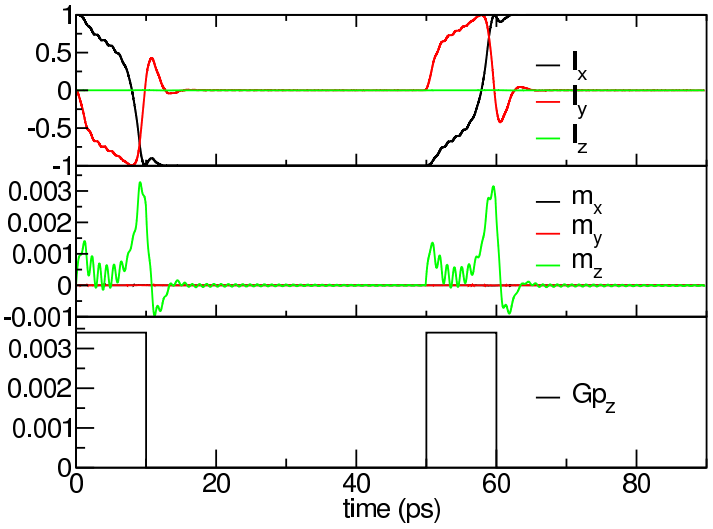

Figure 5.6: Average magnetization (upper panel) and Néel order parameter components (middle panel) for a coupled switching with parameters : $\{\alpha = 0.5,\ K = 2\pi$rad.GHz, J=172.16 rad.THz, $M_s = 5.10^5$A.m$^{-1}\}$. Initial conditions: $\{\boldsymbol{S}^1(0) = -\boldsymbol{S}^2(0) = \hat{\boldsymbol{x}},\ \epsilon^i_{IJ}(0) = 0\}$. The lower panel displays the STT pulses. Here $B_0 = 7.7\mu_0 M_s^2$ and $B_1 = -23\mu_0 M_s^2$.

Conversely to what we observed in Chapter 3, the required stress to enhance the switching speed, even for the purely transverse (compression/tensile stress) stress, is quite small, around $30\mu_0 M_S^2$. A second notable difference is the oscillatory behavior, which is more noticeable for the average magnetization. This is due to the fact that in the case at hand, we have taken into account mechanical inertia effects and also have not imposed a damping term on the mechanical part.

This leads to another interesting question which is how the switching time is affected by the values taken by either B_0 and B_1, *i.e.,* the magnetoelastic constants, that are the coefficients of the interaction between magnetic moment(s) and strain (cf. (5.24)).

We have checked that changing B_0 has no influence on the switching time, because this coefficient does not appear in the precession equation. It does give rise to the Joule magnetostriction effects, as, already, mentioned in reference [6].

However, changing B_1 does have a strong influence.

In Figure 5.7 we display the switching time as a function of R, defined as the ratio of $\tilde{B_1}$ over the reference value which we obtained for NiO, namely, $B_1 = -23$

$$R = \frac{\tilde{B_1}}{B_1} \tag{5.54}$$

We performed different simulations, for each value of R and recorded the time at which the x-component of the Néel vector crosses over to negative values.

One can see that this time decreases, with increasing R, which makes sense, as this enhances the effects of the tensile stress.

When R becomes lower than 1, the effect is opposite. One aspect which is, however,

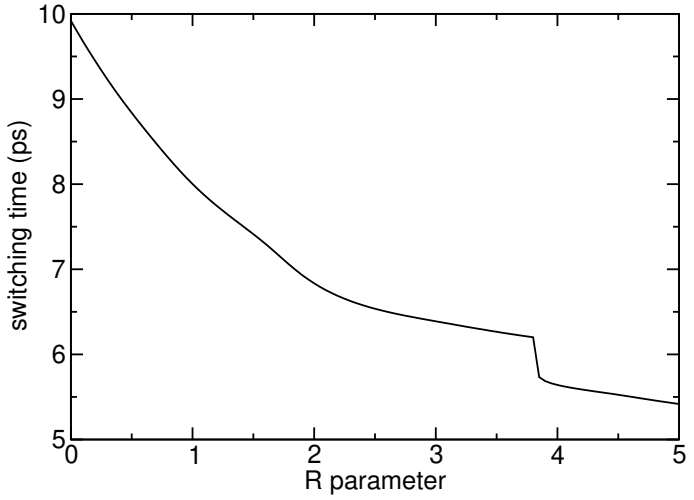

Figure 5.7: Switching time (in ps) as a function of varying B_1 over its natural value in NiO.

surprising is that there is a quick drop of the switching time for $R \approx 4$.

This can be explained as due to the oscillations of the magnetization, induced by the elastic coupling. As this coupling becomes stronger, one of the peaks of this Néel vector dips below 0 and thus the switching time appears to drop in a discontinuous fashion. This is another interesting consequence of the interplay of the magnetization and the strain, that could be captured in real experiments.

Nonetheless, the profile of the magnetization seems to indicate that the magnetization itself has acquired an inertia. It seems that this behavior is specific to AF systems [144], quite likely because of the strength of the exchange interaction in these materials. Results for the strain dynamics in the coupled case, corresponding to the alter ego to Figure 5.6 are given in Figure 5.8

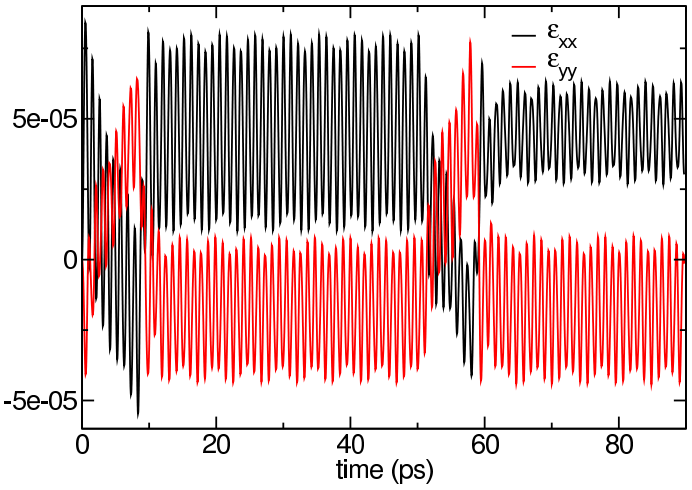

Figure 5.8: Strain components as a function of time with the magnetoelastic constants turned on. Parameters identical to Figure 5.6

Indeed, the mechanical part displays the expected oscillatory behavior due to the quadratic contributions (namely that the equations of motion take the form of two coupled first-order equations for ϵ_{IJ} and π_{IJ}). As the dynamics is not damped, the system keeps oscillating. The specific time scales for which this is a valid hypothesis are very much material dependent and still need to be investigated, in practice.

In the present case, as this behavior is expected, it serves as another consistency check of our framework.

One can also see the influence of the STT pulse on the mechanical structure. Indeed the external stress initiates the oscillations and during the pulse, one can clearly see the strain grows along the x-axis direction and diminish along the y-axis. When the pulse stops, the strain relaxes towards the stress induced deformation. After the second pulse the strain again shifts before relaxing to a similar state than after the first switching, although the amplitude is different. What is further interest is that these mechanical oscillations should be related to the sound velocity of the medium [145], which is controlled by the constants M_0 and M_1. In the present study, we have chosen $M_0 = 0$ and $M_1 = 10000$, but there should be a way to obtain these coefficients of the mass matrix more efficiently, in order to describe these oscillations more accurately from experimentally easily accessible data.

Let us now discuss the checks we have carried out, in order to ensure the consistency of our code.

We monitor the variation of the total energy of the system which should be conserved over time, since there isn't any damping and whose variation can only be due to the external torque. Results for different quality factors of the variable time step integration scheme are found in Figure 5.9

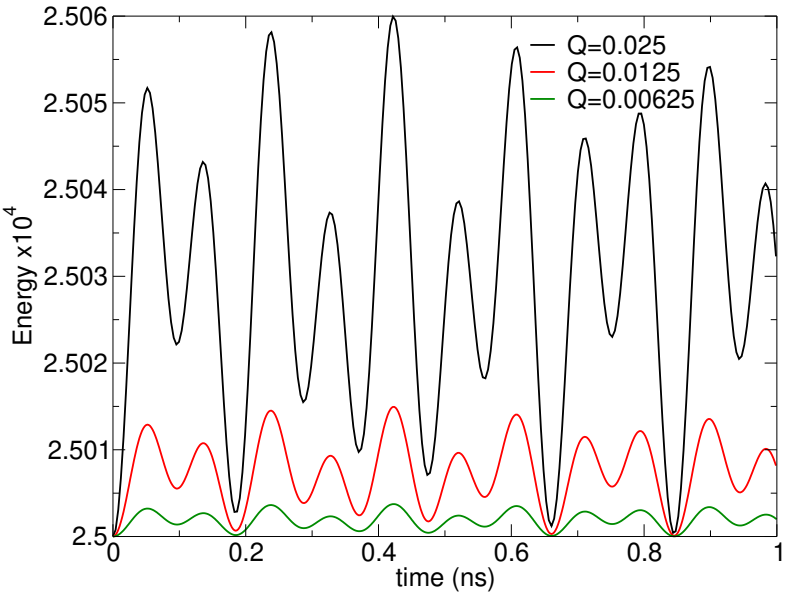

Figure 5.9: Single-site total energy as a function of both time and variable time step Q for scheme $S\pi S\epsilon S\pi S$. Conditions of the simulation are expressed in reduced units: $2C_0/\mu_0 M_s^2 = 5.1 \times 10^5$, $2C_1/\mu_0 M_s^2 = 3.5 \times 10^5$, $M_1 V_0 \mu_0 M_s^2/2\hbar^2 = 1000$, $\boldsymbol{\omega}_{DC} = (0, 0, 2\pi)$ rad.GHz, $\pi_{11}(0) = 1$, $\boldsymbol{s}(0) = (1, 0, 0)$. All the other parameters not reported, included initial conditions are zero.

We have verified that $\boldsymbol{\pi}^{(1)}(t) = \boldsymbol{\pi}^{(2)}(t)$ and $\boldsymbol{\epsilon}^{(1)}(t) = \boldsymbol{\epsilon}^{(2)}(t)$, because there is no non-local mechanical interaction and each site has the same magnetoelastic constants B_0 and B_1. For Figure 5.9 we can verify that, indeed, the energy converges to a constant value, in the present simulation $\dfrac{\pi_{11}^2(0)}{4M_1}$, which is another quality check of our algorithm. Now the last check which remains is to evaluate the influence of the chosen scheme on the quality of the integration by comparing the dynamics. Results are depicted in Figure 5.10.

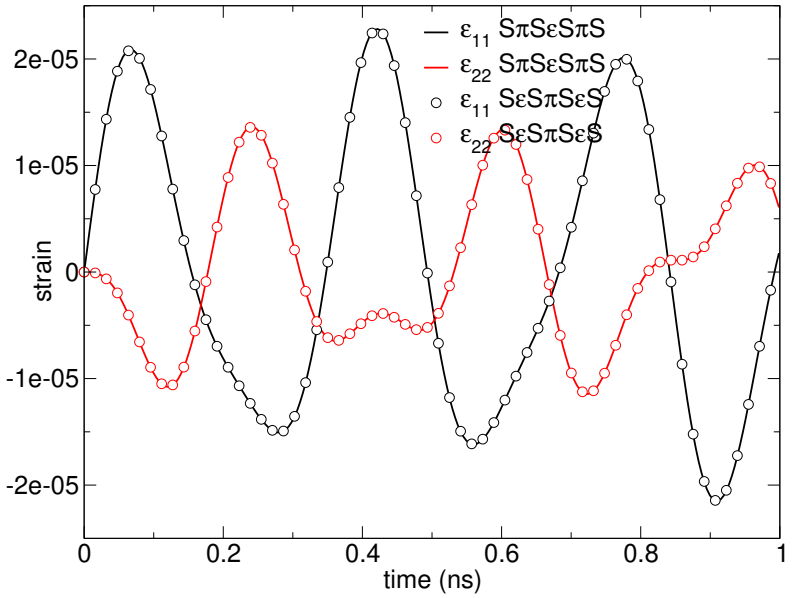

Figure 5.10: Single-site strain components as a function of time for various numerical schemes. Conditions of the simulation are identical to those for Figure 5.9 and the results are produced for $Q = 0.0025$ only.

To obtain these curves, we proceeded in the following way. First, we plotted the $\epsilon_{11}^{(1)}(t)$ and $\epsilon_{22}^{(1)}(t)$ (red and black curves) with the integration scheme corresponding to the operator ordering of the first line of Table 5.1. We then proceeded to plot them again, but with the ordering corresponding to the second line of Table 5.1 (red and black points), so as to compare the results. Although previous studies [146, 147] seemed to indicate a noticeable influence of the integration scheme on the results, here the influence is below 1%.

Summary

- We have defined a Poisson bracket for the coupled magnetoelastic dynamics by using anticommuting variables.
- We have constructed a Hamiltonian for the description of the coupled dynamics for the magnetic and mechanical degrees of freedom and have deduced the equations of motion for this system using the corresponding Poisson bracket.
- We have shown how to generalize the one–particle model in order to describe the interaction of many "particles," that stand for domains in the material. In particular, we showed how to couple these particles by a purely magnetic exchange interaction, that's relevant for describing two magnetically inequivalent sites, as in AFs.
- We simulated the switching of the magnetization, by an external STT, for the case of a model for the NiO AF and showed that it is possible to obtain the influence of external stress on the switching speed. It appears that through this external stress it is possible to adjust the switching speed.

Conclusion

The focus of this study was to contribute to improving our understanding of the properties of magnetic materials, as these are probed by external stimuli such as temperature, pressure and magnetic fields. To this end we have developed a new conceptual framework, that is the basis for our computational methods.

The object of our study is the probability distribution for the magnetization, $P(\boldsymbol{s})$, that, formally, can be written as a path integral:

$$P(\boldsymbol{s}) = Z^{-1} e^{-\int dt\, dt' \frac{1}{2}\left\{e(\boldsymbol{s})^{-1}\left(\frac{d\boldsymbol{s}}{dt}+\boldsymbol{A}(s)\right)(t) G(t-t') e^{-1}(\boldsymbol{s})\left(\frac{d\boldsymbol{s}}{dt}+\boldsymbol{A}(s)\right)(t')\right\}} \left|\det \frac{\delta \eta_I(t)}{\delta s_J(t')}\right| \tag{5.55}$$

where $\boldsymbol{\eta}(t)$ denotes the bath, to which the magnetic moment, $\boldsymbol{s}$ is coupled. This is the result of the stochastic description of the dynamics in terms of the Langevin equation.

The challenge is to understand how to make sense of this expression and to describe the appropriate generalization for describing many-body systems.

In real–and numerical–experiments, this is achieved by computing its moments. We have developed the conceptual and computational tools for doing so, under controlled approximations and our results allow insights into its properties.

In particular, we have developed the Hamiltonian formalism of Berezin and Marinov and of Casalbuoni, for including the spin degrees of freedom, on equal footing with those of the medium, in which the magnetic moment(s) are embedded into an efficient computational framework.

We have, also, developed the generalization of Hamiltonian mechanics, known as Nambu mechanics, in order to take into account dissipative effects in magnetic materials.

We have shown how to test our approximations, both through consistency checks and comparison with real experiments, in particular regarding how to describe switching of the magnetization in the presence of elastic effects.

Let us summarize the results of our work:

In chapter 2 we investigated a model of magnetization dynamics where a "light" spin is interacting with a "heavy" spin, the latter defining a spin bath for the former. This approach was first considered to check if and how it can simulate the coupling between magnetism and elasticity by reproducing effects expected for this coupling (*i.e.*, longitudinal damping and long-term equilibrium with lower norm for both spins), and, on the other hand, to compare stochastic and effective – deterministic – calculations, respectively on

the averaged realizations for the spins and for the moments of their distributions. Indeed, even if the deterministic model is conceptually much more complicated to construct, the stochastic model is computationally much more demanding. We then have been able to show that through this model, longitudinal damping can emerge for both light and heavy spins and depending on initial conditions and simulation parameters, one can even converge to an equilibrium solution for the norm of both light and heavy spins, which is lower than the initial norm, without imposing an *ad hoc* longitudinal Bloch-like damping term on either of both spins. The deterministic computations on the moments using Gaussian closure and independent initial correlators between the light and heavy spins, seem to reproduce a similar behavior even though they diverge at longer time, because the Gaussian closure approximation seems to break down as is shown by the fact that the third-order cumulants grow significantly. Better closing assumptions and initial correlations between the light and heavy spins could be investigated and should allow better agreement between the stochastic and deterministic approaches, for longer simulation times. Another issue is that, even though this model displays longitudinal damping and, depending on simulation parameters, long time equilibrium with lower norm for both spins, which is expected of magnetoelastic coupling, it is not completely trivial how to parametrize these to "mimic" a specific material's properties. An example of a similar approach is given in reference [18] where the properties of the bath are described in terms of the normal sound propagation modes of a given compound. Furthermore, once the relevant parameters are identified, this approach requires preliminary *ab initio* simulations to properly fit these parameters for a given compound. Finally, one may have to consider more noises, suitable to experiments, to describe some materials properties which could make establishing a formula much more complicated as the SL formula and the FND theorem take up different forms for non-Gaussian noise sources.

Subsequently, in chapter 3, to circumvent this difficulty, we studied a Lagrangian model, where we showed that a particular coupling between magnetic and elastic degrees of freedom could be most helpful. We construct the Lagrangian, that describes the precession of a localized magnetic moment around an effective frequency. Next, we defined the Lagrangian for the elastic degrees of freedom, which produces the dynamics for a localized strain tensor and, finally, we constructed the interaction term, that can describe magnetoelasticity. This model is first constructed for a single particle (*i.e.*, single domain), carrying a local magnetization – or spin depending on the scale – and a local strain tensor. The peculiarity of this model is that the spin is not described directly by the variable $\boldsymbol{s}$ but rather by its time derivative, hence being sensitive to the whole history of the underlying variable $\boldsymbol{s}$. This allowed us to obtain first-order EOM for the spin part of ME systems. This model is then extended to multiple interacting particles, by introducing a magnetic exchange between the nearest neighbors, which is expected to be the dominant interaction. We then investigate the magnetic and elastic behavior of a simple toy model for AF NiO and simulate the influence of an external stress on the switching of the Néel order parameter by an external STT pulse. We showed that the switching speed can be improved by an external compression stress but that the required stress is quite large. Conversely, using a shear stress appears to be much more efficient to improve the switching speed, depending on the sign of the ME constants. This model also shows that the equilibrium norm of the spin can be lower than the initial value as both the mechanical and spin sys-

tems exchange energy, resulting in different equilibrium states before and after the STT pulse. This is in agreement with what was observed in chapter 3, where a bath of spins was investigated. This remains true for the second applied pulse, switching the system back to the initial orientation but with still a slightly lower value for the spin norm than initially. This method, however, has some issues. One issue is the non-locality due to the description in terms of $\dot{\boldsymbol{s}}$ makes it impossible to give a simple expression for the magnetic induction $\boldsymbol{B}$, or the vector potential $\boldsymbol{A}$ (which yields the effective precession frequency) .It is, however, this same non-locality which makes the identification possible in the first place. Another problem is that this model does not preserve the phase-space volume and the energy, making it difficult to have feedback on the stability of the integration scheme over time.

In chapter 4, we study the influence of external or internal noise and the way these can be implemented in magnetic systems. First, we explore Nambu dynamics, which naturally takes into account constraints for spinning particles. Here we show how to describe simple – conservative – precession, *i.e.,* Larmor-like precession, by a Nambu model describing the spin phase space as the intersection between a sphere (which encodes the constant norm of the spin) and a plane (representing the constant energy surface). We also inspect ways to extend this model to include dissipation of energy so as to describe damped magnetization precession. We then identify this dissipation implementation with an LLG damping term so as to recover previously well-known dynamics. We then probe the differences between additive and multiplicative noise implementation so as to find out which is better suited for describing the fluctuations of magnetic DOF. We show that in the case of magnetization dynamics, the multiplicative noise implementation is more adapted and through this we present a fluctuating and dissipating Nambu system for the description of the phase space of magnetic degrees of freedom. We then focus on comparing the dynamics for averages of the stochastic realizations of the spins to a deterministic model for the moments of their statistical distributions, obtained by Gaussian closure. The deterministic approach being independent of any number of realizations is much more efficient (*i.e.*, requires less computational resources). However, this deterministic method seems to require stronger closure assumptions than Gaussian closure, for the multiplicative noise, whereas this assumption appears to be strong enough for additive noises. It would be interesting to study further under which assumptions the deterministic model can be accommodated to describe larger amplitudes of multiplicative noises. This implementation for Nambu dynamics gives rise to interesting physical interpretation of the magnetization phase space where regular damping towards an axis can be understood as the plane shifting up until the intersection with a sphere is simply a point, and "fuzzy" surfaces, due to the multiplicative noise coupling, whose "fuzzy" intersection explains how longitudinal damping can emerge.

Finally, in chapter 5, we set up the Hamiltonian formalism for the coupled dynamics of magnetic and elastic degrees of freedom in which each single domain carries a local (uniform) magnetization (or spin), a local (uniform) strain tensor and a local (uniform) strain-rate tensor. In this model, the classical – commuting – spin variable is constructed on the ground of anticommuting – Grassmann – variables. This in turn enables us to reconstruct the spin part of the Poisson bracket developed before to explain why there cannot be a conjugate variable for the spin (except itself), as the conjugate variable to

the Grassmann variable is proportional to itself. Using this, we extend the graded Poisson Bracket to a canonical pair conjugate variables (strain/strain-rate tensors) which can now be used to obtain equations of motion for ME media. The next step was to build a Hamiltonian including all the physics necessary to describe ME media. Combining these two steps, we obtain the magnetoelastic equations of motion for a single domain that are consistent with well-reported equilibrium situations. This model is extended to multiple particle systems, by considering a magnetic exchange interaction only. We then adapt this model to the study of the same AF NiO toy model (chapter 3) to cross-check these two approaches. Here again, we managed to probe the influence of external stress on the switching behavior of the Néel order parameter by an external STT pulse. The observations were the same as in the Lagrangian case, namely that the switching speed can be improved by the external stress, with significantly lower threshold values than required for the Lagrangian model. The main advantages of the Hamiltonian description is that it does not present any non-locality issues and that the energy is conserved over time, which makes it easier to track integration scheme failure. In this specific case, as the integration scheme is symplectic it preserves the phase-space volume which was tracked over time as well in further studies. An issue is that the oscillation frequencies of the elastic medium introduced by the inertia term appear to be very high, which indicates sound velocity much larger than expected. This is due to some arbitrariness of the "mass"-matrix, which could be adapted by studying experimental sound velocity diagrams for specific materials, hence yielding the physically correct oscillations and improving the quality of the simulation scheme altogether. One could also improve this model by implementing a dissipation term for the elastic medium so as to force relaxed oscillations towards an equilibrium state for the mechanical system as well.

Concerning purely mechanical DOF, there are models such as granular field theories and models, that focus on the mechanical degrees of freedom, which can describe spatially correlated strains and effects in solids, beyond elasticity, but these are beyond the scope of this thesis. It would, however, be interesting to study more detailed systems by defining larger lattices using for example "enlarged" ASD models where the elastic behavior is introduced in the fashion we described and where more attention is given to the parametrization of the mass matrix. These results could then, in theory, be compared to experimental magnetization curves or strain mediated switching experiments. It would then also be of interest to couple these models to external baths so as to include thermal effects, induced, for example, by a thermal gradient producing a spin current, and have a better grasp on how a measure of non-equilibrium entropy production can emerge. Indeed, one may wonder how the thermal bath couples to the mechanical DOF, the magnetic system or both, maybe even with two thermostats, thus yielding two different temperatures, as experimental "many temperatures" models seem to indicate. By trying to study directly the moments of the thus obtained distributions, one could formulate effective, deterministic, models for such thermal dynamics, but this will have to be the focus of future works.

Conclusion

Le but de cette étude a été de développer une meilleure compréhension théorique des propriétés des matériaux magnétiques afin de pouvoir élaborer des simulations numériques de leur comportement temporel lorsqu'existent des contraintes externes telles qu'une température, une pression ou un champ magnétique.

Comme présenté en introduction, on peut formellement résumer l'objectif de cette thèse à "donner" sens à la distribution de probabilité pour un moment magnétique $\boldsymbol{s}$ à l'équilibre avec le bain $\boldsymbol{\eta}(t)$ dans lequel il est plongé

$$P(\boldsymbol{s}) = Z^{-1} e^{-\int dt\, dt' \, \frac{1}{2}\left\{e(\boldsymbol{s})^{-1}\left(\frac{d\boldsymbol{s}}{dt}+\boldsymbol{A}(s)\right)(t) G(t-t') e^{-1}(\boldsymbol{s})\left(\frac{d\boldsymbol{s}}{dt}+\boldsymbol{A}(s)\right)(t')\right\}} \left|\det \frac{\delta \eta_I(t)}{\delta s_J(t')}\right| \tag{5.56}$$

En pratique, on travaillera plutôt avec les moments de cette distribution et l'objectif de cette thèse a été de développer des outils numériques, dans le cadre d'approximations dont les conséquences sont contrôlées.

À cette fin, nous avons, dans la continuité des travaux de Berezin, Marinov et Casalbuoni, développé un formalisme Hamiltonien qui permet de traiter les degrés de liberté magnétiques au même niveau que les degrés de liberté du milieu dans lequel ceux-ci "vivent".

Nous avons également développé le formalisme de Nambu, une généralisation du formalisme Hamiltonien, pour tenir compte des effets de dissipation au sein de matériaux magnétiques.

De même, nous avons développé des outils permettant de vérifier la validité de nos approximations de manière auto cohérente, mais aussi en les confrontant à des données expérimentales dans le cadre de l'étude du retournement de l'aimantation pour un système magnétoélastique.

Voici un résumé des travaux de cette thèse :

Dans le chapitre 2, nous avons établi un modèle dans lequel un spin "léger" interagit avec un spin "lourd", ce dernier définissant un bain de spin. Nous avons développé cette approche afin de tenter d'obtenir un modèle effectif qui reproduit les effets du couplage magnétoélastique à savoir un amortissement longitudinal pour la norme du spin et la possibilité d'atteindre un état d'équilibre pour lequel la norme des deux spins est inférieure à leur norme initiale. Nous avons construit ensuite, à partir de ce modèle stochastique, un modèle déterministe sur les moments des distributions des deux spins et nous avons pu reproduire un amortissement longitudinal, à la fois pour le spin léger et le spin lourd. De plus, en fonction des conditions initiales et des autres paramètres matériaux de simulation

(constantes de couplage magnétoélastique, d'élasticité, d'échange magnétique ...), nous avons montré qu'il était possible d'obtenir une solution convergeant vers un état d'équilibre pour lequel la norme des deux spins est inférieure à la norme initiale, sans imposer de façon *ad hoc* une dissipation de Bloch. Les simulations du modèle déterministe, obtenues à partir d'une hypothèse de fermeture Gaussienne et de corrélations initiales nulles, reproduisent un comportement initialement tout à fait similaire au modèle stochastique, mais divergent pour des temps longs, les hypothèses de fermeture n'étant plus valides pour ces temps longs comme le montre la courbe du cumulant qui croît significativement. Il semblerait qu'il faille ici introduire des hypothèses de fermeture plus complexes ainsi que des corrélations initiales non triviales entre les spins léger et lourd, pour pouvoir recouvrir les résultats du modèle stochastique pour des temps longs. Cette approche reproduit les effets attendus du couplage magnétoélastique, à savoir la dissipation longitudinale et l'émergence d'état d'équilibre à norme inférieure à l'état initial, pour les deux spins, mais il n'est néanmoins pas évident de savoir comment les paramétrer pour décrire les propriétés d'un matériau donné. Un exemple d'interprétation est donné dans [18] où la paramétrisation du bain correspond aux modes normaux de propagations du son dans le composé étudié. De plus cette approche doit s'appuyer sur une étude préliminaire qui puisse permettre ce paramétrage afin de mimer un système élastique équivalent donné. Une autre voie ouverte pour ce modèle est de choisir d'étudier des bruits colorés dans ce modèle, mais ceci implique des formes différentes notamment pour les formules de SL et de FND qui sont nettement plus difficiles à manipuler pour ce genre de bruits non Gaussiens. Afin d'outrepasser ces limites, nous avons ensuite développé une approche Lagrangienne pour laquelle les degrés de liberté mécaniques sont étudiés de façon plus explicite.

Dans le (chapitre 3), nous avons bâti un modèle Lagrangien pour le couplage entre les degrés de liberté magnétiques et mécaniques, à partir de 3 termes. Le premier est le Lagrangien magnétique qui décrit la précession d'un moment magnétique local autour d'une pulsation effective. Le second est le Lagrangien élastique qui décrit la dynamique d'un tenseur de déformation mécanique également local. Le dernier est le Lagrangien du couplage magnétoélastique. Dans un premier temps, ce modèle a été construit pour une particule isolée, portant un moment magnétique et un tenseur de déformation mécanique tout deux locaux. La particularité de ce modèle est que le spin n'est pas représenté directement par la variable, $\boldsymbol{s}$ mais plutôt sa dérivée temporelle $\boldsymbol{\mu} = \dot{\boldsymbol{s}}$, et la dynamique est de ce fait sensible à tout l'historique de $\boldsymbol{s}$. Ceci nous a permis d'obtenir des équations du mouvement du premier ordre pour le spin dans ce système magnétoélastique. Ce modèle est ensuite étendu au cas multi particulaire en implémentant un échange purement magnétique entre sites (plus proches voisins), interaction estimée prédominante dans notre modèle. Ce modèle est ensuite utilisé pour étudier un modèle jouet antiferromagnétique appliqué à NiO afin de simuler l'influence d'une contrainte mécanique externe sur la vitesse de retournement du paramètre de Néel par un couple de transfert de spin. Nous avons pu montrer que le retournement pouvait être accéléré par une compression, mais que l'intensité requise est élevée. Inversement, nous avons pu montrer des effets similaires pour une contrainte de cisaillement avec une intensité requise nettement plus faible. Ce modèle montre également que la norme du moment magnétique peut diminuer par rapport à sa valeur initiale, les systèmes mécaniques et magnétiques échangeant de l'énergie après l'application du couple de transfert de spin, et se relaxent vers un état d'équilibre différent

de l'état initial. Ces observations concordent avec le chapitre 2 pour lequel nous avons également observé une relaxation du système vers un état d'équilibre de norme inférieur à la norme initiale pour les deux spins (léger et lourd). Pour la seconde application du couple de transfert de spin, on observe une dynamique similaire, mais bien qu'il y ait retournement dans la direction initiale, l'état d'équilibre n'est pas identique à l'état initial. Cette méthode présente néanmoins des problèmes conceptuels. Puisque la description en $\boldsymbol{\mu}$ implique une non-localité en $\boldsymbol{s}$, il est difficile de fournir une expression simple pour le potentiel vecteur $\boldsymbol{A}$ (ou le champ magnétique $\boldsymbol{B}$) qui engendrent la pulsation effective de précession $\boldsymbol{\omega}$, malgré le fait que ce soit cette non-localité qui permette de relier $\boldsymbol{\omega}$ et $\boldsymbol{A}$. Un autre problème est que ce modèle ne permette pas de construire un système fermé, ce qui rend plus difficile d'évaluer la stabilité du schéma d'intégration en analysant l'évolution temporelle de l'énergie, par exemple. Pour aller plus loin et tenir compte des effets de température pour les propriétés de matériaux magnétiques, une méthode possible est le couplage à un bain stochastique.

Dans le chapitre 4, afin d'étudier l'influence de bruits et de leur implémentation sur les systèmes magnétiques, nous nous sommes intéressés à la dynamique de Nambu qui permet naturellement de traiter les contraintes inhérentes à la description Hamiltonienne de degrés de liberté vectoriels, à savoir la dynamique d'espaces des phases à nombres de degrés de liberté impairs. Dans cette partie nous avons montré comment décrire une précession conservative (à la Larmor), par une dynamique de Nambu dont l'espace des phases est décrit par l'intersection d'un plan et d'une sphère. Nous avons également évalué comment implémenter au sein de ce formalisme des termes dissipatifs afin de décrire la précession amortie de l'aimantation d'un domaine. Ces termes sont ensuite identifiés comme un terme de LLG afin de décrire la dynamique relaxée d'un moment magnétique d'une manière physiquement réaliste. Nous avons évalué les différences entre bruits additifs et multiplicatifs afin de déterminer lequel est le plus adapté à la description de fluctuations pour les milieux magnétiques. Nous avons montré que pour ces derniers, l'implémentation multiplicative semble être la plus adaptée. Nous avons ainsi obtenu pour la première fois une dynamique de Nambu fluctuante et dissipante pour la description de l'espace des phases de degrés de liberté magnétiques. Nous avons ensuite poursuivi cette étude en comparant la dynamique stochastique d'un moment magnétique à un modèle déterministe sur les moments de sa distribution statistique obtenu en imposant une hypothèse de fermeture Gaussienne. Cette dernière, étant indépendante du nombre de réalisations, est numériquement nettement plus efficace. Cependant, cette approche semble indiquer qu'il faille des hypothèses nettement plus élaborées pour la fermeture d'un système à bruit multiplicatif que pour un système à bruit additif. Une extension de ce travail serait d'observer sous quelles hypothèses de fermeture il serait possible d'étudier des bruits multiplicatifs d'amplitude plus élevée. Cette dynamique de Nambu a donné lieu néanmoins à des interprétations intéressantes dans l'espace des phases de l'aimantation où l'amortissement transverse peut être vu comme un plan qui s'élève et dont le cercle d'intersection avec la sphère se réduit progressivement jusqu'à n'être plus qu'un point, d'où la position d'équilibre alignée avec le champ dominant. Sans le cas de surfaces (sphère et plan) bruitées, leur intersection est plus diffuse et fournit une explication plausible des phénomènes d'amortissement longitudinaux, puisque s'il y a intersection en dehors de la sphère, la norme n'est pas conservée. Dans le chapitre 3, une description non locale en

termes de $\boldsymbol{s}$ a été présentée. Une alternative à cette description non locale en termes de variables commutantes est une description locale en termes de variables anticommutantes.

Finalement (chapitre 5), nous avons construit un modèle Hamiltonien pour la dynamique couplée des degrés de liberté magnétiques et élastiques. Dans celui-ci, chaque site d'un réseau porte un moment magnétique, une déformation mécanique et un tenseur conjugué. Le spin classique (commutant) est construit à partir de variables sous-jacentes (anticommutantes, de Grassmann). Ceci nous permet de produire simplement la partie incluant le spin dans un crochet de Poisson construit par Yang et Hirschfelder et ainsi de fournir par la même occasion une explication pour l'absence de variable conjuguée au spin. Dans ce formalisme, le spin est sa propre variable conjuguée (à un facteur constant près). À partir de ce crochet, nous avons construit un crochet de Poisson pour l'espace des phases étendu à la déformation mécanique, son tenseur conjugué et le spin. Ce crochet a été utilisé pour déterminer les équations du mouvement d'un système magnétoélastique couplé. Nous avons ensuite établi un Hamiltonien pour un système magnétoélastique.Nous avons pu déterminer les équations du mouvement pour la dynamique couplée pour une telle particule. Comme dans le chapitre 3, nous avons étendu ce modèle à plusieurs particules, en introduisant un échange purement magnétique entre particules. L'étape suivante fut d'utiliser ce modèle pour étudier le modèle jouet de NiO antiferromagnétique, afin de comparer nos résultats au chapitre 3. Nous avons pu évaluer ici encore l'influence d'une contrainte mécanique externe sur le retournement du paramètre de Néel par un couple de transfert de spin. Nous avons pu constater que la vitesse de retournement peut être accélérée par une contrainte mécanique, mais avec un seuil nettement plus faible que pour le modèle Lagrangien. Ceci peut s'expliquer par l'absence d'implémentation de terme d'amortissement pour les degrés de liberté élastiques. Un des avantages de cette formulation, par rapport à la description Lagrangienne, est qu'elle est locale. Un autre avantage est qu'elle constitue un système fermé pour lequel l'énergie est conservée, ce qui rend plus aisé d'évaluer la stabilité des schémas d'intégration numérique. Dans le cas présent, le schéma d'intégration étant symplectique, il doit conserver le volume de l'espace des phases en plus de l'énergie, ce qui pourrait être vérifié en simulant l'évolution temporelle de la variation du volume de l'espace des phases. Un problème est que les oscillations du milieu élastique semblent se produire à des fréquences très élevées, ce qui devrait impliquer une vitesse de propagation du son dans ce milieu nettement supérieur à la valeur attendue. Ceci est en partie dû aux constantes de la matrice de masse (qui ne de rapport avec une "vraie" masse que le fait qu'elles décrivent une inertie en modulant les oscillations mécaniques caractéristiques du matériau considéré), qui pourraient être adaptées pour des matériaux spécifiques (pour dépasser le modèle jouet), en utilisant par exemple des données expérimentales de vitesse du son dans un matériau étudié. Ceci permettrait de décrire ces oscillations de façon plus réaliste. Une autre voie d'amélioration serait d'implémenter un terme de dissipation mécanique afin de forcer le système à relaxer vers un état d'équilibre mécanique.

Bien évidemment, il existe des modèles de descriptions pour les degrés de liberté mécaniques telles que les théories de champ granulaire ou des modèles non linéaires de déformations qui permettent de décrire des corrélations spatiales pour les contraintes mécaniques dans un solide ou encore des effets au-delà de l'élasticité, mais ceux-ci dépassent le cadre des présents travaux de thèse. Il serait néanmoins intéressant d'étudier des

systèmes plus complexes, notamment avec plus d'une particule, à la manière d'une dynamique de spin atomique "augmentée", où la partie mécanique et le couplage sont introduits de la manière décrite dans le chapitre 5, en accordant plus d'importance à la paramétrisation de la matrice de masse. Ces résultats pourraient ensuite être comparés à des données expérimentales de courbes d'aimantation ou de retournement d'aimantation par contrainte mécanique. Pour aller plus loin encore, l'approche Hamiltonienne pourrait être couplée à des bains, notamment thermiques, afin de permettre de donner un sens physique à la notion de température au sein de chaque sous-partie de ce système. On peut se demander en effet si l'implémentation de températures finies passe par le couplage du seul système magnétique à un bain, ou s'il faut coupler les deux systèmes à des bains de nature différente. Il semble en effet que les interprétations expérimentales définissent plusieurs températures, une pour chacun des sous-systèmes, indiquant plutôt un argument en faveur de la seconde option. Une fois un tel modèle obtenu, il pourrait être intéressant également d'en construire le modèle déterministe équivalent pour ses moments.

Appendix

Appendix A

Articles and communications

A.1 Articles

- T. Nussle, P. Thibaudeau, S. Nicolis, Dynamic magnetostriction for antiferromagnets, ArXiv:1907.01857 [Cond-Mat, Physics:Physics] (2019), accepted for publication in Physical Review B
- T. Nussle, P. Thibaudeau, S. Nicolis, Probing magneto-elastic phenomena through an effective spin-bath coupling model, Eur. Phys. J. B. 92 (2019) 29
- T. Nussle, P. Thibaudeau, S. Nicolis, Coupling magneto-elastic Lagrangians to spin transfer torque sources, J. Magn. Magn. Mater. 469 (2019) 633–637
- P. Thibaudeau, T. Nussle, S. Nicolis, Nambu mechanics for stochastic magnetization dynamics, J. Magn. Magn. Mater. 432 (2017) 175–180
- S. Nicolis, P. Thibaudeau, T. Nussle, A Group Action Principle for Nambu Dynamics of Spin Degrees of Freedom, in: Quantum Theory and Symmetries with Lie Theory and Its Applications in Physics, Dobrev, Vladimir, QTS-X/LT-XII, Varna, Bulgaria, 2017: pp. 411–420

A.2 Oral communications

- "Magnetoelastic Hamiltonian coupling in antiferromagnets", August 28$^{\text{th}}$ 2019, Joint European Magnetic Symposia, Uppsala, Sweden
- "Une approche Hamiltonienne du couplage magnéto-élastique", May 17$^{\text{th}}$ 2019, Colloque Louis Néel, Toulouse, France
- "Modélisation de comportements magnétiques sous contrainte mécanique et thermique", Journées des Jeunes Scientifiques du CEA, November 15$^{\text{th}}$ 2018, Blois, France
- "Thermomécanique dynamique à grande échelle des matériaux magnétiques", November 16$^{\text{th}}$ 2017, Journée des Doctorants de l'Institut Denis Poisson, Tours, France

- "Coupling magnetoelastic Lagrangians with spin transfer torque sources", October 11$^{\text{th}}$ 2017, Ultrafast Magnetism Conference, Kaiserslautern, Germany

A.3 Poster communications

- "A spin-spin bath coupling : comparing the stochastic and deterministic approaches", September 18$^{\text{th}}$ 2018, European School on Magnetism, Krakow, Poland
- "Probing magneto-elastic phenomena through an effective spin-bath coupling", August 7$^{\text{th}}$ 2018, Physics and Application of Spin Phenomena in Solids 10, Linz, Austria
- "Nambu mechanics for stochastic magnetization dynamics", November 1$^{\text{st}}$ 2016, 61$^{\text{st}}$ Annual Conference on Magnetism and Magnetic Materials, New Orleans, USA

Bibliography

[1] R. Skomski, *Simple Models of Magnetism*, Oxford Graduate Texts (Oxford University Press, Oxford, New York, 2008).

[2] R. Kubo and N. Hashitsume, Progress of Theoretical Physics Supplement **46**, 210 (1970).

[3] W. Brown, IEEE Transactions on Magnetics **15**, 1196 (1979).

[4] W. T. Coffey and Y. P. Kalmykov, Journal of Applied Physics **112**, 121301 (2012).

[5] J. Curie and P. Curie, Bulletin de Minéralogie **3**, 90 (1880).

[6] E. Du Trémolet de Lacheisserie, *Magnetostriction: Theory and Applications of Magnetoelasticity* (CRC Press, Boca Raton, 1993).

[7] T. Nussle, P. Thibaudeau, and S. Nicolis, The European Physical Journal B **92**, 29 (2019).

[8] P. Thibaudeau, T. Nussle, and S. Nicolis, Journal of Magnetism and Magnetic Materials **432**, 175 (2017).

[9] T. Nussle, P. Thibaudeau, and S. Nicolis, Journal of Magnetism and Magnetic Materials **469**, 633 (2019), arXiv:1711.08062 .

[10] C. Cohen-Tannoudji, B. Diu, and F. Laloë, *Mécanique quantique* (Hermann, Paris, 2008).

[11] M. A. Wongsam and R. W. Chantrell, Journal of Magnetism and Magnetic Materials **152**, 234 (1996).

[12] V. Bargmann, L. Michel, and V. L. Telegdi, Physical Review Letters **2**, 435 (1959).

[13] T. Fukuyama and A. J. Silenko, International Journal of Modern Physics A **28**, 1350147 (2013).

[14] M. Rivas, *Kinematical Theory of Spinning Particles* (Springer Netherlands, Dordrecht, 2002).

[15] S. Wimmer, K. Chadova, M. Seemann, D. Ködderitzsch, and H. Ebert, Physical Review B **94**, 054415 (2016).

[16] T. Bose and S. Trimper, Physics Letters A **375**, 2452 (2011).

[17] T. L. Gilbert and J. M. Kelly, Conf. Magnetism and Magnetic Materials (1955).

[18] E. Rossi, O. G. Heinonen, and A. H. MacDonald, Physical Review B **72**, 174412 (2005).

[19] K.-H. Yang and J. O. Hirschfelder, Physical Review A **22**, 1814 (1980).

[20] T. Ruijgrok and H. Van der Vlist, Physica A: Statistical Mechanics and its Applications **101**, 571 (1980).

[21] R. Casalbuoni, Il Nuovo Cimento A (1965-1970) **33**, 389 (1976).

[22] F. Berezin and M. Marinov, Annals of Physics **104**, 336 (1977).

[23] L. Brink, P. Di Vecchia, and P. Howe, Nuclear Physics B **118**, 76 (1977).

[24] D. Beaujouan, P. Thibaudeau, and C. Barreteau, Physical Review B **86**, 174409 (2012).

[25] D. Perera, M. Eisenbach, D. M. Nicholson, G. M. Stocks, and D. P. Landau, Physical Review B **93**, 060402 (2016).

[26] P.-W. Ma, S. L. Dudarev, and J. S. Wróbel, Physical Review B **96**, 094418 (2017).

[27] J. Tranchida, S. J. Plimpton, P. Thibaudeau, and A. P. Thompson, Journal of Computational Physics **372**, 406 (2018).

[28] B. Skubic, J. Hellsvik, L. Nordström, and O. Eriksson, Journal of Physics: Condensed Matter **20**, 315203 (2008), arXiv:0806.1582 .

[29] V. P. Antropov, M. I. Katsnelson, M. van Schilfgaarde, and B. N. Harmon, Physical Review Letters **75**, 729 (1995).

[30] W. F. Brown, Physical Review **130**, 1677 (1963).

[31] C. H. Woo, H. Wen, A. A. Semenov, S. L. Dudarev, and P.-W. Ma, Physical Review B **91**, 104306 (2015).

[32] R. F. L. Evans, U. Atxitia, and R. W. Chantrell, Physical Review B **91**, 144425 (2015).

[33] M. D. Kuz'min, Physical Review Letters **94**, 107204 (2005).

[34] V. P. Antropov, M. I. Katsnelson, B. N. Harmon, M. van Schilfgaarde, and D. Kusnezov, Physical Review B **54**, 1019 (1996).

[35] E. Beaurepaire, J.-C. Merle, A. Daunois, and J.-Y. Bigot, Physical Review Letters **76**, 4250 (1996).

[36] P. Thibaudeau and D. Beaujouan, Physica A: Statistical Mechanics and its Applications **391**, 1963 (2012).

[37] G. Bertotti, I. D. Mayergoyz, and C. Serpico, Physica B: Condensed Matter Proceedings of the Fourth Intional Conference on Hysteresis and Micromagnetic Modeling, **343**, 325 (2004).

[38] J. Tranchida, P. Thibaudeau, and S. Nicolis, Physica B: Condensed Matter 10th International Symposium on Hysteresis Modeling and Micromagnetics (HMM 2015), **486**, 57 (2016).

[39] V. E. Shapiro and V. M. Loginov, Physica A: Statistical Mechanics and its Applications **91**, 563 (1978).

[40] R. V. Bobryk, Physical Review E **83**, 057701 (2011).

[41] D. A. Garanin, Physical Review B **55**, 3050 (1997).

[42] A. V. Chumak, V. I. Vasyuchka, A. A. Serga, and B. Hillebrands, Nature Physics **11**, 453 (2015).

[43] V. Zapf, M. Jaime, and C. D. Batista, Reviews of Modern Physics **86**, 563 (2014).

[44] W.-S. Dai and M. Xie, Journal of Statistical Mechanics: Theory and Experiment **2009**, P04021 (2009).

[45] Y. Nambu, Physical Review D **7**, 2405 (1973).

[46] N. Mukunda and E. C. G. Sudarshan, Physical Review D **13**, 2846 (1976).

[47] M. Axenides, E. Floratos, and S. Nicolis, Journal of Physics A: Mathematical and Theoretical **42**, 275201 (2009), arXiv:0901.2638 .

[48] P. Névir and R. Blender, Journal of Physics A: Mathematical and General **26**, L1189 (1993).

[49] R. Blender and G. Badin, Journal of Physics A: Mathematical and Theoretical **48**, 105501 (2015).

[50] P.-M. Ho, Nuclear Physics A Proceedings of the 4th International Symposium on Symmetries in Subatomic Physics, **844**, 95c (2010).

[51] M. Axenides and E. Floratos, Journal of High Energy Physics **2010** (2010), 10.1007/JHEP04(2010)036.

[52] J. Tranchida, P. Thibaudeau, and S. Nicolis, Journal of Physics: Conference Series **574**, 012146 (2015).

[53] B. Carter, Physical Review Letters **74**, 3098 (1995).

[54] V. V. Sokolov, P. A. Eminov, and K. N. Fotov, Physics Procedia 12th International Conference on Magnetic Fluids (ICMF12), **9**, 131 (2010).

[55] C. Kittel, Reviews of Modern Physics **21**, 541 (1949).

[56] E. Callen and H. Callen, Physical Review **139**, 455 (1965).

[57] D. Fritsch and C. Ederer, Physical Review B **86**, 014406 (2012).

[58] W. F. Brown, *Magnetoelastic Interactions*, english ed., edited by C. Truesdell, R. Aris, L. Collatz, G. Fichera, P. Germain, J. Keller, M. M. Schiffer, and A. Seeger, Springer Tracts in Natural Philosophy, Vol. 9 (Springer Berlin Heidelberg, Berlin, Heidelberg, 1966).

[59] G. Grimvall, *Thermophysical Properties of Materials*, enl. and rev. ed ed. (Elsevier, Amsterdam, 1999).

[60] J. Zinn-Justin, *Quantum Field Theory and Critical Phenomena*, 4th ed., International Series of Monographs on Physics No. 113 (Clarendon Press ; Oxford University Press, Oxford : New York, 2002).

[61] L. Corwin, Y. Ne'eman, and S. Sternberg, Reviews of Modern Physics **47**, 573 (1975).

[62] N. Mueller and R. Venugopalan, arXiv:1901.10492 [hep-ph, physics:hep-th, physics:nucl-th] (2019), arXiv:1901.10492 [hep-ph, physics:hep-th, physics:nucl-th] .

[63] G. Bacher, A. A. Maksimov, H. Schömig, V. D. Kulakovskii, M. K. Welsch, A. Forchel, P. S. Dorozhkin, A. V. Chernenko, S. Lee, M. Dobrowolska, and J. K. Furdyna, Physical Review Letters **89**, 127201 (2002).

[64] N. Prokof'ev and P. Stamp, Reports on Progress in Physics **63**, 669 (2000), arXiv:cond-mat/0001080 .

[65] A. Rebei and G. J. Parker, Physical Review B **67**, 104434 (2003).

[66] S. A. Crooker, D. G. Rickel, A. V. Balatsky, and D. L. Smith, Nature **431**, 49 (2004).

[67] N. G. V. Van Kampen, *Stochastic Processes in Physics and Chemistry* (Elsevier, 1992).

[68] P. Mazur, Physica **43**, 533 (1969).

[69] K. Miyazaki and K. Seki, The Journal of Chemical Physics **108**, 7052 (1998).

[70] R. Casalbuoni, A. Deandrea, N. Di Bartolomeo, R. Gatto, F. Feruglio, and G. Nardulli, Physics Letters B **299**, 139 (1993).

[71] R. Wieser, The European Physical Journal B **88** (2015), 10.1140/epjb/e2015-50832-0.

[72] G. Bertotti, I. D. Mayergoyz, and C. Serpico, *Nonlinear Magnetization Dynamics in Nanosystems* (Elsevier, 2009).

[73] J. Tranchida, P. Thibaudeau, and S. Nicolis, Physical Review E **98**, 042101 (2018).

[74] K. Kim and D.-H. Lee, Journal of Korean Physical Society **35**, 387 (1999).

[75] M. Suzuki, Communications in Mathematical Physics **183**, 339 (1997).

[76] P.-W. Ma and S. L. Dudarev, Physical Review B **83**, 134418 (2011).

[77] W. Greiner and J. Reinhardt, *Field Quantization* (Springer-Verlag, Berlin Heidelberg, 1996).

[78] E. Hairer, C. Lubich, and G. Wanner, *Geometric Numerical Integration: Structure-Preserving Algorithms for Ordinary Differential Equations*, 2nd ed., Springer Series in Computational Mathematics (Springer-Verlag, Berlin Heidelberg, 2006).

[79] S. Blanes, F. Casas, J. A. Oteo, and J. Ros, Physics Reports **470**, 151 (2009).

[80] O. Eriksson, A. Bergman, L. Bergqvist, and J. Hellsvik, *Atomistic Spin Dynamics: Foundations and Applications*, first edition ed. (Oxford University Press, Oxford, 2017).

[81] J. Frank, W. Huang, and B. Leimkuhler, Journal of Computational Physics **133**, 160 (1997).

[82] J. C. Butcher, *Numerical Methods for Ordinary Differential Equations*, third edition ed. (Wiley, Chichester, West Sussex, 2016).

[83] P. E. Kloeden and E. Platen, *Numerical Solution of Stochastic Differential Equations* (Springer Berlin Heidelberg, Berlin, Heidelberg, 1992).

[84] B. Gough, *GNU Scientific Library Reference Manual - Third Edition*, 3rd ed. (Network Theory Ltd., 2009).

[85] J. R. Dormand and P. J. Prince, Journal of Computational and Applied Mathematics **6**, 19 (1980).

[86] V. Jakšić and C.-A. Pillet, Communications in Mathematical Physics **178**, 627 (1996).

[87] J. Simoni, M. Stamenova, and S. Sanvito, Physical Review B **95**, 024412 (2017).

[88] J. D. Jackson, *Classical Electrodynamics*, 3rd ed. (Wiley, Hoboken, NY, 2009) oCLC: 552107820.

[89] K. Y. Bliokh, A. Niv, V. Kleiner, and E. Hasman, Nature Photonics **2**, 748 (2008).

[90] C. Truesdell and W. Noll, *The Non-Linear Field Theories of Mechanics*, 3rd ed., edited by S. S. Antman (Springer Berlin Heidelberg, Berlin, Heidelberg, 2004).

[91] R. P. Feynman, R. B. Leighton, M. Sands, and R. P. Feynman, *Le cours de physique de Feynman*, Vol. 2 (InterEditions, Paris, 1992).

[92] A. A. Deriglazov, Modern Physics Letters A **25**, 2769 (2010).

[93] T. Tomé and M. J. de Oliveira, Physical Review A **41**, 4251 (1990).

[94] N. A. Doughty, *Lagrangian Interaction: An Introduction to Relativistic Symmetry in Electrodynamics and Gravitation*, 1st ed. (Addison-Wesley, Sydney, 1990).

[95] D. G. Edelen, *Lagrangian Mechanics of Nonconservative Nonholonomic Systems.* (Springer, Amsterdam, 2010).

[96] E. DeGiuli, Physical Review E **98**, 033001 (2018), arXiv:1804.04834 .

[97] S. Chikazumi, *Physics of Ferromagnetism* (Oxford Science Publications, 1997).

[98] G. Roepke, Theoretical and Mathematical Physics **6**, 216 (1971).

[99] H. V. Gomonay and V. M. Loktev, Physical Review B **81**, 144427 (2010).

[100] R. Cheng, J. Xiao, Q. Niu, and A. Brataas, Physical Review Letters **113**, 057601 (2014).

[101] R. Cheng, M. W. Daniels, J.-G. Zhu, and D. Xiao, Physical Review B **91**, 064423 (2015).

[102] P. d. V. D. Plessis, S. J. van Tonder, and L. Alberts, Journal of Physics C: Solid State Physics **4**, 1983 (1971).

[103] P.-d.-V. du Plessis, S. J. van Tonder, and L. Alberts, Journal of Physics C: Solid State Physics **4**, 2565 (1971).

[104] N. Koon, C. Williams, and B. Das, Journal of Magnetism and Magnetic Materials **100**, 173 (1991).

[105] A. E. Clark, M. Wun-Fogle, J. B. Restorff, and T. A. Lograsso, Materials Transactions **43**, 881 (2002).

[106] H. H. Rugh, Journal of Physics A: Mathematical and General **31**, 7761 (1998).

[107] J. E. Marsden and T. S. Ratiu, *Introduction to Mechanics and Symmetry*, edited by J. E. Marsden, L. Sirovich, M. Golubitsky, and W. Jäger, Texts in Applied Mathematics, Vol. 17 (Springer New York, New York, NY, 1999).

[108] R. Ibáñez, M. de León, J. C. Marrero, and D. M. de Diego, Journal of Mathematical Physics **38**, 2332 (1997).

[109] H. Bhatia, G. Norgard, V. Pascucci, and P. Bremer, IEEE Transactions on Visualization and Computer Graphics **19**, 1386 (2013).

[110] P. Griffiths and J. Harris, *Principles of Algebraic Geometry* (John Wiley & Sons, 2014).

[111] J.-Z. Wu, H.-y. Ma, and M.-D. Zhou, *Vorticity and Vortex Dynamics* (Springer Science & Business Media, 2007).

[112] M. Axenides and E. Floratos, in *Chaos, Information Processing and Paradoxical Games* (WORLD SCIENTIFIC, 2014) pp. 27–41.

[113] R. Graham and D. Roekaerts, Physics Letters A **109**, 436 (1985).

[114] G. E. Uhlenbeck and L. S. Ornstein, Physical Review **36**, 823 (1930).

[115] H. Risken, *The Fokker-Planck Equation*, edited by H. Haken, Springer Series in Synergetics, Vol. 18 (Springer-Verlag, Berlin, Heidelberg, 1989).

[116] D. Walton, Journal of Magnetism and Magnetic Materials **62**, 392 (1986).

[117] T. Nussle, P. Thibaudeau, and S. Nicolis, arXiv:1907.01857 [cond-mat, physics:physics] (2019), arXiv:1907.01857 [cond-mat, physics:physics] .

[118] J. Scherk, Reviews of Modern Physics **47**, 123 (1975).

[119] G. Binasch, P. Grünberg, F. Saurenbach, and W. Zinn, Physical Review B **39**, 4828 (1989).

[120] M. N. Baibich, J. M. Broto, A. Fert, F. N. Van Dau, F. Petroff, P. Etienne, G. Creuzet, A. Friederich, and J. Chazelas, Physical Review Letters **61**, 2472 (1988).

[121] L. Brink, O. Lindgren, and B. E.W. Nilsson, Physics Letters B **123**, 323 (1983).

[122] M. B. Green and J. H. Schwarz, Physics Letters B **122**, 143 (1983).

[123] A. Barducci, R. Casalbuoni, and L. Lusanna, Nuclear Physics B **124**, 93 (1977).

[124] B. Thaller, *The Dirac Equation* (Springer Science & Business Media, 2013).

[125] J. Alicea, Reports on Progress in Physics **75**, 076501 (2012).

[126] R. Casalbuoni, Il Nuovo Cimento A (1965-1970) **33**, 115 (1976).

[127] J. Gomis, J. París, and S. Samuel, Physics Reports **259**, 1 (1995).

[128] J. E. Marsden, R. Montgomery, P. J. Morrison, and W. B. Thompson, Annals of Physics **169**, 29 (1986).

[129] J. Kijowski and W. Szczyrba, Communications in Mathematical Physics **46**, 183 (1976).

[130] W. Szczyrba, Communications in Mathematical Physics **51**, 163 (1976).

[131] B. K. D. Gairola, Physica Status Solidi (b) **85**, 577 (1978).

[132] A. C. Eringen, ed., *Nonlocal Continuum Field Theories* (Springer New York, New York, NY, 2004).

[133] L. D. Landau, E. M. Lifshitz, and L. D. Landau, *Theory of Elasticity*, 3rd ed., Course of Theoretical Physics No. Vol. 7 (Elsevier, Amsterdam, 2008).

[134] J. H. van Vleck, Physical Review **52**, 1178 (1937).

[135] L. Néel, Journal de Physique et le Radium **15**, 225 (1954).

[136] E. W. Lee, Reports on Progress in Physics **18**, 184 (1955).

[137] H. Callen and E. Callen, Journal of Physics and Chemistry of Solids **27**, 1271 (1966).

[138] P. Lu, P. Zhang, H. Lee, C. Wang, and J. Reddy, Proceedings of the Royal Society A: Mathematical, Physical and Engineering Sciences **463**, 3225 (2007).

[139] A. C. Eringen, Journal of Applied Physics **54**, 4703 (1983).

[140] I. Radu, K. Vahaplar, C. Stamm, T. Kachel, N. Pontius, H. Dürr, T. Ostler, J. Barker, R. Evans, R. Chantrell, *et al.*, Nature **472**, 205 (2011).

[141] T. Jungwirth, X. Marti, P. Wadley, and J. Wunderlich, Nature Nanotechnology **11**, 231 (2016).

[142] O. Rodrigues, Journal de Mathématiques Pures et Appliquées **5**, 380 (1840).

[143] J. Honerkamp and H. Römer, *Theoretical Physics: A Classical Approach* (Springer, Berlin; New York, 1993).

[144] R. Cheng, X. Wu, and D. Xiao, Physical Review B **96**, 054409 (2017).

[145] R. W. Ogden, *Non-Linear Elastic Deformations*, dover ed ed., Dover Books on Physics (Dover, Mineola, NY, 1997).

[146] D. Beaujouan, *Simulation des matériaux magnétiques à base Cobalt par Dynamique Moléculaire Magnétique*, Ph.D. thesis, Université Paris Sud, Orsay (2012).

[147] P. F. Batcho and T. Schlick, The Journal of Chemical Physics **115**, 4019 (2001).

Notations

- DOS : Density Of States
- DOF : Degrees Of Freedom
- QFDR : Quantum Fluctuation Dissipation Relation
- AF : AntiFerromagnetic
- EOM : Equation(s) Of Motion
- MMD : Magnetic Molecular Dynamics
- STT : Spin Transfer Torque
- RHS : Right-Hand-Side
- LHS : Left-Hand-Side
- LL : Landau-Lifshitz
- LLG : Landau-Lifshitz-Gilbert
- LLB : Landau-Lifshitz-Bloch
- RK : Runge-Kutta

- GSL : GNU Scientific Library
- ODE : Ordinary Differential Equation
- GNU : GNU is Not Unix
- SL : Shapiro-Loginov
- FND : Furutsu-Novikov-Donsker
- ME : magnetoelastic

Résumé :

Le magnétisme est l'un des plus anciens phénomènes rapportés de l'histoire des sciences naturelles et probablement l'un des plus fascinants. Véritable manifestation macroscopique de la physique quantique, il subit en s'y couplant, l'influence de nombreux réservoirs énergétiques et statistiques, dont ceux de la thermique et de la mécanique.

En remarquant qu'un moment magnétique élémentaire est un objet composite formé grâce à des variables anticommutantes inobservables, on peut engendrer une dynamique Hamiltonienne couplant ce degré de liberté à ceux provenant des autres réservoirs, eux-mêmes décrits par la dynamique de variables aléatoires.

La première étape est d'étudier la dynamique d'un moment magnétique, vu comme un spin classique dans de tels bains. À cette fin on considère un bain magnétique afin d'évaluer la possibilité de mimer les effets de couplage entre moments magnétiques ainsi que le couplage magnétoélastique par un tel modèle effectif.

Par la suite, nous montrons que la précession d'un spin classique peut être modélisée par une dynamique de Nambu qui facilite la description de la nature, additive ou multiplicative, des couplages stochastiques. La dynamique ainsi produite est d'abord étudiée numériquement de façon stochastique en moyennant les différentes réalisations obtenues; ensuite, un modèle déterministe sur la hiérarchie des moments statistiques est établi puis fermé afin de développer une méthode à la fois plus rapide, mais également déterministe de déduction des propriétés magnétiques.

Finalement, pour illustrer la pertinence tangible de toutes ces notions, nous construisons une dynamique étendue de particules "fictives" portant à la fois un moment magnétique et une déformation mécanique locaux exprimant la magnétoélasticité, d'une part dans une approche Lagrangienne puis Hamiltonienne. Pour chacune des deux approches nous étudierons la dynamique du retournement ultrarapide d'aimantation pour NiO, oxyde antiferromagnétique prototype, sous sollicitations mécanique et électrique.

Le formalisme, exposé ici, aussi bien conceptuel qu'informatique, ne sert pas, seulement, comme un exemple de l'état de l'art, mais permet une description des propriétés des milieux magnétiques, qui est fondamentale aussi bien pour la conception de nouveaux matériaux, que comme modèle pour aborder d'autres questions portant sur l'interaction entre bruit et variables dynamiques, plus généralement.

Mots clés :

Dynamique stochastique de spin, fermeture de hiérarchie, magnétoélasticité, couplages magnétomécanique Lagrangien et Hamiltonien, dynamique de Nambu, antiferromagnétisme, intégration symplectique/géométrique, retournement du paramètre d'ordre de Néel, couple de transfert de spin.

Abstract :

One of the utmost interesting properties of matter is magnetism. This property, which is a macroscopic consequence of quantum physics, is subjected and couples to several reservoirs. Among them, two are most relevant, namely the thermal and mechanical reservoirs. We build a Hamiltonian model for the coupling between – classical – magnetism and elasticity, which relies on the – underlying – anticommuting nature of spin, so as to describe the coupled dynamics of these degrees of freedom.

The first step is to study the behavior of the classical spin – or magnetic moment – when coupled to different – stochastic – baths. First a spin bath, so as to investigate if and how such an effective model can mimic the couplings, to different magnetic moments but also to the elastic structure of the compound. A different approach is then followed where, through a Nambu dynamics model for spin precession, the ways in which this spin can be coupled to a bath, additively or multiplicatively, are studied in order to make out which is better suited to describe coupling phenomena in magnetism. Those are then studied numerically, initially stochastically, with the appropriate averaging procedure over different realizations and then deterministically, by building an effective model for the moments of the statistical distributions. This model is obtained by truncating the thus derived hierarchy of moments, so as to construct a quicker and deterministic method to deduce magnetic properties of a system.

The second step is to construct models for magnetoelastic coupling, which we do via "virtual" particles carrying both localized magnetic moment and mechanical strain tensor. We begin by a Lagrangian formulation for the precession of spin, which is coupled to a dynamical elastic solid by a magnetoelastic coupling term. This enables us to study their coupled dynamics in a way that is fully consistent with all the symmetries, which ensures a consistent description.

We then shift to a Hamiltonian description where spin is interpreted as a composite – commuting – variable, which is a product of underlying and not observable – anticommuting – variables. Such a spin interacts with a couple of canonically conjugate variables representing the elastic medium, in an extended Poisson structure. Finally, for each of these two models, we numerically study the influence of an external stress on the switching behavior of the Néel order parameter and spin accumulation for a NiO toy model antiferromagnet, induced by an external spin-transfer-torque.

Keywords :

Stochastic spin dynamics, hierarchy closing, magnetoelasticity, Lagrangian and Hamiltonian magnetomechanical coupling, Nambu dynamics, antiferromagnetism, symplectic/geometric integration, Néel order parameter switching, spin transfer torque.